Alexandra Eugénio Fernandes

B. A. Anthropology

Pterosaurs from the Late Cretaceous of Angola

Dissertação para obtenção do Grau de Mestre em
Paleontologia

Orientador: Octávio Mateus, PhD, Prof. Associado FCT-UNL
Co-orientador: Brian Andres, PhD, Associado University of Sheffield

FACULDADE DE CIÊNCIAS E TECNOLOGIA
UNIVERSIDADE NOVA DE LISBOA

Março 2020

Pterosaurs from the Late Cretaceous of Angola

Alexandra Eugénio Fernandes
B.A. Anthropology

Dissertação para obtenção do Grau de Mestre em
Paleontologia

Março 2020

Orientador: Octávio Mateus, PhD, Prof. Associado FCT-UNL
Co-orientador: Brian Andres, PhD, Associado University of Sheffield

Pterosaurs from the Late Cretaceous of Angola

Dedicated to Tia Teresa, who, with every bowl of soup, convinced me that I could.

Acknowledgements

Heartfelt thanks are extended to Maria, Alvaro, Nicki, and Joe Fernandes, for their encouragements and tolerance of my pipe dream of pursuing this course. Thank you to my aunt and godmother Ana Fontoura: you are the best personal librarian anyone could ever dream of. Thank you to Mike Eklund, the most entertaining fossil preparation mentor and cheese connoisseur I've ever met. Thank you to Jack Conrad, who planted this seed (when many others would have just pulled it out by the root). Thank you Călin Șuteu, digitization wizard and life running partner. Thank you to Elizabeth Eugenio, Kimberley Aparisio, Carl Mehling, Fiona Brady, Ana Balcarcel, Eileen Westwig, and all of my beloved family and friends (who, to name individually, might just exceed the length of this thesis).

I would like to deeply thank the members of the PaleoAngola Project, to Louis Jacobs, Mike Polcyn, Octavio Mateus, Bill Johnson, and my brother Miguel Marx (meet me at "The Old Monk" when this is all over), Euridice Pacheco (for her naming creativity) and the rest of the Dream Team. Sincerest gratitude is extended to Carla Alexandra Tomás for her impeccable preparation and guidance, the staff of the Museu da Lourinhã, to the Lourinhã PaleoTeam for countless laughs and incomparable brute strength, and the SMU and FCT-UNL staff. Thank you to Brian Andres for so many superb insights and such generosity in sharing profuse pterosaurian knowledge, to Miguel Moreno-Azanza (for teaching me almost everything I learned throughout this degree), to Eduardo Puertolas-Pascual (for teaching me whatever Miguel didn't), and to Filippo Rotatori (pro auxilio sunt Latin).

Many thanks to the participants of Flugsaurier 2018 for extending me a warm welcome into their club, and an especial round of gratitude to Oliver Rauhut, Matyas Vremir, Mark Norell, Mike Habib, Chris Bennett, Nick Longrich, Dave Martill, Olaf Dulfer, Pia Schucht, and Elsa Marlene Vorderwuelbecke.

Abstract

Fourteen fossil bones from the Lower Maastrichtian marine locality of Bentiaba in the Namibe Basin of Angola, Africa, identified as pterosaurs, are here described and attributed to Pteranodontia. One articulated set of bones from within the fossil assemblage can be further attributed to the Nyctosauridae, gen. et sp. nov. This is the first record of pterosaur material from the central west coast of Africa, contributing new information about the paleoecological environment of Gondwana during this time frame. Ontogenetic deductions are also drawn from preliminary histological work. This fossil assemblage provides a first glimpse of Angolan pterosaur paleobiodiversity, giving further insight into the ecosystems of the Late Cretaceous.

Keywords: Pterosauria, Lower Maastrichtian, Angola, Namibe Basin

Resumo

Quatorze ossos fósseis da localidade marinha de Bentiaba, no Maastrichtiano Inferior, na Bacia do Namibe, em Angola, África, identificados como pterossauros, são aqui descritos e atribuídos a Pteranodontia. Um conjunto articulado de ossos da assembléia fóssil pode ser ainda atribuído a Nyctosauridae, gen. et sp. nov. Este é o primeiro registo de material de pterossauro da costa oeste central da África, contribuindo com novas informações sobre o ambiente paleoecológico de Gondwana durante esse período. Informações ontogenéticos também são extraídas de trabalhos histológicos preliminares. Este conjunto fóssil fornece um primeiro vislumbre da paleobiodiversidade Angolano dos pterossauros, fornecendo uma visão mais detalhada dos ecossistemas do final do Cretáceo.

Palavras-chave: Pterosauria, Maastrichtiano Inferior, Angola, Bacia do Namibe

Table of Contents

Figures

Tables

Abbreviations: MGUAN, Museu Geologico Universidade Agostinho Neto/Museu Nacional de História Natural of Luanda, Angola; MGUAN-PA, PaleoAngola Project.

INTRODUCTION

Pterosaurs are the first vertebrates to have evolved powered flight and are highly diverse ecologically, with a successful global distribution throughout nearly their entire temporal range from the Late Triassic through the Cretaceous (Barrett et al., 2008). Pterosaurs are also widely considered to be a relatively challenging group to study for reasons such as a sparse fossil record, lack of intact fossil material due to their physical bone fragility, and a propensity for fossils to have undergone drastic taphonomic duress (Butler et al., 2013). Additionally, remains that are successfully recovered are usually done so in great quantity mainly from Lagerstätten environments, which creates a sampling bias for very select areas (Buffetaut & Mazin, 2003). However, this dearth of worldwide fossil material does not detract from pterosaurs having played a crucial role in reconstructing paleoecological faunas. In this work, a morphological description and attribution is given for fossil pterosaur material retrieved from present-day Angola, increasing recognized taxonomic diversity of Late Cretaceous Gondwanan paleoenvironments.

Angola is a country with a richly-preserved paleontological record, although much of it remains vastly unexplored due to a history of more than forty years of civil unrest (up until as recently as 2002), as well as insufficient scientific funding, which has caused students and researchers to lack reliable access to scientific data (Lourenço, 2019). The specimens described here were collected during several expeditions, carried out by PaleoAngola Project members, who collected fossils throughout multiple field seasons in various localities, beginning in 2005 and up until the present day (Mateus et al., 2019). Although past excavations were fraught by complications, the efforts thus far have already been greatly successful in increasing known taxon diversity (including many new species) for the region in the Late Cretaceous, including: dinosaurs, marine reptiles, turtles, fish, etc. (Araujo et al., 2015a, 2015b; Jacobs et al., 2006, 2009; Mateus et al., 2009, 2011, 2019; Polcyn et al., 2010; Schulp et al., 2006, 2008), and now here in greater detail, pterosaurs.

Within Angola, the pterosaur material yielded from these ongoing expeditions has thus far only been discovered and retrieved from the single locality of Bentiaba. Existing stratigraphic data indicates that this interval, which is part of the Mocuio Formation, is of lower Maastrichtian Stage (uppermost Cretaceous) age (Strganac et al., 2014).

The PaleoAngola Project comprises an international team of paleontological researchers from Southern Methodist University in the United States of America, The Universidade Nova de Lisboa in Portugal, the Maastricht Natural History Museum in Holland, Agostinho Neto University in Angola, and with the support of the following Angolan Institutions: Tundavala Private University and the Methodist University of Angola. The mission statement of the PaleoAngola project encompasses creating a strong and lasting tradition of Angolan paleontological research and pride in cultural heritage through scientific dissemination, which is intended to proliferate Angola's own internal academic growth.

History and Record of Pterosaur Discoveries on the African Continent

Pterosaur discoveries in Africa have been relatively sparse when compared with the majority of the world, with main fossil concentrations on the continent occurring in northern countries, and disparate occurrences occurring further south. This distribution is likely due to poor field sampling and the potential unavailability of Mesozoic exposures throughout sub-Saharan Africa (Mateus, pers. comm.). In addition, much of what has been unearthed are isolated bones, rather than articulated skeletons (Kellner et al., 2007). Most localities are Cretaceous in age, with some Jurassic sites as well. Below is a brief summary of reported discoveries from the continent, through the current publication date:

From Tunisia, in the Chenini Formation of the Tataouine region, an unnumbered isolated tooth attributed to an ornithocheirid pterosaur was reported by Benton et al. (2000). This specimen might correspond to the Anhangueria (Rodrigues & Kellner, 2013) or even Ornithocheiromorpha (Andres et al. 2014) and is currently under study (Andres, pers. comm.). Other teeth were reported from the Douiret sand member of the same horizon by Fanti et al. (2012) and attributed to "Ornithocheiroidea". From the Oum ed Diab Member of the Aïn el Guettar Formation (Early Cretaceous, Albian), a tooth was also assigned to "Ornithocheiroidea" (Martill et al., 2018).

Morocco is the African country with the most abundant pterosaur fossil material recorded to date, and is also notable for being one of the few countries with not just isolated elements but also articulated skeletal material. Although fragmentary remains are still most abundant, several species have been named from this country.

From the non-marine Cretaceous (Albian/Cenomanian) deposits of Ksar es Souk, the anhanguerid *Siroccopteryx moroccensis* Mader & Kellner, 1999 was described based on the anterior part of a rostrum with teeth, and a complete azhdarchid cervical vertebra was also reported, along with isolated *Anhanguera* teeth (Kellner & Mader, 1997).

From the Cenomanian Kem Kem beds of Takmout, near Erfoud in southern Morocco, *Afrotapejara zouhri* Martill et al. 2020 is a tapejarid based on a jaw fragment. The thalassodromine *Alanqa saharica* Ibrahim et al. 2010 (Longrich et al. 2018) is based on the anterior end of a rostrum, and is also represented by a mandibular symphysis from the Kem Beds (Martill et al., 2018). *Xericeps curvirostris* Martill et al. 2017 is an azhdarchid, based on a partial mandible. *Coloborhynchus fluviferox* Jacobs et al. 2019 is an "ornithocheirid", based on an anterior rostrum fragment. Several other clades are also reported from these beds, such as "ornithocheirids" represented by more than thirty teeth, a tapejarid rostrum, and three jaw fragments first attributed to a pteranodontid (Wellnhofer & Buffetaut, 1999), but which may instead be an azhdarchid (Averianov, 2008). A jaw fragment attributed to Dsungeripteroidea, two mid-cervical vertebrae attributed to Azhdarchidae, and a humerus attributed to Azhdarchoidea were also reported (Rodrigues et al., 2011).

From the Lower Cretaceous (possibly Berriasian) of Anoual, Morocco, various teeth from a microverebrate assemblage were reported and attributed to the "ornithocheirds" and gnathosaurines (Knoll, 2000).

A series of cervical vertebrae from Oulad Abdoun Basin and other isolated vertebrae from Sidi Daoui, from a locality near Khouribga were referred to *Phosphatodraco mauritanicus* Pereda et al. 2003,

and from the Upper Maastrichtian phosphate mines of the Ouled Abdoun Basin, two cervical vertebrae of the same species were recovered (Longrich et al., 2018). *Tethydraco regalis* Longrich et al. 2018 was described based on a humerus compared to two ulnae, femora, and a tibia; *Alcione elainus* Longrich et al. 2018 was described based on a partial skeleton including humerus, sternum, scapulocoracoid, and femur, and other referred material; *Simurghia robusta* Longrich et al. 2018 was described based on a humerus; *Barbaridactylus grandis* Longrich et al. 2018 was described based on an associated skeleton including a left humerus, radius and ulna, right femur, left scapulocoracoid, partial right mandible, and referred material. Also, an azhdarchid cervical vertebra and ulna were reported (Longrich et al., 2018).

Senegal yielded a pterodactyloid cervical vertebra and a suspected shaft of a tibia from the Upper Cretaceous locality of Paki, southeast of Dakar in the Sénégala Basin (Monteillet et al., 1982).

From Niger, in the Lower Cretaceous Elrhaz Formation, at the western edge of the Ténéré Desert, an undescribed tooth attributed to the "Ornithocheiridae" was found (Sereno & Brusatte, 2008). From the Aptian-aged Elrhaz Formation, one potential tapejaroid was reported based on a humerus, and one potential anhanguerid based on a partial wing (Blackburn & Sereno, 2002).

From Cameroon, a fleeting mention of the preliminary identification of a pterosaur vertebra was reported from the Campanian Douala sub-basin (Ntamak-Nida et al., 2006).

From the Democratic Republic of the Congo (at the time referred to as Belgian Congo), a single fragmentary distal left metacarpal IV was recovered in 1947 from the Cretaceous locality of Bibanga, and attributed to the "Ornithocheiridae" (Swinton, 1948).

From Kenya, an isolated caudalmost cervical or cranialmost (non-notarial) dorsal vertebra was retrieved from Cretaceous fluvial deposits in West Turkana and tentatively attributed to Azhdarchidae (O'Connor et al., 2010).

From Tanzania, the Upper Jurassic Tendaguru Formation deposits have yielded pterosaur material (including some three-dimensional) from as early as 1931, deposited in the Museum für Naturkunde Berlin. A radius and ulna were identified as *Rhamphorhynchus* sp. An ulna and first phalanx were identified as *Pterodactylus* sp. (Reck, 1931). The tibiotarsus, fibula, and first phalanx were identified as Dsungaripteroidea (sensu Young, 1964), gen. et sp. indet. (Galton, 1980; Unwin & Heinrich, 1999). Two humeri were referred to Archaeopterodactyloidea (Costa & Kellner, 2009). Two cervical vertebrae were suggested to be azhdarchids (Costa et al. 2015) but had been previously phylogenetically determined to be ctenochasmatids (Andres and Ji, 2008). A coracoid was referred to a basal pterodactyloid (Costa et al., 2014). A wing metacarpal was referred to Pterodactyloidea (Costa et al., 2014). Finally, a short section of a mandibular symphysis was attributed to the pterosaur *Tendaguripterus recki* Unwin & Heinrich, 1999.

From South Africa, undescribed isolated pterosaur bones are reported as having been collected from the Lower Jurassic Elliott Formation (Blackbeard & Yates, 2007).

Madagascar has yielded four fossil teeth, attributed to non-pterodactyloid pterosaurs, from the Middle Jurassic (Bathonian Stage) sediments of the Mahajanga Basin (Dal Sasso & Pasini, 2003). Many other isolated teeth and a single pneumatized caudal vertebra from the Ambondromamy region were also attributed to non-pterodactyloids (Flynn et al., 2006).

Although pterosaur material was only found in very recent years, Angola's own formal history of geological study and fossil collecting in general began in the nineteenth century with names such as José de Anchieta, Carlos Friere de Andrade, Augusto Eduardo Neuparth, and others (Mateus et al., 2019). This was a time in which scientists were more akin to adventurers, making overarching observations on flora and fauna as naturalists. Records exist from as early as 1818 of mainly government-supported expeditions, perhaps most notably the expedition between 1853 and 1860 led by Friedrich Welwitsch, who described the African shield and its sedimentary cover, even describing its Mesozoic strata succession. Interest developed towards fossils themselves closer to 1882, when mining expeditions to Benguela were made to discover potential ore deposits, which uncovered a horde of Cretaceous fossils in West Africa. These were then shipped to Paul Choffat, a geologist living in Portugal who worked for the Portuguese Geological Survey, who then began publishing internationally on the specimens found. He named a number of new taxa and went on to co-author papers with other paleontologists on ammonites, lamellibranchs, gastropods, and echinoids (Masse & Laurent, 2015; Rocha & Kullberg, 2008). Although Choffat was able to correctly identify the locality of Bentiaba as Cretaceous after examining cf. *Triqonoarca* invertebrate fossils from the region (Choffat, 1905), his works were not always entirely accurate geologically, but still proved seminal in proliferating interest in the region. He even drew comparisons of Angola to the geology of Brazil, noting "these countries are located opposite each other, and… during the Cretaceous period, they had to be bathed by the same sea, presenting the same climatological conditions" (Choffat: 1890: p. 121), an idea which twenty years later supported Alfred Wegener in defending his revolutionary theory of continental drift (Rocha & Kullberg, 2008).

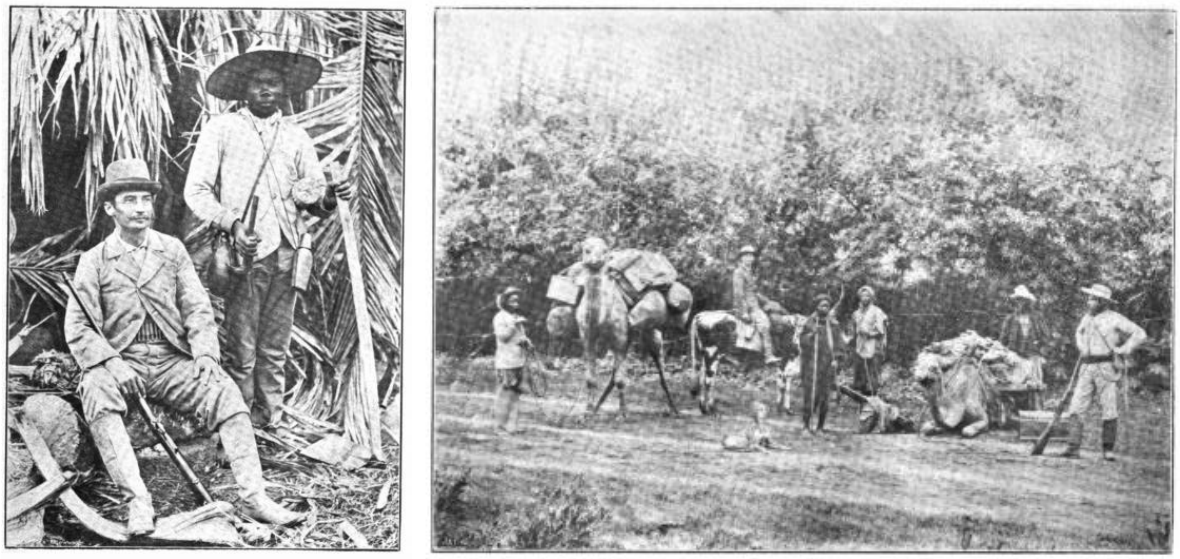

Figure 1. José Pereira do Nascimento and his campaign in Angola, circa 1894 (images taken from do Nascimento, 1898)

José Pereira do Nascimento (Fig. 1) was another geologist who worked extensively (on camelback) in the Namibe region of Angola from 1894 to 1895, studying the mineralogical wealth of the provinces, taking detailed documentation of the landscape geology and sedimentology, and publishing a scientific journal in 1894 with his findings. Do Nascimento even passed through the locality of Bentiaba (referred to as São Nicolau at that time, Fig. 2B), collecting and cataloging geological and

fossil samples, while in close communication with Choffat about the discoveries that he was making there (do Nascimento, 1898).

The construction of the Benguela railway system between 1903 and 1929 also accelerated scientific expeditions greatly to south-west Angola. John Walter Gregory was one such geologist who took advantage of the technological advance in transport, and in 1915-1916, published a geological map of the igneous formations near Huambo as well as collected fossils extensively throughout the region. This also precipitated the production of more geological mapping, notably one such venture by the Vernay campaign of 1925, which also collected fossils in Benguela and sent them to the American Museum of Natural History in New York for study. There, Otto Haas determined that this fossil fauna was of Campanian–Maastrichtian age (Masse & Laurent, 2015).

Although the Namibe region was less explored in the early days, Raoul Dartevelle (1907–1956), a Belgian geologist, did publish some paleontological observations on the area throughout his lifetime. Momentum for this region picked up closer to the 1960's, when the Namibe coastal sedimentary series was studied and published on by G. Soares de Carvalho (1961), who created a 1/40,000 map, and provided extensive detail of each formation, and also in 1972 when Luís Gonzaga Projecto Lapão published a geological map series for the provincial government. Paleontological studies soon followed these works, with ammonite assemblages from the Cenomanian–Turonian at Punta Negra described by Howarth (1965, 1966) and Cooper (1972) (Masse & Laurent, 2015). Many other paleontologists during that time also conducted fieldwork in the country, but perhaps none more significantly than Miguel Telles Antunes, whose fieldwork in the 1960's and thereafter on the Cretaceous and Paleogene series and their paleontological context set the precedent for present-day expeditions, including those of the PaleoAngola project.

Since the 1960's, Agostinho Neto University of Luanda has continually hosted many geological expeditions and collaborations with scientific researchers throughout Angola, including those involved with the PaleoAngola project. Although civil war had essentially halted these activities for many years, the end of the war in 2002 allowed for a gradual renovation of infrastructure, making research again possible on the national and international level (Lourenço, 2019). The first PaleoAngola Project expedition occurred in 2005 (the first since the acceptance of plate tectonics), with the intention of conducting geological and paleontological field expeditions focused on the effects of the opening of the South Atlantic Ocean on life through geologic time (from 130 Ma to the present), the efforts of which have yielded a vast variety of fossil bone throughout the years.

Materials and Methods

All specimen preparation was completed mechanically at the laboratory of the Museu da Lourinhã in Lourinhã, Portugal or at the Universidade Nova de Lisboa in Lisbon, Portugal, using a Paleo Tools ME-9100 for the bulk removal of the surrounding matrix, a Paleo Tools Micro Jack 6 for more precise matrix removal, a Presslufthammer HW 322 for more delicate work, and a variety of manual tools and wooden dowels for precision work. Throughout this process, all bone surfaces were consolidated with 5% Paraloid B-72 diluted in acetone, and any breaks or deep fissures were glued and reinforced with 20% or 50% Paraloid B-72 in acetone, as required. Specimen numbers MGUAN-

PA654 and MGUAN-PA655 were fully prepared by the author, as was the partial preparation and stabilization of MGUAN-PA652, MGUAN-PA653, MGUAN-PA656, MGUAN-PA658, MGUAN-PA659, and MGUAN-PA661 and MGUAN-PA662, altogether totaling over 300+ hours of work performed by the author (not including three weeks of full-time fieldwork in Angola for fossil collection). Bones were then three-dimensionally scanned using an Artec Space Spider, and all scans were processed using Artec Studio 14.

Phylogenetic analysis was conducted using T.N.T. v1.5 (Goloboff & Catalano, 2016). The matrix used was from Longrich et al. (2018), which added new additional characters to the Andres et al. (2014) matrix and also added additional taxa from the Late Cretaceous. The matrix contains continuous and discrete partitions. *Euparkeria capensis* Broom 1913 was used as the outgroup. The matrix also incorporated ordered characters (characters 0-51, 53, 63, 64, 79, 83, 85, 97, 101, 110, 111, 119, 139, 140, 158, 160, 167, 174, 175, 177, 180, 183-185, 194, 206, 213, 242, 250, 265, 269, 270) and unordered characters. It should be noted that T.N.T. begins numbering characters and taxa from 0. All characters were equally weighted, although the continuous characters were rescaled from a minimum of 0.000 to a maximum of 1.000 so that their maximum change would equal the maximum change along a branch of a binary character (i.e., one step). Ambiguous branch support was not used, zero-length branches were automatically collapsed, and resultant trees were filtered for the best score. A basic traditional tree-search analysis was conducted with 1,000 random addition sequence replicates. Analytical protocols are expanded upon in the supplementary material of Andres et al. (2014). No new characters were added here to the matrix, although character 236 on *Cretornis hlavaci* was deactivated as per a coding error (Andres, pers. comm.). Two new taxa were added, one to each software run: one based on all existing elements as though they were one taxon and labeled “Angola_ pterosaurs”, and another separate taxon represented by just the articulated MGUAN-PA650 humerus and MGUAN-PA651 ulna (the material from a single known individual, exhibiting the most characters), labeled “MGUAN_PA650&651”. It cannot be definitively assumed that all of the pterosaur material encompasses only one species. Much more extensive fossil sampling is required to ascertain if all of the bones, especially the fragmentary remains (which in some cases do not exhibit any known diagnostic characters), even individually represent the same species. However, in order to phylogenetically assess the possibility of all specimens belonging to a single species, two separate taxa were created, one in each taxon-character matrix.

Paleohistological analysis was conducted by creating bone thin sections, similar to petrographic methodologies and involved destructive sampling. These thin sections were produced by slicing bone, embedding the sample in epoxy resin, and then thin-slicing and grinding the section by hand in order to produce the thinnest possible layer to be analyzed under a microscope. In the case of pterosaur bones, histology can have an especially risky aspect due to the inherent thinness of the bones, which heightens the risk of over-grinding and potentially ruining the sample, so caution must be taken. For histological analysis, a fragment of the MGUAN-PA653 ulnar shaft was used. Thin section slides were prepared partially by the author according to current standards at the time of publication in the laboratory of the Rheinische Friedrich-Wilhelms-Universität Bonn. Due to the characteristic thinness of pterosaur bone, fossil samples were embedded in Araldite 2020/A clear adhesive epoxy and catalyzed with Araldite 2020/B in order to facilitate handling and analysis. These epoxy blocks were then cut down using a circular rotating diamond-tipped disc saw blade on a Buehler Isomet precision sectioning saw to cut through and section the block and sample. The

mounting-side of the samples were wet-ground using a Jean Wirtz TF 250 metallographic polishing machine, fitted with abrasive paper. After mounting to a slide, the exposed side of the sample was hand wet-ground with silicon carbide grinding powder and water on glass plates, in decreasing coarseness, beginning with F220 grit and then refining with F400 and F600 grits, prior to covering with a slide cover, using the method described by Lamm (2013). To observe the histological structures of the sample, the thin sections were analyzed with a Nikon Eclipse E400Pol petrographic microscope under normal light, under crossed plane polarized light, and also through a lambda filter.

The material described here is temporarily housed and curated, while on indefinite loan, at the Museu da Lourinhã, in Lourinhã, Portugal. The Geological Museum of Agostinho Neto University in Luanda, Angola will be the permanent repository for the material, once the museum has completed proposed renovation plans and initiates a call for the repatriation of the material.

Geographical and Geological Setting

The Republic of Angola is a country of 1,246,700 km^2 on the west coast of southern Africa, lying between 4° 22′ and 18° 02′ south latitude, and 11° 41′ and 24° 05′ east longitude, and bordered by the Democratic Republic of Congo to the north, Zambia to the east, and Namibia to the south (Fig. 2A). Currently, Angola occupies only four percent of the terrestrial area out of the entirety of Africa, yet it possesses the highest number of biomes of any African country - seven out of the nine present on the continent (Huntley, 2019). The arid Namibe region is home to abundant fossiliferous outcrops, and even the sole habitat of *Welwitschia mirabilis* Hooker 1859, commonly referred to by the local people as a 'living fossil' plant of the desert. Yet, despite having significant natural wealth, Angola remains one of the least well-documented countries in the world in terms of its biodiversity (Lourenço, 2019) – present or past.

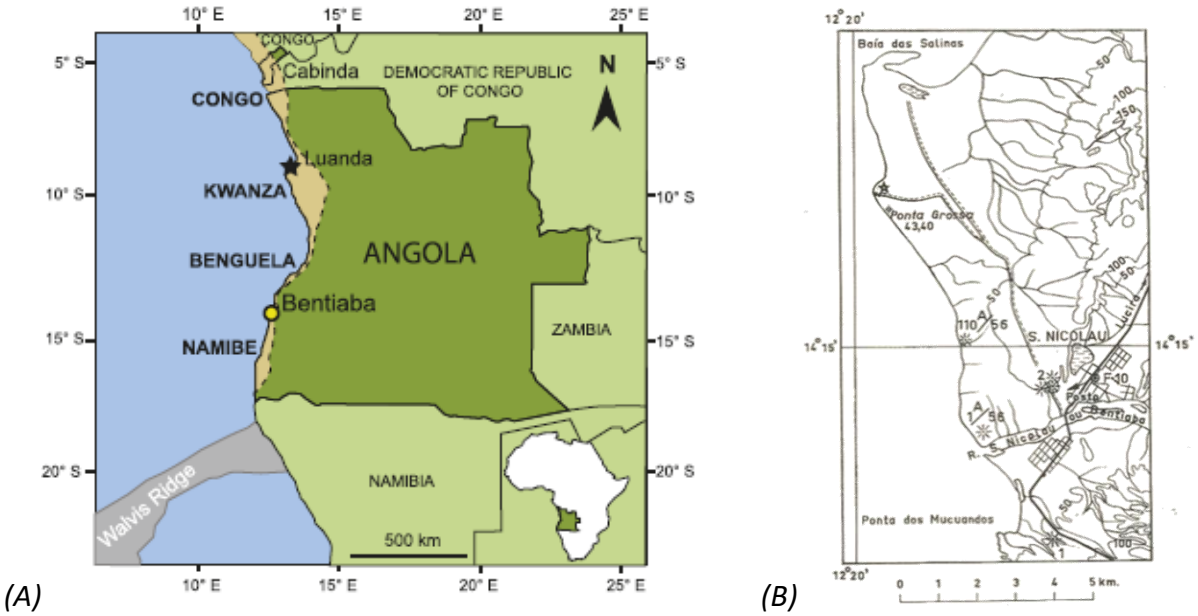

Figure 2. A. Location of Bentiaba, taken from Strganac et al. (2015), and B. region of Bentiaba (formerly known as S. Nicolau) of the Moçâmedes Basin, taken from Antunes (1964).

Information about the paleobiodiversity of Angola is drawn from over 1300 fossil taxa, largely from fossil-bearing marine Cretaceous and Cenozoic outcrops (Fig. 3), which are the most readily abundant (Mateus et al., 2019). Angola has substantial paleogeographic significance in the geologic record, mainly for forming and preserving the eastern continental border of the south Atlantic Ocean during the splitting of the continents during the Cretaceous Period, beginning at about 134 Ma (Jacobs et al., 2006). The Cretaceous is also of particular geological importance to Gondwana as a whole, because Africa was still linked to South America and Euramerica at the beginning of this time period, but nearing the end of the epoch, land connections were becoming severed (Jacobs et al. 2016). As Gondwana then drifted apart and the south Atlantic Ocean opened, many marine species began colonizing the area from the southern waters, with a first known marine animal occurrence beginning at about 88 Ma (Mateus et al., 2019). By the Upper Maastrichtian, Angola's present-day coastline was formed, and Africa essentially had become isolated from other continental landmasses, meaning that inhabitant species could begin to further endemically specialize, creating a unique paleobiology (Sampson et al., 1998; Benton et al., 2000).

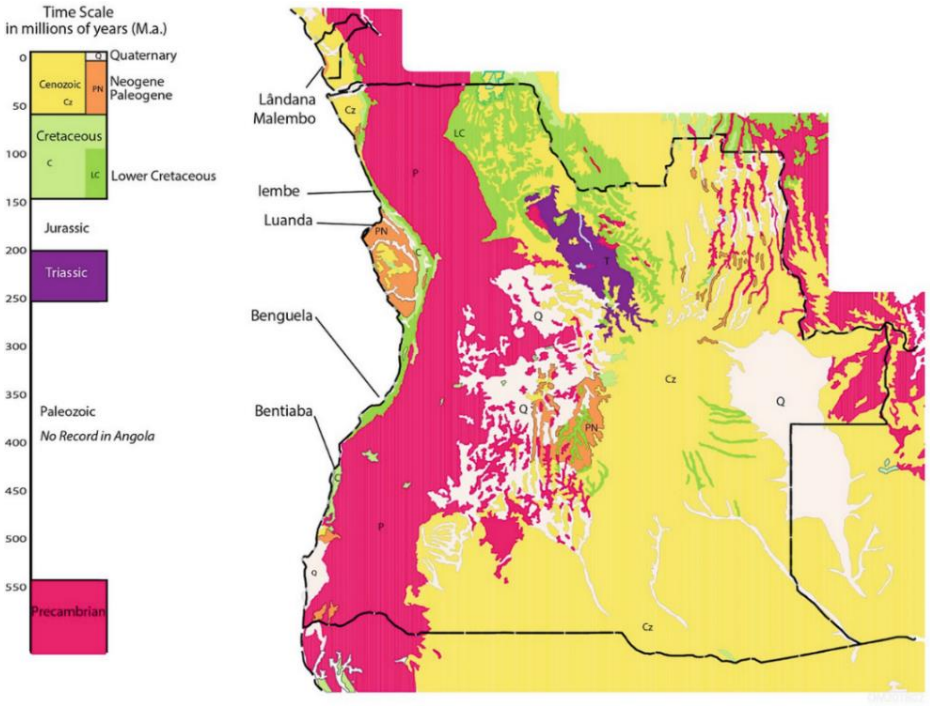

Figure 3. Geological map of Angola, scale: 1:30.000.000
(U.S. Geological Survey, 2002) taken from Mateus et al. 2019.

Presently, the Cretaceous outcrops of Angola are found along the coast, with the presence of inland basins as well (Mateus et al., 2019). The fossiliferous coastline outcrops of the Namibe region are mainly composed of marine sandstones, the component sediments of which were deposited prior to oceanic rifting and can be up to 200 m thick (Jacobs et al., 2006). These sandstones sit atop a basalt layer, which appeared after rifting at about 84.6 Ma and is part of the Ombe Formation. Above the Ombe Formation are the Baba Formation, and the Mocuio Formation (encompassing the Bentiaba locality), which were created as a result of oceanic shelf infill. Further inland, the outcrops change

from shallow marine facies to terrestrial facies until a metamorphic crystalline basement is reached (Strganac et al., 2014). The locality of Bentiaba is located in the southwest of the country (Fig. 2) on the coastline of the Namibe Desert and contains a vast marine fossil assemblage, which represents a remarkably-preserved diversity of life.

Based on vertebrate and invertebrate faunas (Antunes, 1965), as well as carbon isotope analysis, and magnetostratigraphy and $^{40}Ar/^{39}Ar$ dates for the section at Bentiaba (Strganac et al., 2014), the age of this locality is found be early Maastrichtian, at approximately 71.64–71.40 Ma.

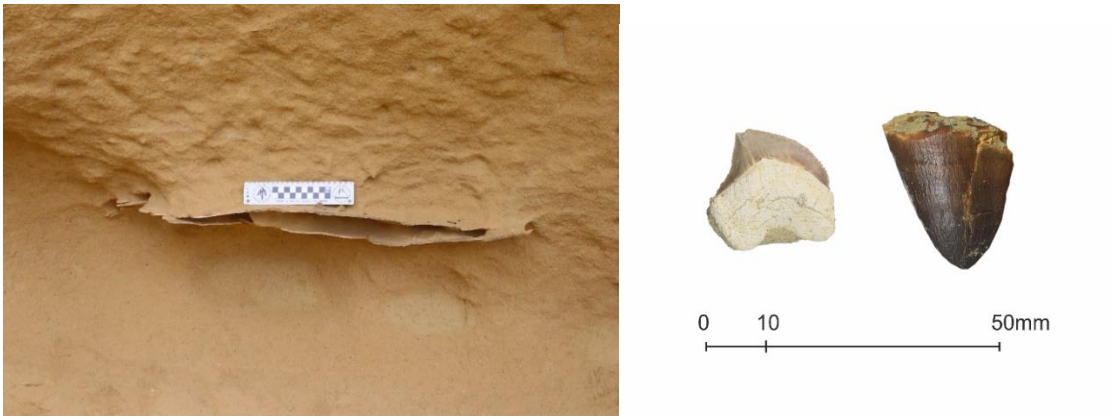

Figure 4. Some examples of Bentiaba invertebrate and vertebrate fauna: cf. Inoceramus *in situ (scale: 190 mm) at Bench 19 (left) and MGUAN-PA* Squalicorax *shark and mosasaur teeth recovered in pterosaur field jackets during preparation (right).*

The invertebrate fauna of the overall region includes mollusks (representing about 61% of taxa, over half of which are Cretaceous ammonites), including *Trigonoarca angolensis* Rennie 1929, bivalves such as cf. *Inoceramus* (Fig. 4), ammonites such as *Baculites* aff. *asper*, and even nautiloids such as *Eutrephoceras indicum* d'Orbigny 1850 (Antunes, 1964; Mateus et al., 2019). Cretaceous foraminifera make up about 16% of fossil faunal diversity, and vertebrates represent about 15% of taxa (Mateus et al., 2019).

There are an abundance of scattered fossiliferous vertebrate remains throughout the sediments of Bentiaba itself, including fossil assemblages composed mainly of fishes such as *Enchodus* sp., marine reptiles such as the mosasaurs *Globidens phosphaticus* Bardet et al. 2005 and *Prognathodon kianda* Schulp et al. 2008, elasmosaurid plesiosaurs (Araujo et al., 2015), sharks such as *Anacorax pristodontus* Antunes 1964 and *Squalicorax pristodontus* Agassiz 1843, turtles such as *Angolachelys mbaxi* Mateus et al. 2009, and pterosaurs (Polcyn et al., 2010; Jacobs et al., 2009; Mateus et al., 2009; Schulp et al., 2008; Schulp et al., 2006; Jacobs et al., 2006).

The pterosaur specimens discussed herein were collected from within a 0.15 km² area (Fig. 5), and within the same stratigraphic level, and thus, despite not being found in association, possibly represent the same taxon. Three articulated sets of pterosaur remains were discovered, as well as several other isolated individual bones. MGUAN-PA650 and MGUAN-PA651 consist of two articulated bones from one individual: a left humerus distal fragment articulated with a complete left ulna. MGUAN-PA654 and MGUAN-PA655 consist of two articulated bones from another individual: a right metacarpal IV distal fragment articulated with a right digit IV first phalanx proximal

fragment. MGUAN-PA661 and MGUAN-PA662 consist of two articulated bones from another individual: a left ulna articulated with a left radius. All other bones were found in isolation.

Figure 5. Map of Angolan localities where pterosaur material was recovered (Google Earth, 2020).

The lithology of Bentiaba is characterized by fine-grained pinkish-white to reddish-yellow sandstones capped every so often by slightly coarser-grained compacted sandstone layers, which erode into bench-like horizontal protuberances (Fig. 6). These layers occur with some regularity throughout the stratigraphy, and so were ascribed numbers in previous expeditions, beginning with the number one pertaining to the most basal bench at the bottom of the formation, and all the way through “Bench 19”, which is the top-most of the compacted layers. Thus far, pterosaur material has only been preserved and recovered from the finer-grained layer above Bench 19, which is abundantly fossiliferous (Fig. 6). In fact, most vertebrate specimens recovered by the PaleoAngola Project thus far are found concentrated in a 1–2 m thick zone directly overlying Bench 19 (Strganac et al., 2014). This upper section is capped by about 10 m of fine-grained sandstone, the base of which is characterized by pale yellow to white fine-grain and weakly-cemented sediments, which then change to a darker slightly coarser yellow silty sand within the first few meters, in which most of the the pterosaur material was found.

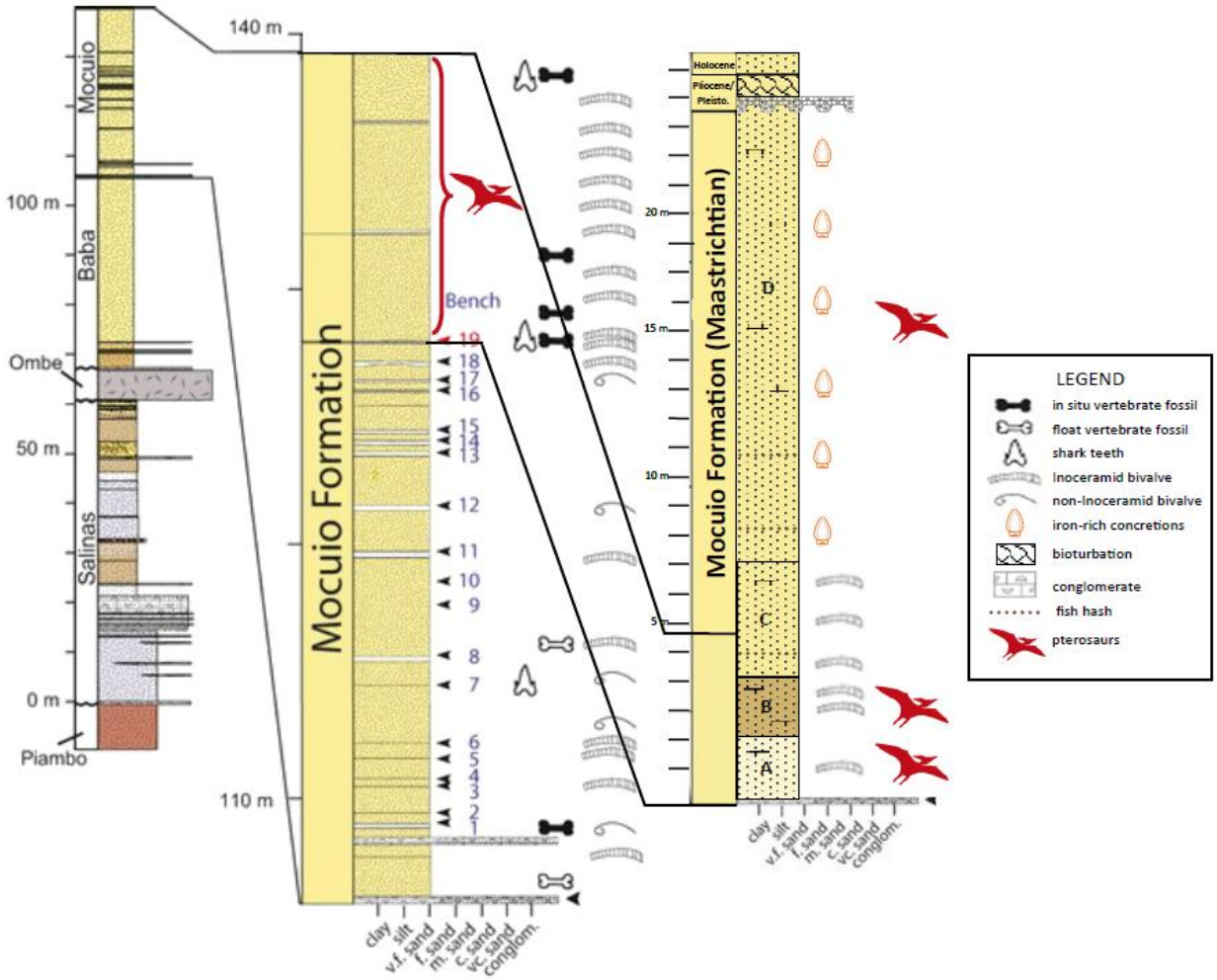

Figure 6. Stratigraphic Section of Bentiaba, with section yielding pterosaur fossils demarcated in red (modified from Strganac et al., 2014).

Based on the paleogeography of the Bentiaba coastline, the locality containing the Bench 19 layer was previously a narrow, shallow marine shelf near the shoreline, at approximately 24°S paleolatitude in waters between 50 and 100 m in depth and 18°C paleotemperature based on δ18O from bivalve shells (Jacobs et al., 2016). Based on the found fossil assemblage, this was a highly-productive marine environment characterized by relatively low sedimentation rates compared to bone input (Strganac et al., 2014). The manner in which the fossils are interspersed throughout the layer implies general taphonomic scattering over the sea floor, because there is very little erosion or signs of transport on the bone surfaces and the bones are in fairly pristine condition (Strganac et al., 2014). Disarticulation of skeletons may have been due to scavenging, as is evidenced by the visible bite marks and scratches that are found on certain bones (Strganac et al., 2014), a premise which is potentially supported by the abundant shark and other predatory teeth (Fig. 4) that have been recovered from the locality.

RESULTS

Systematic Paleontology

For taxon MGUAN-PA650 & MGUAN-PA651, the following taxonomic attribution was given:
PTEROSAURIA Owen, 1842
PTERODACTYLOIDEA Plieninger, 1901 sensu Padian 2004
PTERANODONTIA Marsh, 1887
NYCTOSAURIDAE Nicholson and Lyddekker 1889, gen. et sp. nov.

For all of the remaining Angola specimens, the following taxonomic attribution was given:
PTEROSAURIA Owen, 1842
PTERODACTYLOIDEA Plieninger, 1901 sensu Padian 2004
PTERANODONTIA Marsh, 1887

Description

The total number of pterosaur specimens collected consists of 11 individuals including 14 elements, all collected in the same stratigraphic layer (Table 1). The hollowness of these particular bones indicated that they are representative of either a member of the Theropoda (including Aves) or Pterosauria (Gauthier, 1986; Sereno et al., 1993; Novas, 1993). Following the typical criteria for Pterosauria (Currey and Alexander, 1985), all of the Angola specimens have very thin cortical bone, varying in thickness between 0.3 to 1.6 mm. All of the fossils preserve their three-dimensionality with no great apparent taphonomic distortion, although cortical bone surfaces are superficially fractured overall on all of the specimens, likely due to lithostatic pressure. The bones are a light pinkish-white in color with a more reddish-yellow sedimentary infilling, matching their surrounding matrix, which also yielded many fragmentary remains of various fishes, as well as the teeth of sharks and mosasaurs (Fig. 4). All of the following descriptions of wing limb elements are oriented as in flight, and leg elements are oriented as in standing position.

Table 1. Bentiaba Pterosaur elements (bones of the same individuals are demarcated using superscripts)

Specimen Number	Material	Taxonomic Identification
MGUAN-PA163	Left Femur	*Pteranodontia*
MGUAN-PA650	Left Humerus fragment[1] (proximal)	*Nyctosauridae, gen. et sp. nov.*
MGUAN-PA651	Left Ulna[1]	*Nyctosauridae, gen. et sp. nov.*
MGUAN-PA652	Left Manual Digit IV Phalanx 2 fragment (proximal)	*Pteranodontia*
MGUAN-PA653	Left Ulna fragment (distal)	*Pteranodontia*
MGUAN-PA654	Right Metacarpal IV fragment[2] (distal)	*Pteranodontia*
MGUAN-PA655	Right Manual Digit IV Phalanx 1 fragment[2] (proximal)	*Pteranodontia*
MGUAN-PA656	Manual Digit IV Phalanx 2 fragment (distal)	*Pteranodontia*
MGUAN-PA657	Right Metacarpal IV fragment (proximal)	*Pteranodontia*
MGUAN-PA658	Wing fragment	*Pteranodontia*
MGUAN-PA659	Right Manual Digit IV phalanx 1	*Pteranodontia*
MGUAN-PA660	Right Metacarpal IV fragment (proximal)	*Pteranodontia*
MGUAN-PA661	Left Ulna[3]	*Pteranodontia*
MGUAN-PA662	Left Radius[3]	*Pteranodontia*

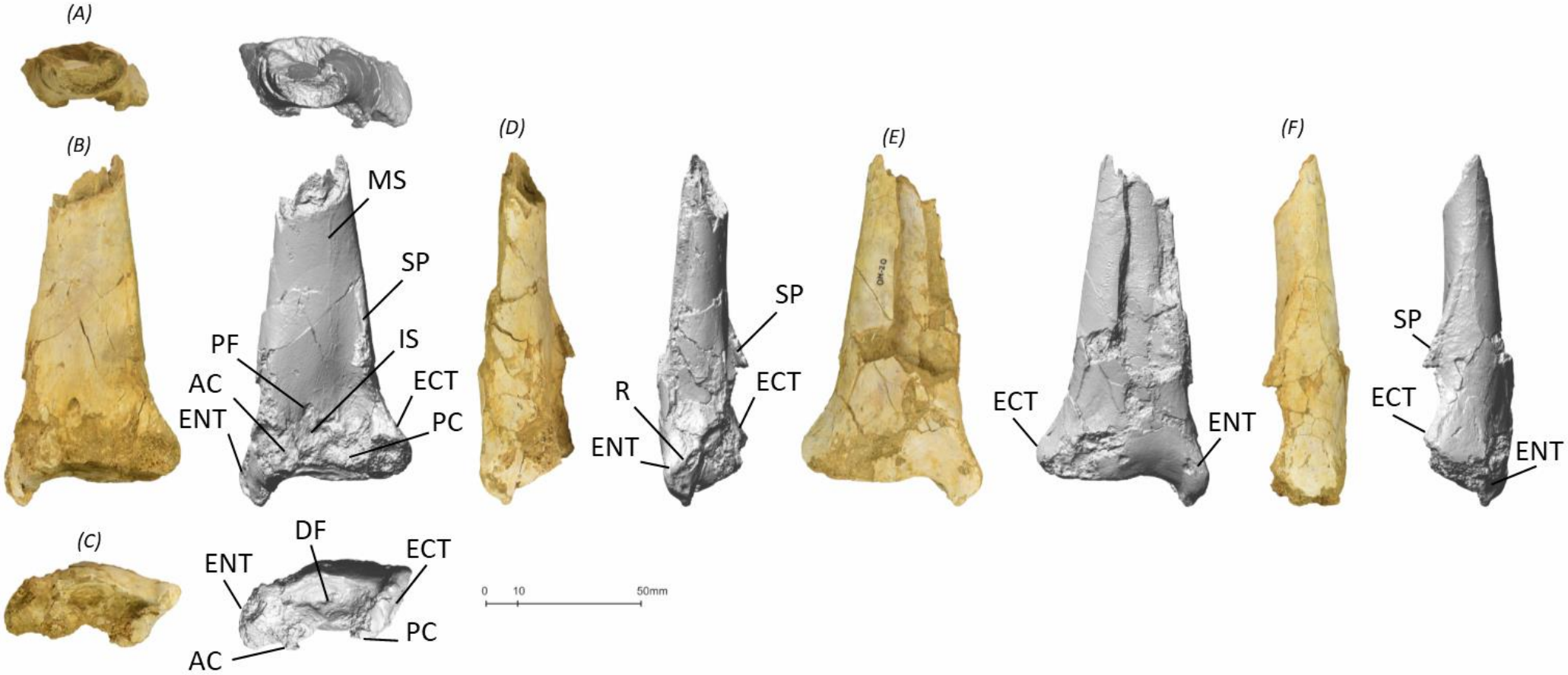

Figure 7. MGUAN-PA650 left humerus fragment photographs and surface scans in (A) proximal (B) ventral (C) distal (D) posterior (E) dorsal (F) anterior views
Abbreviations: AC, anterior condyle; DF, distal fossa; ECT, ectepicondyle; ENT, entepicondyle; IS, intercondylar sulcus; MS, muscle scar;
PC, posterior condyle; PF, pneumatic foramen; R, ridge; SP, supracondylar process.

Humerus MGUAN-PA650

MGUAN-PA650 (Fig. 7) is a left humerus fragment, comprised of a partial shaft through the distal end, which was found in situ articulated with the ulna fragment MGUAN-PA651. The bone surface is superficially fractured overall and is crushed inward for a section of the shaft on the dorsal surface, although it retains its original three-dimensional shape at its distal-most end. The anterior and posterior condyles are damaged, missing parts of the ventral areas.

Anteroposteriorly, the bone is relatively planar. Dorsoventrally, the shaft expands gradually toward the distal edge of the condylar area. The shaft is elliptical in cross-section. Overall, the proximodistal length of the fragment measures 108.3 mm in length, putting the estimated overall length of the humerus at about 212 mm (estimation methodology discussed further on in the text). Anteroposteriorly, the humerus is 57.6 mm at the widest part of its distal end and 24.9 mm minimum mid-width at the narrowest part of the shaft, making the distal end well over twice the width of the thinnest part of the extant shaft. The dorsoventral mid-depth measures 15.7 mm at the narrowest end of the shaft and measures 24.3 mm at the distal-most end. The cortical bone ranges from about 0.5 mm to 1.4 mm in thickness. The supracondylar process is a thin prominent crest running along the anteroventral edge of the shaft, beginning approximately 64.5 mm from the distal-most end of the ectepicondyle, reaching its apex at 36.9 mm from the end, and diminishing gradually toward the ectepicondyle. Posteriorly bordering the supracondylar process and proximal to the lateral condyle, lies the shallow triangular fossa. The shaft of the humerus bears a slightly-raised, thin, and longitudinal scar proximodistally along its ventral margin closer to its anterior edge that is likely the origin of the brachialis muscle (Bennett, 2003).

The entepicondyle is 18.6 mm in anteroposterior length and in 10.6 mm in dorsoventral width and is elongated. The ectepicondyle, which is 14.4 mm in anteroposterior length and in 16.3 mm in dorsoventral width, is rounded in horizontal outline. The entepicondyle expands prominently posterodistally from the anterior condyle, which is not very well developed and somewhat eroded. The dorsal surface of the entepicondyle bulges to form a posterodorsal ridge, sloping anterodistally into a tapered point on the distal surface. In contrast, the ectepicondyle only projects anteriorly and slightly ventrally from the posterior condyle. On the ventral surface, a 4.9 mm long by 2.7 mm wide elliptical pneumatic foramen is clearly visible proximal to the anterior and posterior condyles at the end of the intercondylar sulcus, slightly closer to the anterior condyle. The proximal margin of the foramen is deeper and well-defined, but the margin diminishes as the foramen becomes shallower distally. Rugosities are visible on the posterior surface of the shaft proximal to the entepicondyle that are likely the origin for the carpus and digit extensors (Bennett, 2003), as well as on the anterior surface of the shaft proximal to the ectepicondyle that are likely the origin for the lateral head of the triceps (Bennett, 2003).

Distally, the entepicondyle forms a posterodorsally-elongated projection, which is distally flattened on the ventral-most surface and comes to a point dorsally. In contrast, the ectepicondyle forms a broad subtriangular surface, flattened distally. Between the condyles lies an anteroposteriorly-oriented figure eight-shaped distal fossa. The distal fossa is positioned posteriorly and halved by a shallow prominence. The ventral margin of the fossa is partially eroded, but seems to assume a concave shape. The dorsal margin of the fossa is sinusoidal, the anterior region more concave and posteriorly more convex. The surface of the distal fossa is dotted with small circular pits, some more

elongated than others. A larger ovoid pit on the dorsal wall of the posterior end of the fossa could potentially be a pneumatic foramen.

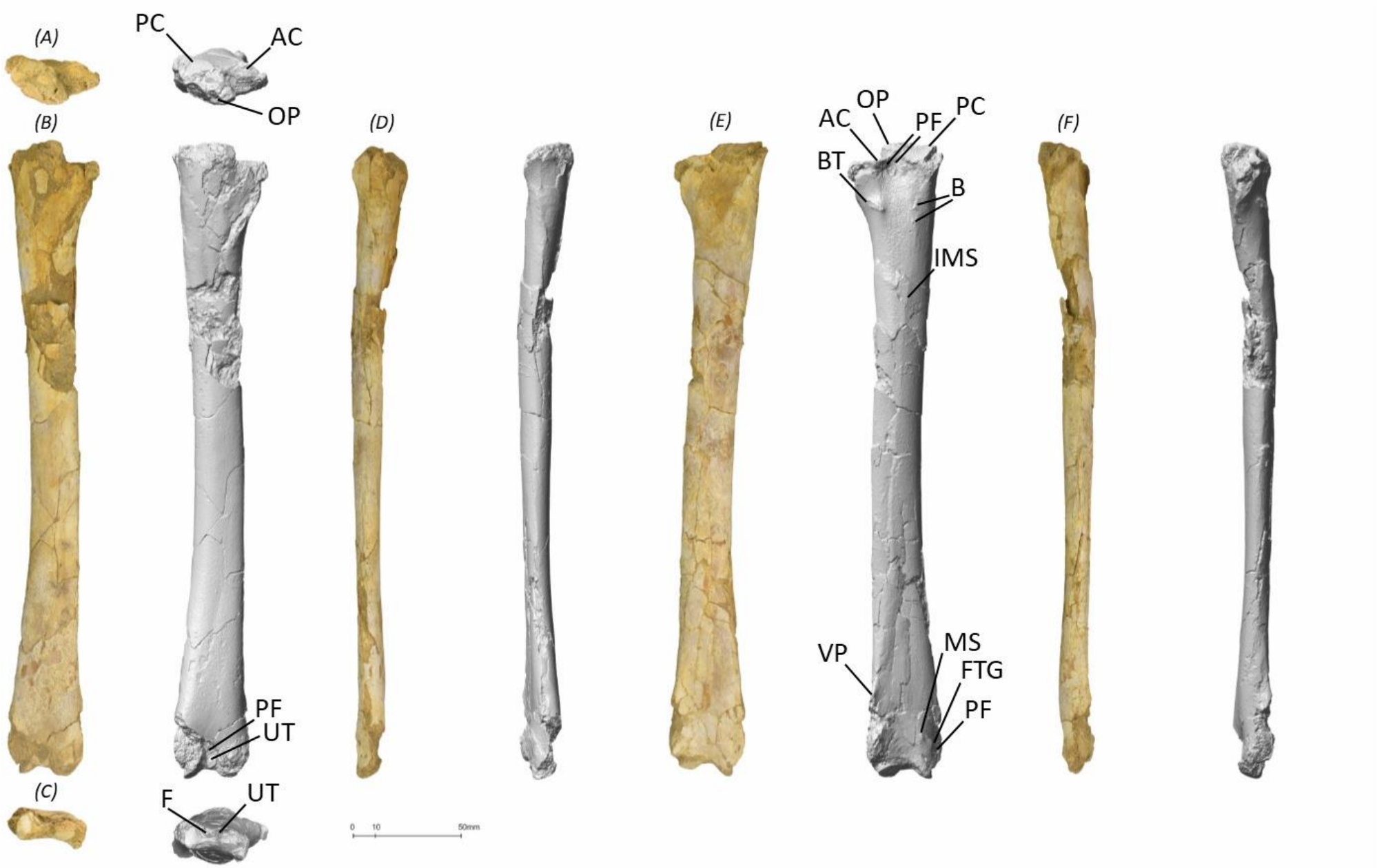

Figure 8. MGUAN-PA651 left ulna in (A) proximal (B) dorsal (C) distal (D) anterior (E) ventral (F) posterior views
Abbreviations: AC, anterior cotyle; B, bumps; BT, biceps tubercle; F, fovea; FTG, flexor tendon groove; MS, muscle scar; OP, olecranon process; PC, posterior cotyle; PF, pneumatic foramen; UT, ulnar tubercle;

Ulna MGUAN-PA651

MGUAN-PA651 (Fig. 8) is a left ulna, which was found articulated in situ with humerus fragment MGUAN-PA650. The entire bone surface is superficially fractured overall. It is very nearly complete, save for a few sections missing cortical bones along the olecranon process, the dorsal side of the proximal shaft, as well as on both the dorsal-to-dorsoanterior and posterior distal terminal expansions, which are partially eroded. Sediment infill in those missing regions helps retain the bone's overall three-dimensionality, which is otherwise preserved.

Overall, the ulna is elongate and straight. In horizontal outline, the proximal and distal ends of the ulna expand very slightly outward from the shaft. The ulna measures 290.1 mm in total length, and in anteroposterior width measures 44.1 mm at the widest point of the proximal end, 22.4 mm at the midpoint of the shaft, and 35.3 mm at the at the widest point of the distal end. The cortical bone ranges from about 0.5 mm to 1.6 mm in thickness. In the transverse plane, the shaft is dorsoventrally-flattened and elliptical in cross-section. Dorsoventrally, the height of the shaft measures 11.8 mm at its narrowest point, 18.2 mm at the broadest proximal end, and 14.1 mm at the broadest part of the distal end. The shaft's ventral surface exhibits a faintly raised longitudinal ridge, likely the interosseus membrane scar (Avarianov, 2010), which begins somewhat anteriorly at the proximal end and then extends parallel to the center of the shaft for almost the proximal half of the ulna. Near the proximal end of the ulna, two elliptical foramina are evident on the shaft's ventral surface, just distal to where the anterior and posterior cotyles meet. The larger foramen measures 4.9 mm in proximodistal length and 2.8 mm in anteroposterior width, and lies anterior to the smaller one, which measures 1.8 mm in length and 1.2 mm in width. The biceps tubercle is posteriorly offset, just distal to the posterior cotyle, and is a slightly anterodistally-elongated rugose protuberance 9.7 mm in length. Posterior to the biceps tubercle and distal to the posterior cotyle, lie two significantly smaller bumps, perhaps the anchor for the radioulnar ligament (Bennet, 2001a). The more proximal bump distally borders a small rugose area on the shaft surface. The dorsal surface of the ulnar shaft is relatively featureless.

In horizontal outline, the proximal articular area of the ulna is asymmetrical. The posterior expansion is oriented posteriorly and slightly ventrally away from the shaft and capped by the posterior cotyle, whereas the anterior side, apart from a slight ventral curvature, exhibits hardly any expansion. The proximal end of the ulna is kidney-shaped in cross-section with the concavity on the ventral side, while the shaft is elliptical in cross-section. The olecranon process is slightly eroded. A small intercotylar crest subdivides the articular surfaces. The anterior cotyle is saddle-shaped (concave anteroposteriorly and convex dorsoventrally) with an overall gentle ventrodistal tilt. The posterior cotyle is more proximally placed than the anterior cotyle, forming a step between both articular surfaces. The posterior cotyle is anteroposteriorly concave.

On the distal end of the ulna, starting about 44.8 mm from the distal-most edge, the beginning of the posterior expansion is preserved as a slight ridge, although the majority of the distal portion has been eroded. In ventral view, on the anterior side of the shaft, lies the flexor tendon groove, with an apparent foramen located on its distal end. On the posterior margin of the groove is a rugose ridge, which exhibits as a raised tubercle with a muscle scar. On the dorsal surface, a large pneumatic foramen measuring 9.34 mm in length and 3.64 mm in width lies between and proximal to the distal articular facets.

On the distal surface, the three distinct articular surfaces for the proximal syncarpal lie side-by-side in a figure eight-shaped configuration, with the fovea in between. Both surfaces are partially eroded to the point where trabecular bone is visible. What remains of the rounded anterior articular surface is dorsoventrally-projected from the center, and oriented proximodorsally. The distal tuberculum lies posterior to the anterior articular surface, is projected anteroposteriorly from the center point of the distal end of the ulna, and inclined proximoventrally.

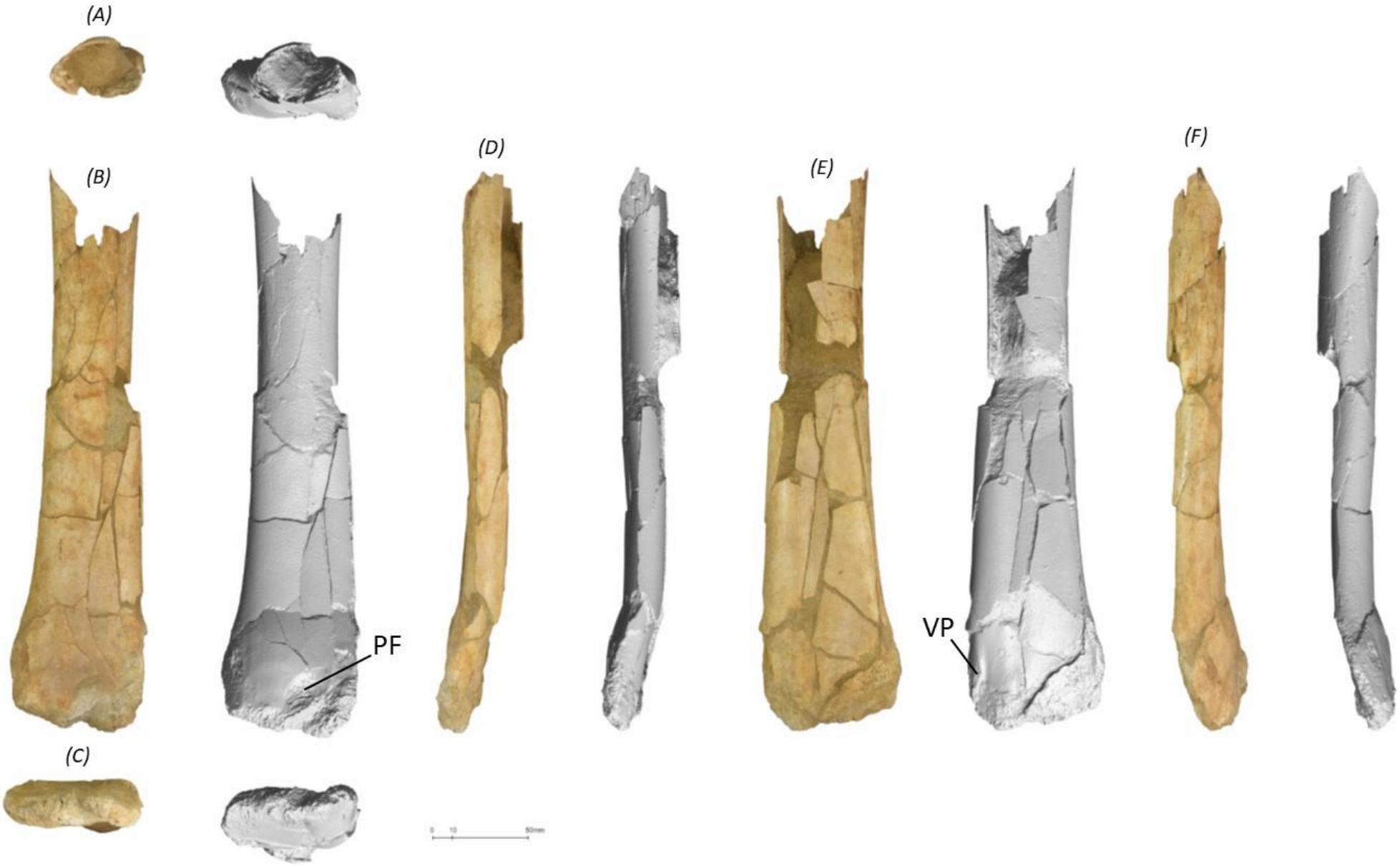

Figure 9. MGUAN-PA653 left ulna fragment in (A) proximal (B) dorsal (C) distal (D) anterior (E) ventral (F) posterior views
Abbreviations: PF, pneumatic foramen; VP, ventral process

ULNA MGUAN-PA653

MGUAN-PA653 (Fig. 9) is a distal left ulna fragment that is missing the proximal end, as well as the distal-most articular portion, which seems to have been eroded away. The entire bone surface is superficially fractured overall with sections of cortical bone missing on the dorsal, ventral, and posterior sides, making features difficult to discern. The entire specimen measures 185.8 mm in proximodistal length by 70.2 mm in anteroposterior width at the widest proximal point by 48.6 mm in anteroposterior width at the narrowest complete distal point, and in cross-section it measures roughly 20.6 mm dorsoventrally throughout. Overall, it is slightly crushed dorsoventrally, but this does not greatly affect its three-dimensionality. The cortical bone ranges from about 0.6 mm to 1.6 mm in thickness.

In horizontal outline, the shaft expands gradually as it approaches the distal end. The shaft is straight in the transverse plane, although the distal end of the fragment has been dorsally offset slightly due to taphonomy. The shaft is elliptical in cross-section. In dorsal view, part of a possible large foramen is visible and slightly posteriorly-positioned on the distal-most end of the fragment. The cortical bone surrounding the preserved margins of this foramen are slightly sloped inward. In ventral view, the shaft exhibits the beginning of an anteroposteriorly-extending raised ridge on the posterodistal corner, possibly the beginning of the posterior expansion, with a shallow groove running anteriorly alongside it.

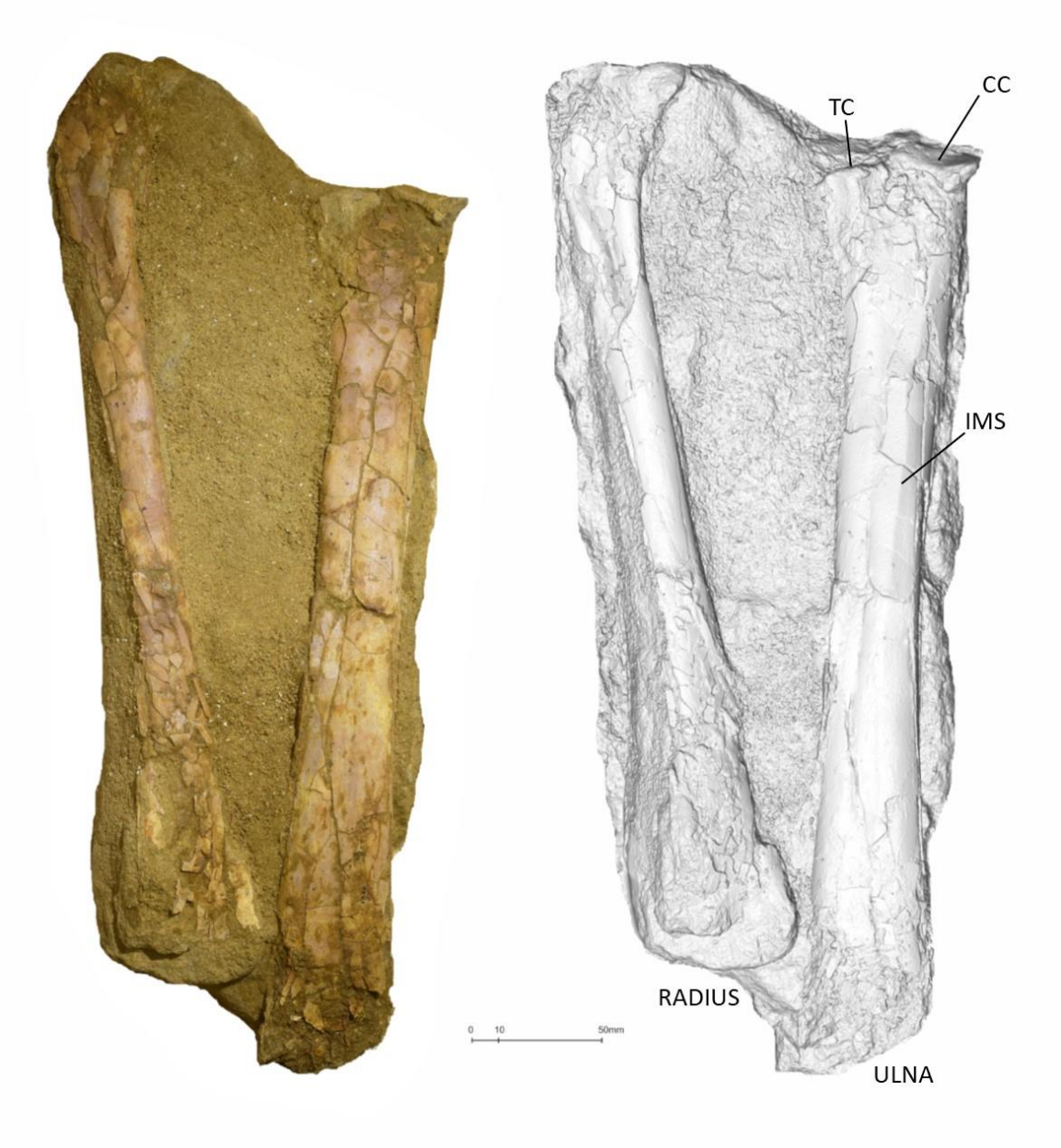

Figure 10. MGUAN-PA661 left ulna and MGUAN-PA662 left radius in ventral view
Abbreviations: TC, trochlear cotyle; CC, capitular cotyle; IMS, interosseous membrane scar

ULNA MGUAN-PA661 and RADIUS MGUAN-PA662

MGUAN-PA661 (Fig. 10) is a nearly complete left ulna, which was found in articulation with radius MGUAN-PA662. The ulna measures 341.0 mm in proximodistal length by 62.3 mm in anteroposterior width at the widest part of the proximal end, 34.3 mm at the midpoint of the shaft, and 53.3 mm in anteroposterior width at the distal end. It is 9.3 mm in dorsoventral height at the broken distal end of the shaft, and 19.7 mm in dorsoventral height at the widest past of the proximal articular end. The bone ranges from about 0.5 mm to 1.0 mm in cortical thickness. It is fairly well-preserved, with an overall intact three-dimensional shape. The cortical bone surface is cracked throughout, although it has no real overall loss of bone surface except for a few areas near the distal end, which is

significantly eroded, making features difficult to discern. There appears to be low overall taphonomic distortion. In distal view, the shaft is elliptical in cross-section, flattened dorsoventrally. Only the proximal, ventral, and distal surfaces of the preserved bone have been prepared out of the surrounding matrix for purposes of stabilization. Overall, the ulna is elongate and straight, and the shaft exhibits a faintly raised longitudinal ridge, likely the interosseus membrane scar, which appears to run parallel to and posteriorly-offset from the long axis of the shaft for as long as it can be distinguished on the damaged bone surface.

In ventral view, the shaft expands slightly anteroposteriorly from the center of the shaft as it approaches both articular ends. At the proximal end, the capitular cotyle manifests as a concave crescentic articular facet, spanning just over half of the anteroposterior width of the ulna from the anterior-most point of the shaft to just past the central region of the shaft, and is angled at a slight ventrodistal tilt. The trochlear cotyle occupies the rest of the proximal surface of the ulna and is slightly anteroposteriorly concave.

MGUAN-PA662 is a nearly complete left radius, which was found in articulation with ulna MGUAN-PA661. The shaft appears to have been relatively straight and elliptical in cross-section. The shaft expands anteroposteriorly as it approaches both articular ends. It measures 332.0 mm in proximodistal length and 52.1 mm in anteroposterior width at the distal end of the preserved shaft, 19.1 mm in anteroposterior width at the midpoint of the shaft, and 30.4 mm in anteroposterior width at the proximal end. It measures 14.8 mm in dorsoventral height at the distal end of the shaft, and 7.1 mm in dorsoventral height at proximal end. The cortical bone ranges from about 0.4 mm to 1.0 mm in thickness. Although it maintains its three-dimensional shape, it is highly eroded in areas, particularly around the proximal and the distal articular surfaces, making it difficult to distinguish any specific features. The bone surface is heavily fractured throughout, and an area near the proximal end of the shaft has been crushed inward. There is minimal taphonomic distortion. Only the proximal, ventral, and distal sides are freed from the surrounding matrix for purposes of stabilization.

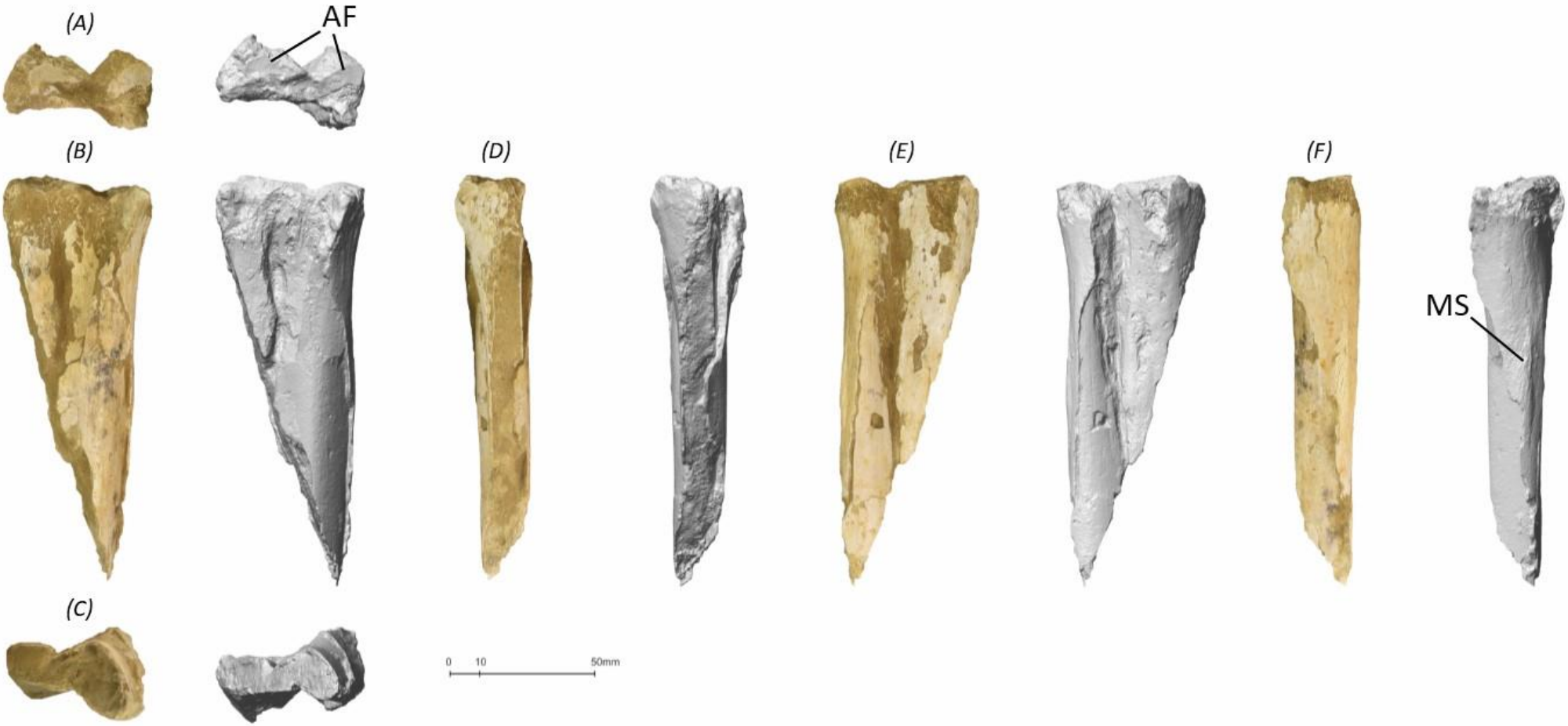

Figure 11. MGUAN-PA660 right metacarpal IV fragment in (A) proximal (B) ventral (C) distal (D) anterior (E) dorsal (F) posterior views
Abbreviations: AF, articular facet; MS, muscle scar

METACARPAL IV MGUAN-PA660

MGUAN-PA660 (Fig. 11) is a proximal right end fragment of an extensively damaged left metacarpal IV. Although it remains three-dimensional, fracturing of the cortical bone overall has meant that some sections of bone have buckled inward on the dorsal and ventral bone surfaces, particularly at the center of the shaft, which gives it an overall figure eight-shaped cross-section in proximal view. Sections of cortical bone have also been altogether eroded from many sections on the dorsal and ventral surfaces. Almost the entire anterior side of the fragment has been sheared off in a posterodistal angle, due to this side corresponding to the exposed portion of the bone when found in situ. The proximal end of the fragment remains complete, although extensive weathering has exposed the trabecular bone on the ventral, posterior, and dorsal sides. The fragment measures 145.2 mm in preserved proximodistal length, and 49.2 mm in dorsoventral width at the proximal-most end. It measures 27.7 mm anteroposteriorly at its widest point and 16.6 mm anteroposteriorly at its narrowest complete point. The cortical bone ranges from about 0.4 mm to 1.1 mm in thickness.

On the posterior surface of the bone, rugose muscle scarring is evident close to the ventral margin, likely the area for attachment of the extensor carpi ulnaris. At least one miniscule foramen is evident on the ventral surface, slightly offset from the center of the shaft. However, determination of the number of foramina present is made difficult by many marks and holes pitting the bone surface, which could be from erosion. Additionally, the bone surface is distinctly scratched in certain areas, which could be related to post-mortem scavenging.

In proximal view, two distinct articular facets are visible, although notably eroded, the dorsal and ventral articular surfaces for the distal syncarpal. The preserved portion of the dorsal articular surface is heavily damaged, but likely subcircular in outline. The preserved portion of the ventral articular surface is larger than the posterior, and although more difficult to distinguish, a definite planar surface is visible extending dorsoventrally.

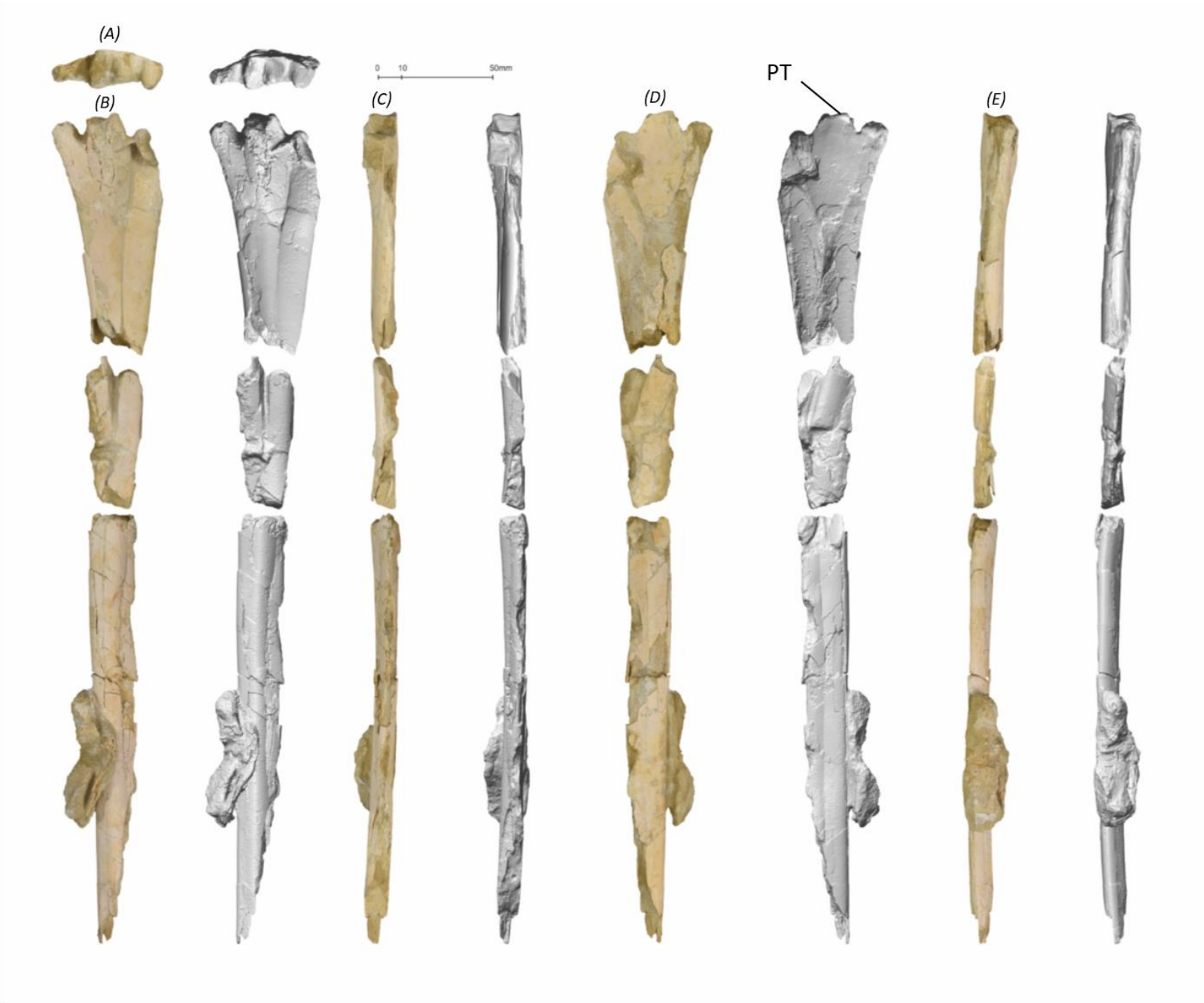

Figure 12. MGUAN-PA657 right metacarpal IV fragment in (A) proximal (B) dorsal (C) anterior (D) ventral (E) posterior views
Abbreviations: PT, proximal tuburculum

METACARPAL IV MGUAN-PA657

MGUAN-PA657 (Fig. 12) is a right proximal metacarpal IV fragment, which is broken into three pieces with minimal sections of bone missing from between each, as can be inferred from the overall dimensions of the shaft as the articular end is approached. It is missing the distal articular end. Overall, the shaft is well-preserved and has almost no taphonomic distortion. A few areas have surface bone loss, but the element is virtually uncrushed with an intact three-dimensional shape. The shaft is proximodistally straight, flattened dorsoventrally, subrectangular in cross-section at the proximal-most end. It approaches a more sub-triangular cross-section at the distal-most end, which is so eroded as to just diminish into an interior sediment mold. There is overall fracturing of the cortical bone surface, with some segments missing entirely from the dorsal, ventral, and posterior surfaces. In horizontal outline, the shaft expands anteroposteriorly as it approaches the proximal end. The cortical bone ranges from about 0.7 mm to 1.5 mm in thickness. On the ventral surface of the metacarpal, centered on the proximal-most edge of the bone, the proximal tuburculum is just visible, extending proximoventrally away from the bone shaft.

The proximal fragment measures 100.6 mm in proximodistal length, 41.2 mm in anteroposterior width at the proximal-most complete end and 25.4 mm in anteroposterior width at the distal-most complete end. The center fragment measures 62.5 mm in proximodistal length, 24.1 mm in anteroposterior width at the proximal-most complete end and 17.1 mm in anteroposterior width at the distal-most complete end. The distal fragment measures 179 mm in proximodistal length, 20.1 mm in anteroposterior width at the proximal-most complete end and 17.1 mm in anteroposterior width at the distal-most complete end.

The proximal fragment measures 15.1 mm in dorsoventral height at the proximal-most complete end and 12.1 mm in dorsoventral height at the distal-most complete end. The center fragment measures 8.3 mm in dorsoventral height at the proximal-most complete end and 9.1 mm in dorsoventral height at the distal-most complete end. The distal fragment measures 11.2 mm in dorsoventral height at the proximal-most complete end and 9.6 mm in dorsoventral height at the distal-most complete end.

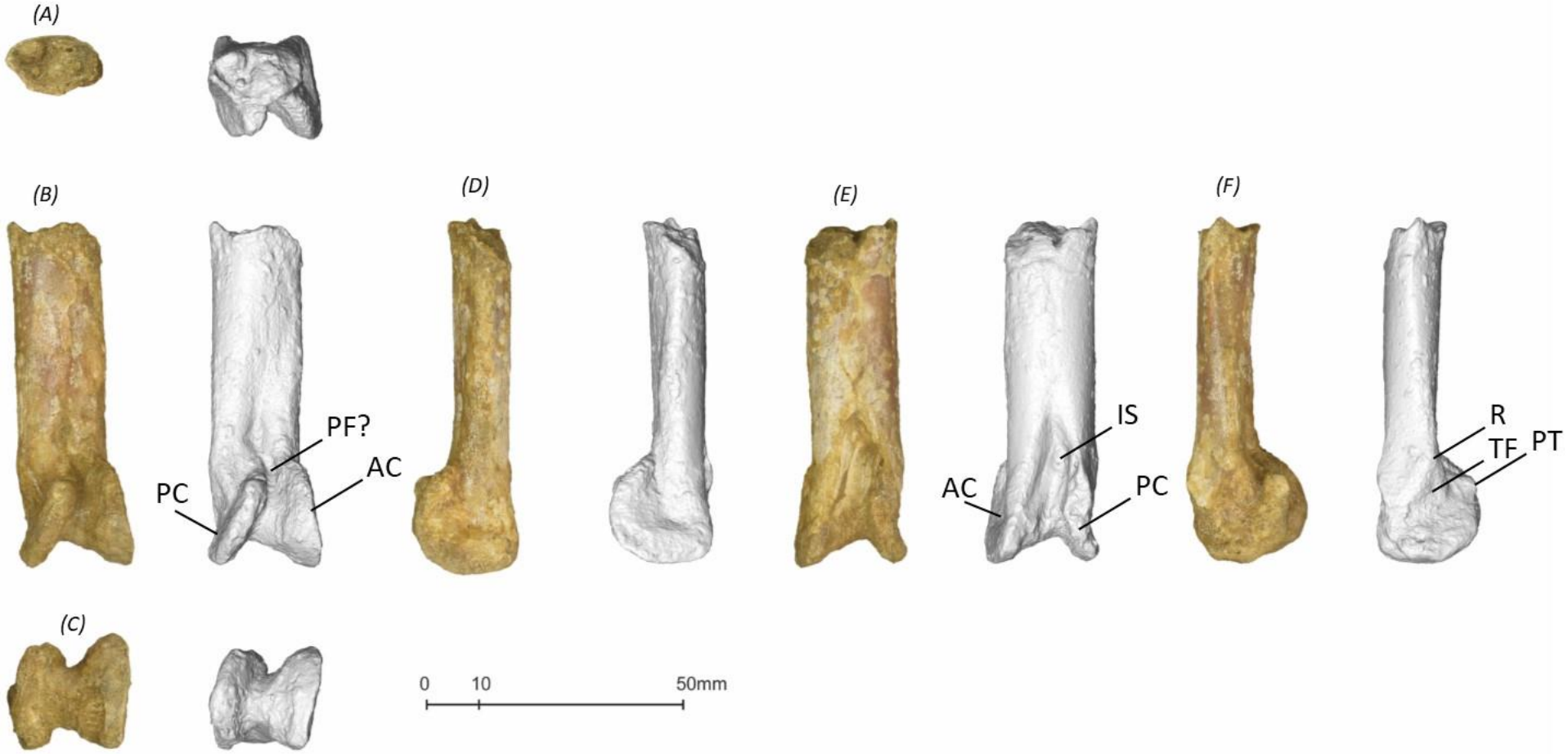

Figure 13. MGUAN-PA654 right metacarpal IV fragment in (A) proximal (B) posterior (C) distal (D) dorsal (E) anterior (F) ventral views
Abbreviation: AC, anterior condyle; IS, intercondylar sulcus; PC, posterior condyle; PF, pneumatic foramen; PT, posterior tubercle; r, ridge; TF, triangular fossa

METACARPAL IV MGUAN-PA654

MGUAN-PA654 (Fig. 13) is a right metacarpal IV fragment composed of a distal shaft and articular end articulated with MGUAN-PA655. It measures 65.3 mm in proximodistal length, 17.1 mm in dorsoventral width at the narrowest part of the shaft, and 18.49 mm in dorsoventral width at the widest part of the condylar area. In the transverse plane, it measures 11.6 mm in anteroposterior breadth at the narrowest part of the shaft and 20.7 mm in anteroposterior breadth at the widest part of the condylar area. The cortical bone ranges from about 0.6 mm to 1.1 mm in thickness. It is very well-preserved, which is not surprising due to its robustness, making it one of the most resistant parts of the skeleton (Bennett, 2003). The fragment has no real overall loss of bone surface, is virtually uncrushed, and has an overall intact three-dimensional shape. The shaft is straight, elliptical in cross-section, and flattened anteroposteriorly.

In the transverse plane, the distal-most condylar area is slightly deflected dorsally at about a 12.1 mm offset from the center of the shaft, and the condyles have about a 6° condylar skew from each other. Centered on the shaft and about 28.4 mm from the distal end, a V-shaped intercondylar sulcus begins, expanding distally and becoming the central concavity between the condyles. The dorsal and ventral borders of this depression manifest as slight ridges, which converge with the distal condyles themselves. On the dorsal surface of the distal end, the metacarpal expands posteriorly to form the ventral condyle. The condylar area forms a pulley-like shape, with the ventral condyle having a ventrodistal deflection, and the dorsal condyle deflecting dorsodistally at a lesser degree.

On the dorsal surface, as the shaft approaches the condylar area, it begins to form a slight ridge on the posterior side, which tapers into a triangular ventrodistally-oriented facet, buttressing the condyle. From this point of convergence, the condyle splays out distally and posteriorly into a fan-like, lunate projection, terminating ventrally with a posterior tubercle. Unlike the dorsal surface of the shaft, the shaft remains straight on the ventral side until an abrupt intersection with the lunate anterior condyle, which also projects distally and posteriorly.

In posterior view, a proximodistally-oriented lenticular fossa is positioned just proximal to the pulley-shaped condylar area on the central shaft. Distal to this fossa and between the bases of the condyles, is a potential pneumatic foramen, although sediment infilling makes this difficult to determine absolutely. The dorsal condyle deflects strongly dorsodistally, and the ventral condyle has a subtle ventrodistal deflection. The distal intercondylar sulcus is asymmetrical, with the deepest part of the concavity occurring more dorsally.

In distal view, the condylar area forms a vertically-oriented hourglass shape, and as the central constriction occurs slightly dorsally, the dorsal condyle is more slender than the ventral condyle.

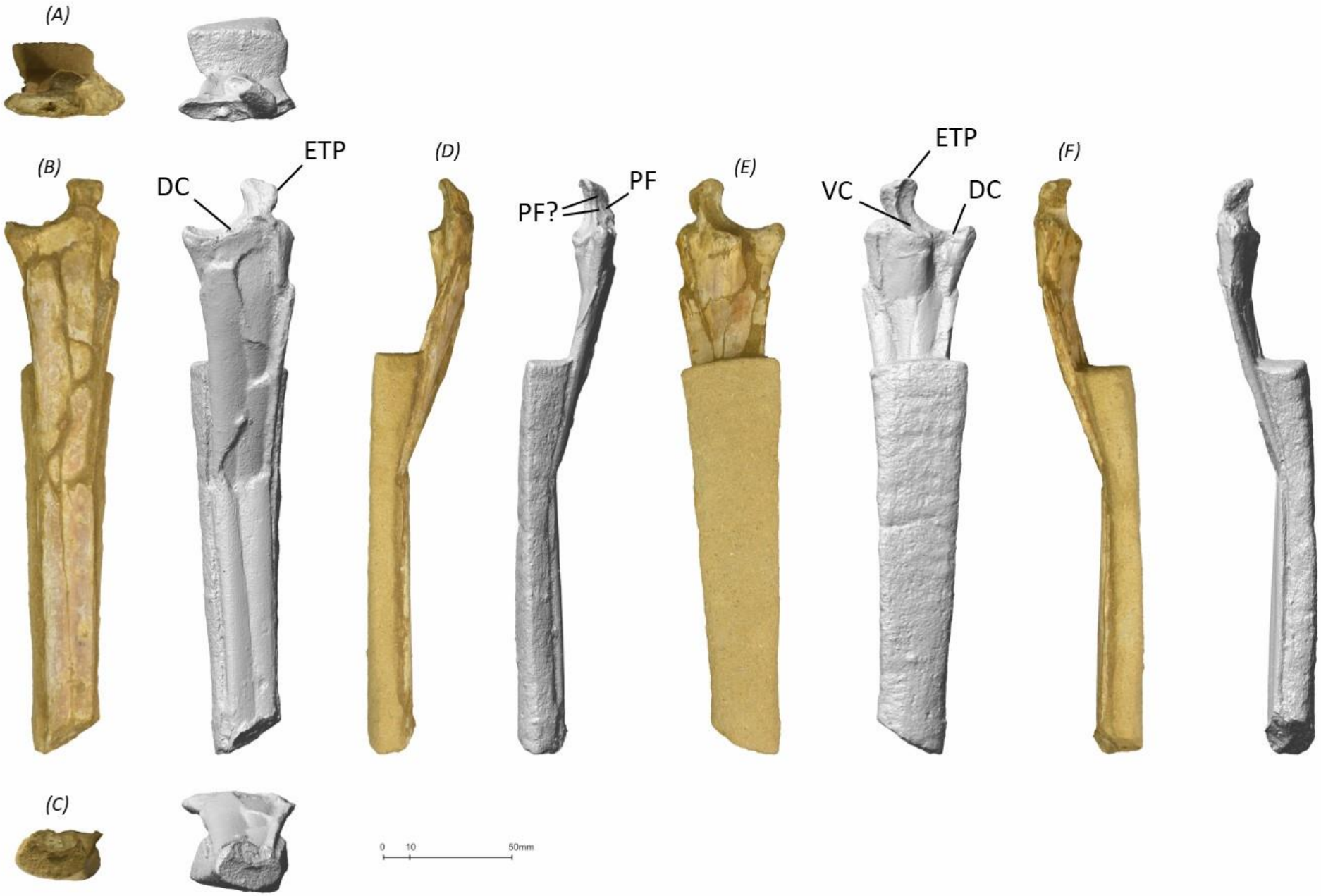

Figure 14. MGUAN-PA655 right manual digit IV phalanx 1 fragment in (A) proximal (B) dorsal (C) distal (D) posterior (E) ventral (F) anterior views
Abbreviations: DC, dorsal cotyle; ETP, extensor tendon process; PF, pneumatic foramen; VC, ventral cotyle

MANUAL DIGIT IV PHALANX 1 MGUAN-PA655

MGUAN-PA655 (Fig. 14) is a right manual digit IV phalanx 1, consisting of a proximal articular end and shaft fragment. The fragment measures 215.1 mm in preserved proximodistal length (including the extensor tendon process), 42.2 mm in anteroposterior width at the widest part of the proximal end, and 18.4 mm in anteroposterior width at the distal end of the shaft. It is 8.7 mm in dorsoventral height at the broken end of the shaft, and 16.1 mm in dorsoventral height at the deepest part of the articular end. The extensor tendon process measures 11.4 mm in width at its base, and in 15.5 mm in height. The cortical bone ranges from about 0.3 mm to 0.7 mm in thickness. It is relatively well-preserved, with an overall intact three-dimensional shape. The cortical bone surface is cracked throughout, although it has no real overall loss of bone surface. The extensor tendon process is fully fused to the rest of the phalanx on its proximal end, which would categorize the specimen as a skeletally mature adult (Bennett, 1993). There appears to be low overall taphonomic distortion, only visible in a small section of the shaft on the posterior side distal to the extensor tendon process, which can be seen offset slightly anteriorly, overlapping the shaft that originally lay alongside it. In the transverse plane, the preserved shaft has broken and flexed dorsally at its preserved midpoint, which gives the specimen a slightly V-shaped form, whereas it would otherwise have been relatively straight, as can be seen in either preserved end. In distal view, the broken end of the shaft is elliptical in cross-section and flattened dorsoventrally. In ventral view, only the proximal one-third of the preserved bone has been prepared out of the surrounding matrix for purposes of stabilization.

In horizontal outline, the shaft expands slightly anteroposteriorly as it approaches the proximal end. In ventral view, the ventral cotyle manifests at the proximal end of the phalanx as a concave crescent from the midpoint of the shaft to the tip of the extensor tendon process, forming an articular facet. The extensor tendon process projects proximally and is sub-rectangular in horizontal outline with a constriction at its base. At this constriction, on its posterior surface and dorsal to the ventral cotyle, lies a lenticular foramen. Two other possible foramina lie alongside this foramen, one an elongated groove infilled with sediment ventral to the lenticular foramen, and the other a small divot proximal to the lenticular foramen. On the anterior edge of the extensor tendon process, a convex protuberance rises anterodorsally.

Dorsally, the posterior side of the articular end is delineated by the tip of the dorsal cotyle. Anterior to this point, the phalanx shaft is bisected by the ventral cotyle, the anterior-most end of which projects posteroventrally from the central region of the shaft. From there, the dorsal border of the ventral cotyle merges with the ventral border of the dorsal cotyle to form an intercotylar ridge. The ventral border of the ventral cotyle also manifests as a sharp longitudinal ridge.

In proximal view, the bicondylar ginglymus at the end of the phalanx is most clearly observed. This articular structure consists of two cotyles that are bifurcated by an intercotylar ridge. This ridge originates at the anteroventral-most point of the dorsal cotyle, flanks the junction created by the meeting of both cotyles, and terminates proximally on the rise of the extensor tendon process. The dorsal cotyle spans the posterior half of the phalanx, excluding the area of the extensor tendon process. The ventral cotyle is posteriorly positioned, almost half the anteroposterior span of the dorsal cotyle, and tear-drop in outline, with the reduction in width occurring proximally as it approaches the extensor tendon process. In this view, the extensor tendon process is sub-rectangular in outline, with the widest side directed anterodorsally.

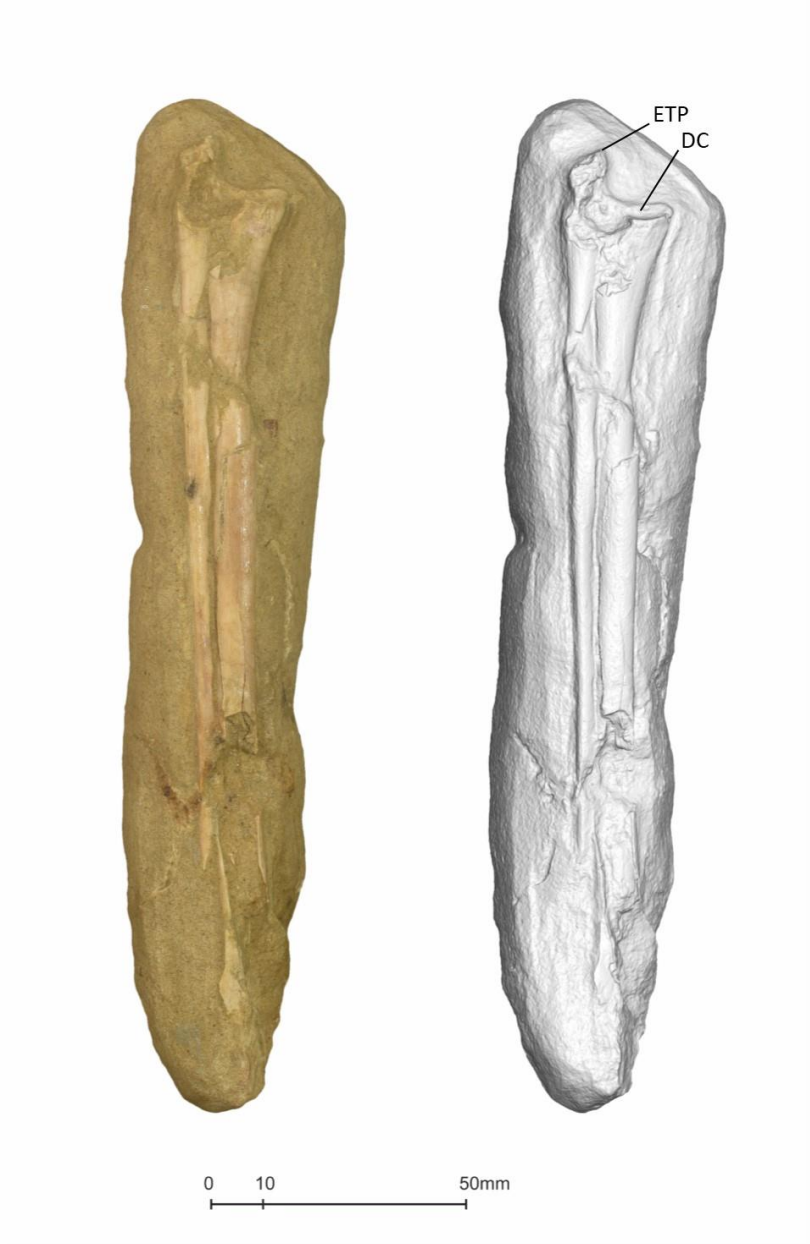

Figure 15. MGUAN-PA659 manual digit IV phalanx 1 in ventral view
Abbreviations: DC, dorsal cotyle; ETP, extensor tendon process

MANUAL DIGIT IV PHALANX 1 MGUAN-PA659

MGUAN-PA659 (Fig. 15) is a nearly complete right manual digit IV phalanx 1, although it is missing major sections of cortical bone at the distal end. The bone has been prepared out of the surrounding matrix on only three sides for purposes of stabilization. It measures 166.0 mm in preserved proximodistal length (including the extensor tendon process) and 9.3 mm in anteroposterior width at the narrowest part of the preserved shaft and 20.8 mm in anteroposterior width at the widest part of the articular area. It is 8.7 mm in dorsoventral height at the broken end of the shaft, and 16.1 mm in dorsoventral height at the articular end. The extendor tendon process is 7.9 mm in width at

the base, and 7.6 mm in height. The cortical bone ranges from about 0.5 mm to 0.8 mm in thickness and is cracked throughout. It is highly eroded in areas, although the intact regions are well-preserved, and it maintains its three-dimensional shape. The proximal region surrounding the cotyles and extensor tendon process is also very damaged, missing the ventral cotyle entirely, and making it difficult to determine the extent of fusion of the extensor tendon process to the rest of the phalanx. However, it does appear to be fused, which is an ontogenetic sign of skeletal maturity (Bennett, 1993). Taphonomic distortion is mostly evident in areas where entire sections of the bone have been offset from their original position, but there does not otherwise seem to be evident warping of bone shape, and the shaft seems to be relatively straight and elliptical in cross-section.

The shaft expands slightly anteroposteriorly as it approaches the proximal articular end. The posterior side of the articular end is delineated by the tip of the dorsal cotyle. Anterior to this point, the dorsal cotyle forms a concavity, the dorsal and ventral margins of which form a rim. The anterior end of the ventral cotyle is too damaged to distinguish. The extensor tendon process has a slightly constricted base, although most of the rest of it is too eroded to glean much information.

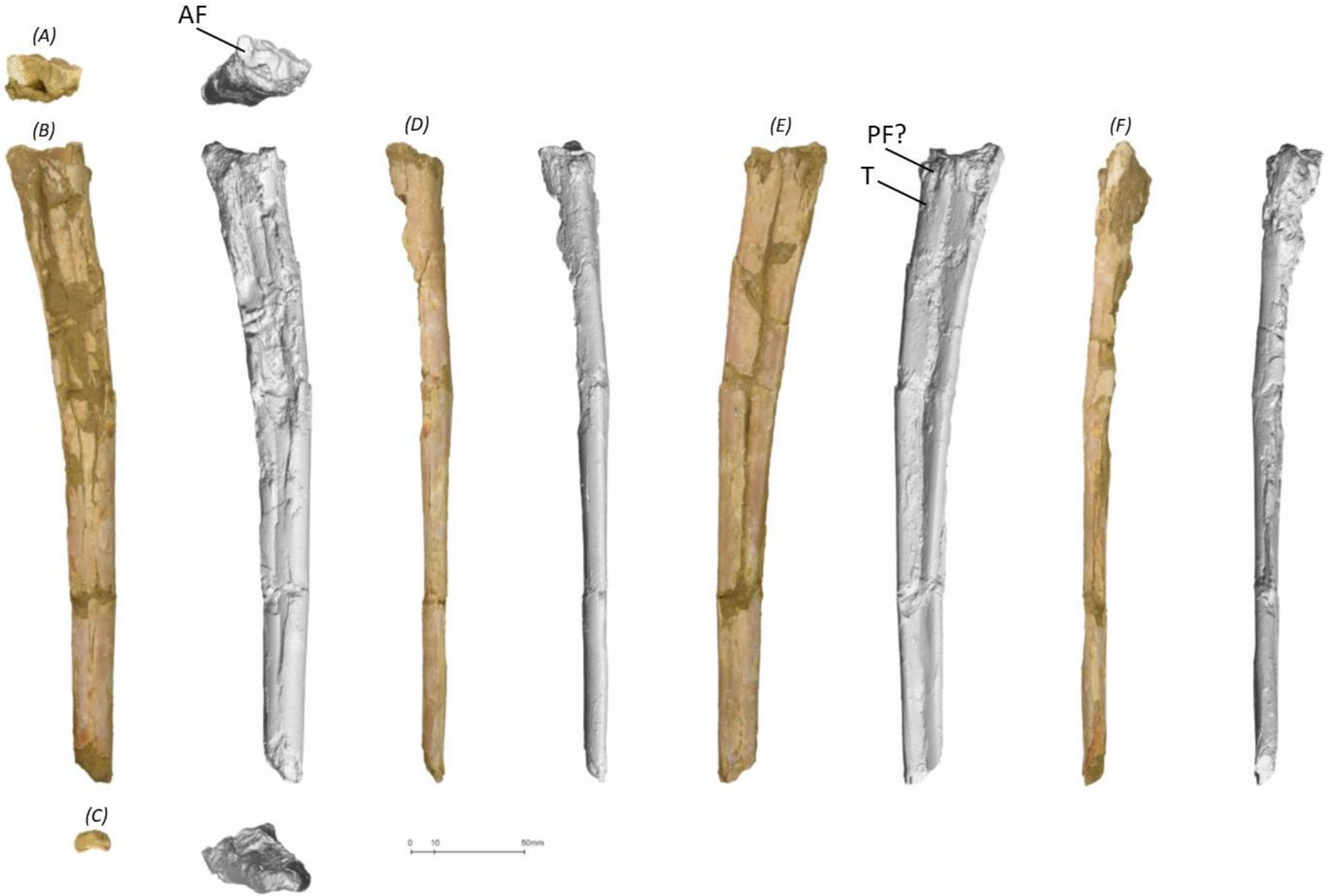

Figure 16. MGUAN-PA652 left manual digit IV phalanx 2 fragment in (A) proximal (B) dorsal (C) distal (D) anterior (E) ventral (F) posterior views
Abbreviations: AF, articular facet; T, tuberosity; PF, pneumatic foramen; T, tuberosity

MANUAL DIGIT IV PHALANX 2 MGUAN-PA652

MGUAN-PA652 (Fig. 16) is the proximal end of an extensively damaged left manual digit IV phalanx 2. It does retain some overall three-dimensionality. There is significant fracturing of the cortical bone surface, with some segments missing entirely from the dorsal, ventral, and posterior sides. Some of the longitudinal fractures along the shaft length have buckled inward. The shaft tapers gradually as it approaches the proximal end, both anteroposteriorly and dorsoventrally. The cross-section of the shaft is difficult to distinguish because of damage, but it appears to be sub-oval to sub-rectangular at the preserved proximal end of the shaft, gradually assuming a kidney shape approaching the distal end with the concavity on the ventral surface. The shaft is straight overall, although has a slight anterodistal curvature, which may be a relic of taphonomy. The proximal end of the phalanx remains fully complete, although extensive weathering has exposed the internal trabecular bone on all sides.

The fragment measures 282.0 mm in preserved proximodistal length, 38.6 mm in anteroposterior width at the widest part of the proximal end, and 18.3 mm in anteroposterior width at the distal end of the preserved shaft. It is 21.9 mm in dorsoventral height at the widest part of the proximal end, and 10 mm in dorsoventral height at the distal end of the preserved shaft. Cortical bone ranges from about 0.6 mm to 1.3 mm in thickness.

In proximal view, the overall articular surface is kidney-shaped, with the convexity facing ventrally. Although the entire surface is too eroded to preserve many features, one distinct articular facet is visible on the posterodorsal corner, the distal edge of which slants at a ventral tilt.

In ventral view, a lenticular foramen extends proximodistally, and is visible on the posterior proximal-most end of the shaft. The proximal margin of the foramen has been eroded away. Distal to the foramen, a small tuberosity is visible.

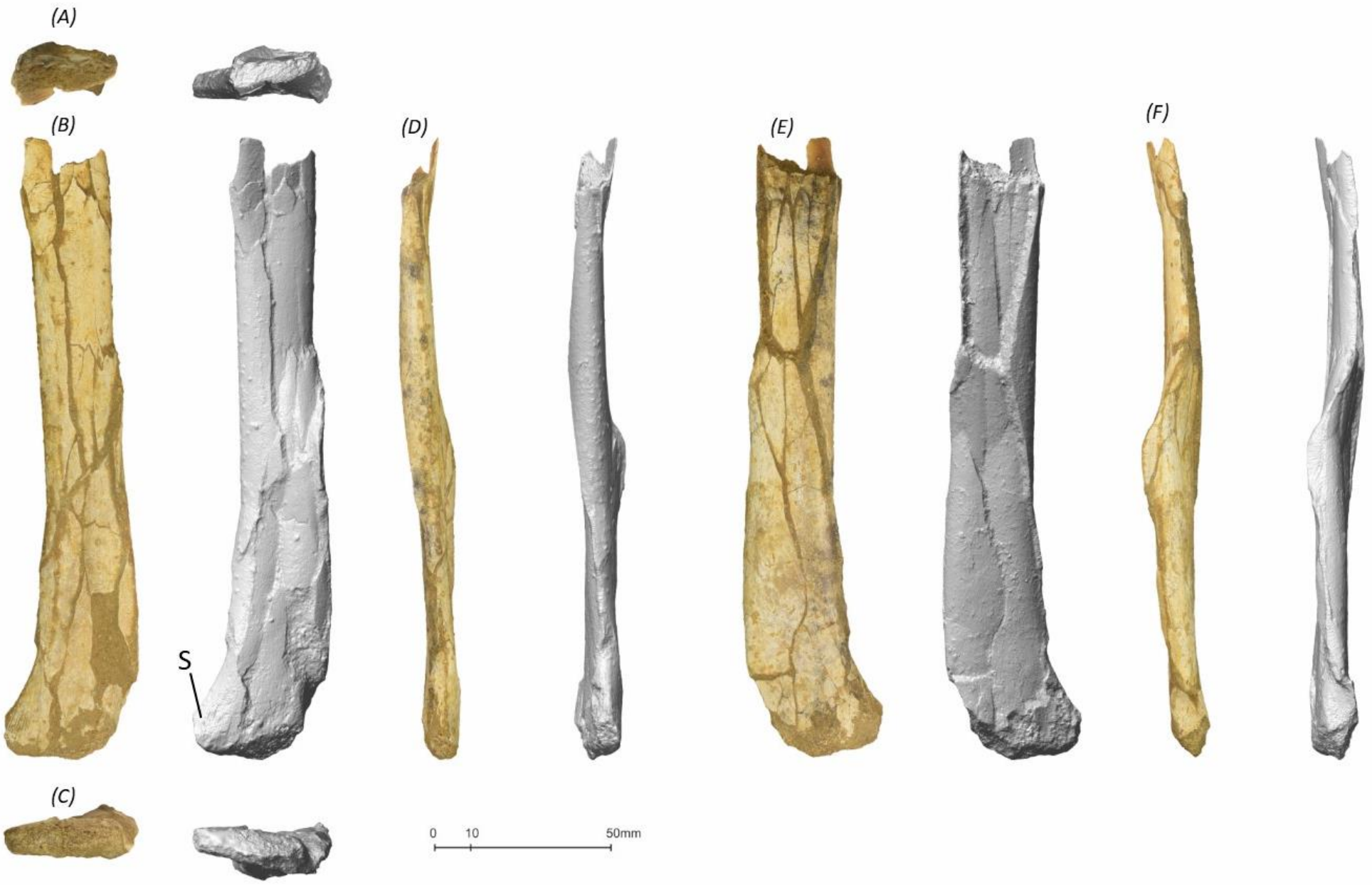

Figure 17. MGUAN-PA656 manual digit IV phalanx 2 fragment in (A) proximal (B) ventral (C) distal (D) anterior (E) dorsal (F) posterior views
Abbreviations: S, striations

MANUAL DIGIT IV PHALANX 2 MGUAN-PA656

MGUAN-PA656 (Fig. 17) is a distal shaft fragment of a manual digit IV phalanx 2, missing the proximal half. It measures 166.0 mm in preserved proximodistal length. It measures 22.5 mm in anteroposterior width at the proximal part of the preserved shaft and 29.7 mm in anteroposterior width at the distal end. It is 6.3 mm in dorsoventral height at the proximal end of the shaft, and 10.2 mm in dorsoventral height at distal end. The cortical bone ranges from about 0.5 mm to 1.0 mm in thickness. It is well-preserved, maintains its three-dimensional shape, but is eroded in areas. The cortical bone surface is cracked throughout, with a region missing in the proximal dorsal part of the shaft. Taphonomic distortion is mostly evident in areas where entire sections of the bone have been offset from their original position, slightly warping the entire shape. The shaft seems to have been relatively straight and elliptical in cross-section. It expands slightly anteroposteriorly as it approaches the distal articular end. The articular end is too eroded to glean much information, save for some longitudinal proximodistal striations at the anterodorsal tip of the bone.

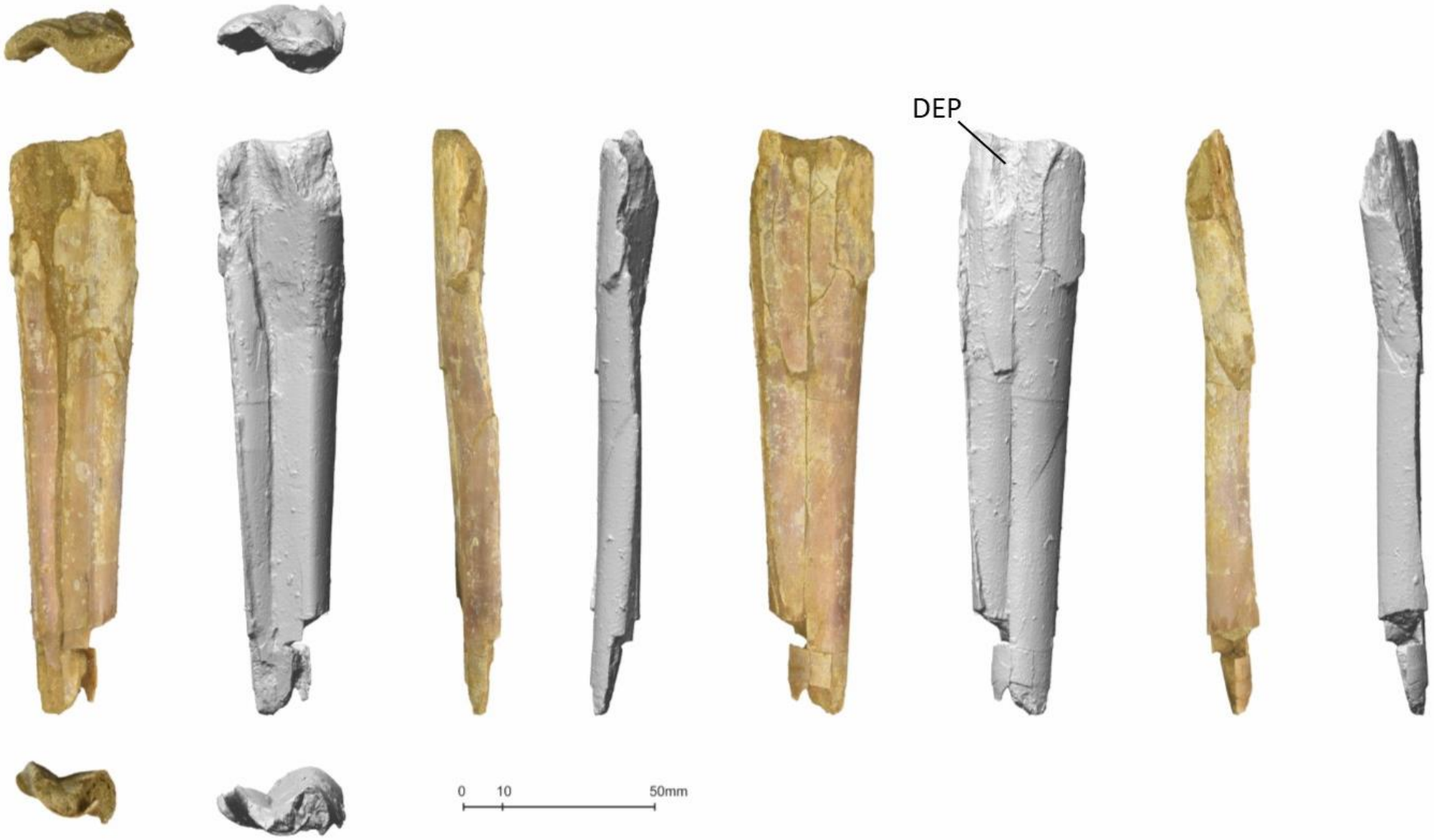

Figure 18. MGUAN-PA658 indeterminate shaft fragment
Abbreviations: DEP, depression

SHAFT FRAGMENT MGUAN-PA658

MGUAN-PA658 (Fig. 18) is an indeterminate shaft fragment, which is likely a wing finger element due to overall shape. It is extensively damaged, although it retains some overall three-dimensionality. There is extensive fracturing of the cortical bone surface, with portions missing entirely from both ends. Some of the longitudinal fractures along the shaft length have become inwardly compressed toward the center of the shaft on the dorsal surface, giving a false sigmoidal cross-section, when in reality the cross-section would have likely been closer to sub-rectangular. The shaft shows a gradual anteroposterior expansion in horizontal outline, likely indicating an approach to an articular end. The most expanded end of the fragment is very eroded, although a depression is visible, slightly off-center on the shaft.

The fragment is straight and measures 140.1 mm in preserved proximodistal length, 21.2 mm at the narrowest width of the complete shaft, 30.3 mm at the widest part of the shaft, 10 mm at the narrowest depth of the shaft, and 21.9 mm dorsoventrally at the greatest depth. Cortical bone ranges from about 0.6 mm to 0.7 mm in thickness.

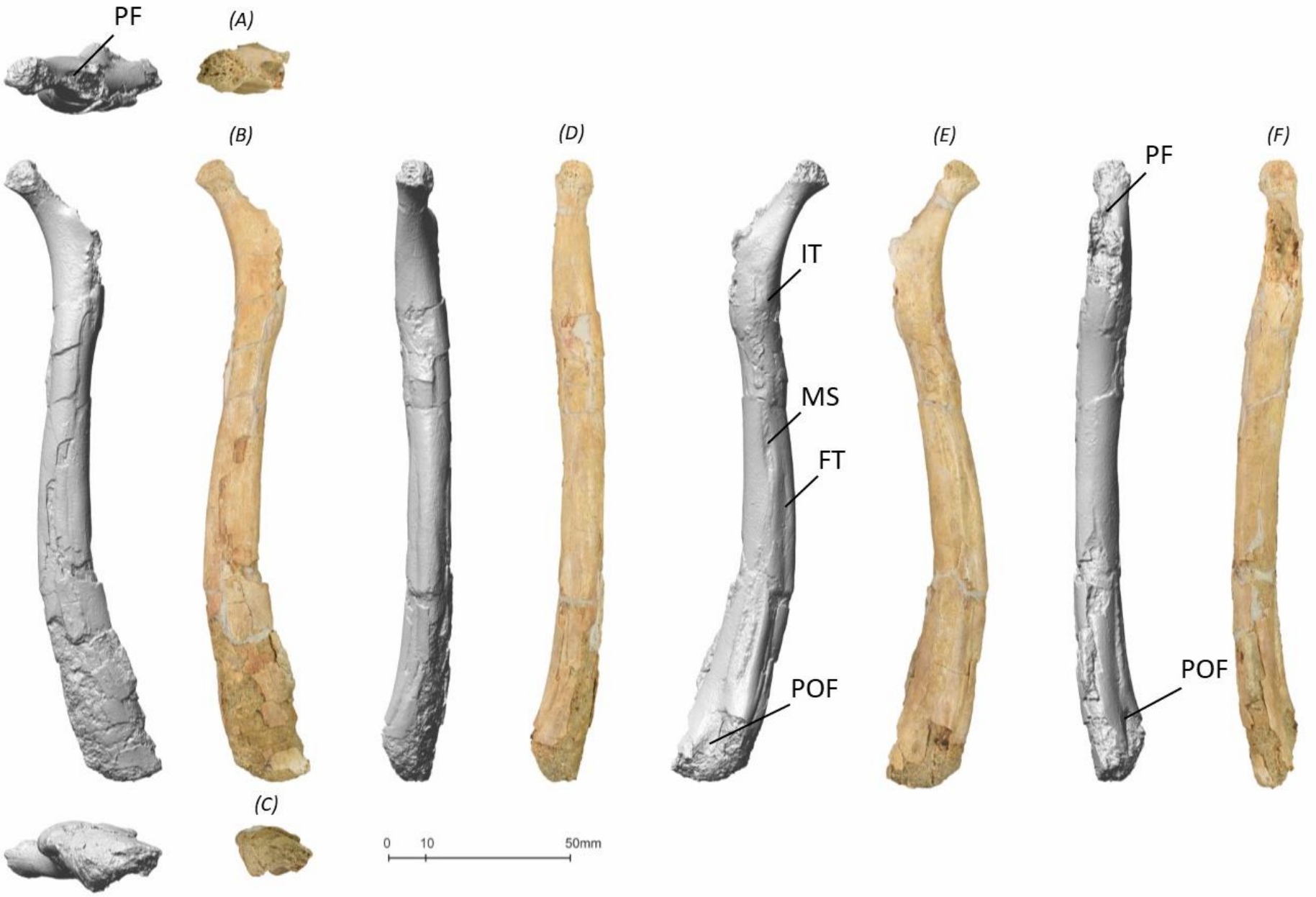

Figure 19. MGUAN-PA163 left femur in (A) proximal (B) anterior (C) distal (D) medial (E) posterior (F) lateral views.
Abbreviations: FT, fourth trochanter scar; IT, internal trochanter; MS, muscle scar; PF, pneumatic foramina; POF, popliteal fossa

FEMUR MGUAN-PA163

MGUAN-PA163 (Fig. 19) is a left femur (Mateus et al. 2012) that is relatively complete but lacks the greater trochanter, the distal condyles, and a few sections of cortical bone at the distal-most end on the lateral and anterior sides of the shaft, where a sedimentary interior mold remains, preserving its original shape. The femoral head has been lightly eroded revealing the trabecular bone, and damage is also evident around the base of the neck. The entire bone surface is superficially fractured. Cortical bone ranges from about 0.4 mm to 0.7 mm in thickness.

The proximodistal preserved length of the femur is 155.8 mm. The narrowest part of the shaft is in the upper third, where it measures 11.2 mm in mediolateral width, the width increasing steadily distally to reach 12.8 mm at the midpoint of the femur, and reaching almost double its mediolateral width at 18.8 mm at the distal condylar area.

The femoral head is bulbous and rounded, projecting proximomedially from a long, constricted neck that exhibits a slight anterior curvature, positioned at a 146° angle to the shaft. Although most of the greater trochanter and the internal trochanter have been eroded away, they are conspicuous as the distal margins of the shaft that border these areas are distinctly sloped to meet them. Trabecular bone is readily visible along the broken margins of the trochanters. In proximal view, a mediolaterally-oriented lenticular pneumatic foramen is sunken into the large concave ventral intertrochanteric fossa. The length of the femoral neck, from the intertrochlear fossa to the head, is 16.5 mm, and the neck has a circular cross-section.

In the transverse plane, the shaft of the femur is bowed posterolaterally, exhibiting a gradual curvature. In cross-section, the shaft begins as circular at the base of the trochanters and expands distally, gradually becoming more subtriangular and twisting slightly as it approaches the distal end. In lateral view, the femur has a minimum anteroposterior width of 10.9 mm, the narrowest part occurring about halfway down the shaft. It is 12.4 mm in anteroposterior at the widest part of the proximal shaft, 11.9 mm in anteroposterior width at the widest part of the distal complete shaft.

In posterior view, the internal trochanter is visible as a slightly raised ridge distal to the proximal end, centered on the shaft. Distal to this scar, the fourth trochanter scar presents as a rugose ridge located centrally and extending distally for approximately 60.5 mm down the length of the shaft of the femur, stopping at about 23.6 mm from the distal end of the femur. Distal to the end of the fourth trochanter scar begins a slight depression, the beginning of the popliteal fossa.

The distal condyles have been completely eroded away, and in distal view the interior sedimentary mold exhibits a reniform shape, posteriorly concave and anteriorly convex toward the area of the intercondylar sulcus.

Additional material:

Figure 20. Articulated MGUAN-PA digit IV metacarpal fragment and first phalanx fragment, in situ (scale: 190 mm)

In addition to the above-mentioned specimens, more pterosaur material remains both in situ, as well as in storage in Angola, awaiting customs clearance. Worth particular mention is a partial manual digit IV metacarpal fragment articulated with a first phalanx fragment, which in its partially-preserved state, measures at least 830 mm alone (Fig. 20). This indicates an extreme size variation among the specimens of the region.

A few other extremely damaged isolated bone fragments were also recovered from the Bentiaba locality, but these shards were overall too shattered and indeterminate to add any descriptive or diagnostic value to this work. However, they do retain inherent value for future histological studies or destructive testing, and therefore their existence is mentioned here.

Phylogenetic Analysis

Two phylogenetic analyses were run: “MGUAN_PA650&651” and the relationships of the Pterosauria, and also all of the Angola pterosaur material combined into a single taxon “Angola_pterosaurs” and the relationships of the Pterosauria. Both results were the same, in five equally parsimonious trees. These trees are each the result of four phylogenetic positions for *Volgadraco bogolubovi* Averianov et al. 2008 and two phylogenetic positions for “Angola_pterosaurs” and “MGUAN_PA650&651”. The “Angola_pterosaurs” taxa are recovered as a sister group in a trichotomy with *Simurghia robusta* Longrich et al. 2018 and *Alcione elainus* Longrich et al. 2018, although the position changes with manipulation of some dubious characters on non-Angolan sister groups, in particular *Cretornis hlavaci* Averianov & Ekrt 2015. Executing the analysis with only one of the Angola taxa results in “MGUAN_PA650&651” also being recovered in the same trichotomy with *Simurghia robusta* Longrich et al. 2018 and *Alcione elainus* Longrich et al. 2018.

Keeping in mind the possibility of sheer coincidence or the dearth of overall characters on the bones available, both taxa nonetheless were recovered in the same position in the cladograms (Fig. 21), which would at least indicate a basic overall similarity. However, more extensive fossil sampling would be required to definitively make any further claims. According to the Longrich et al. (2018) matrix, both representations of the Angola material fell within Pteranodontia, with "MGUAN_PA650&651" falling more specifically within Nyctosauridae in a trichotomy with its fellow African species (Fig. 20).

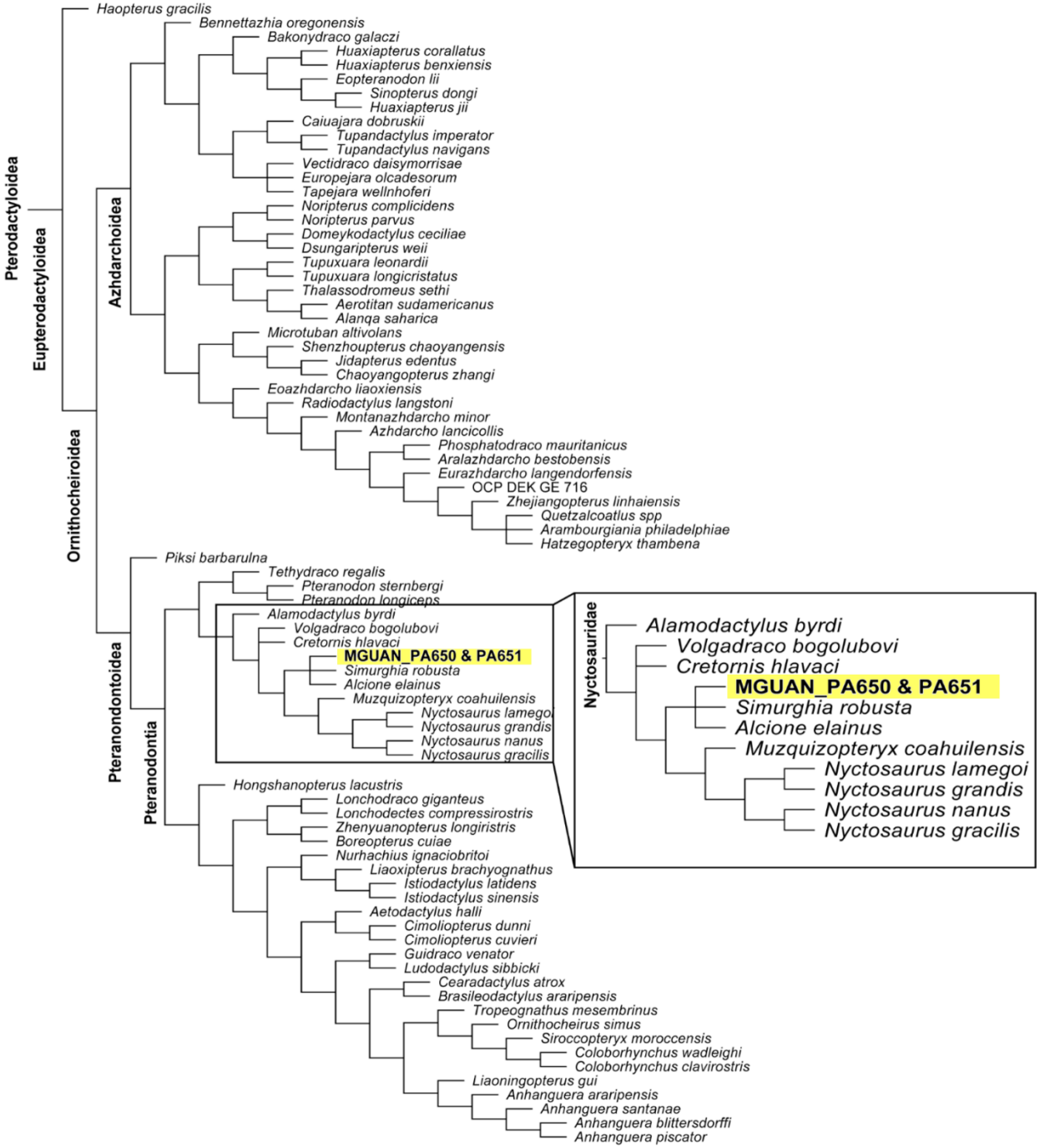

Figure 21. Strict consensus cladogram based on the phylogenetic analysis of Longrich et al. (2018) with the addition of "MGUAN_PA650&651" articulated humerus and ulna.

Wingspan

If all of the specimens recovered from Bentiaba are in fact one distinct species, then the variation in size among the same elements present in the fossil assemblage could indicate great ontogenetic variety, individual variation, or sexual dimorphism as seen in the case of *Pteranodon* (Bennett, 1992, 2017). In order to determine an overall body size of a specimen, average lengths were interpolated from the scatter plot in Bennett (2001b) for *Pteranodon* (a comparable taxon according to the cladogram results) using the length of the "MGUAN_PA650&651" taxon's complete ulna, MGUAN-PA651. This ulna then generated an average overall estimate for the "MGUAN_PA650&651" humerus at around 213.5 mm, plausibly indicating that just over half of the humerus is preserved in MGUAN-PA650.

Table 2. "MGUAN_PA650&651" estimated MGUAN-PA650 humerus length (dashed line) and known MGUAN-PA651 ulna length (solid line) measurements, plotted against each other in orange, against the known dimensions of a large fossil assemblage of Pteranodon (modified from Bennett, 2001b), with a list of accordingly-projected individual wing element lengths of the "MGUAN_PA650&651" taxon.

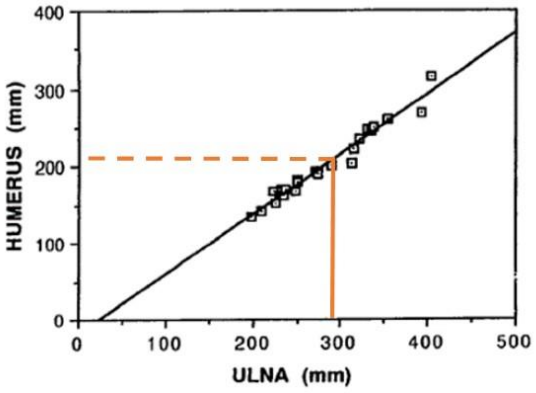

Element	Length
Humerus	213.5 mm (extrapolated)
Ulna	290.1 mm
Metacarpal IV	459.8 mm (extrapolated)
Digit IV Phalanx I	518.3 mm (extrapolated)
Digit IV Phalanx II	421.9 mm (extrapolated)
Digit IV Phalanx III	307.4 mm (extrapolated)
Digit IV Phalanx IV	153.9 mm (extrapolated)
Extrapolated Individual Wing Length = 2.4 m	
Total Extrapolated Wingspan = 4.8 m	

Further inferences can then accordingly be made into wingspan estimates using the ratios of the individual wing elements to deduce individual measurements, which were built in to the Longrich et al. (2018) matrix as continuous characters. Using the Andres et al. (2014) matrix to get average lengths of missing wing elements via ratios to the lengths of the ulna and humerus, and the Bennett (2001b) method to sum the humerus, ulna, metacarpal IV, and the four phalanges of digit IV, each wing is found to measure just over 2.4 meters, giving the MGUAN_PA650&651 taxon approximately a 4.8 m wingspan. These dimensional proportions could then also be scaled up and down, and used to size other individuals with complete bones: the individual with the MGUAN-PA659 digit IV phalanx I, which would yield a 1.5 m wingspan for that individual, and the individual with the articulated MGUAN-PA661 ulna and MGUAN-PA 662 radius would yield a 5.6 m wingspan. However, the existence of other size-variable individuals in the fossil assemblage, namely the much larger MGUAN-PA653 ulna (not to mention the even larger specimen still in Angola), indicate that there was an even wider size variability in the group than we find definitively here. This could be due to intraspecific variation, size variation within sexual dimorphism, as in the case of *Pteranodon*, where the smallest known individuals of each sex were found to be approximately 70% of the size of the largest individuals (Bennett 1991, 1992), ontogeny, or possibly that the assemblage represents several different species (interspecific variation).

Bone Histology

Histology involves the study of tissues in order to reveal their detailed cellular makeup at the microscopic level. It is often used in paleontology in relation to skeletal bone to assess the relative age and skeletal and sexual maturity of an animal (Lamm, 2013), and can be particularly useful as a tool to make inferences about the ontogenetic stage and growth rate of an animal based on recorded growth rings, vascularization patterns, and the organization of collagen fibers within the bones (de Ricqlès, 2000). As bone grows, cartilaginous or fibrous tissues are replaced by bone, with deposition of the new bone tissue occurring on its outer surface, while previously-extant bone is simultaneously eroded from the inner medullary cavity. This outer deposition leaves lines of arrested growth (LAG), which can be counted and used to determine age much like tree rings, and can also manifest in a concentrated outer layer (external fundamental system) as skeletal maturity is reached, giving insight into when determinate growth is exhibited and maturity reached in a taxon (Fig. 23). Another indicator of maturity is if pre-existing vascular canals have begun to be infilled with bone, while new vascular canals appear interspersed throughout the cortex (Padian, 2013).

Interpreting the ontogenetic stage of a fossil taxon is traditionally reliant on the degree of fusion of bones (both in the epiphyseal regions and between different elements), the extent of element ossification, surface textures, and histology (Padian, 1995; Bennett, 1993). In order to further explore the ontogenetic variability of the Angolan fossil assemblage, a sample was taken for histological analysis in order to have a better understanding of the skeletal maturity of the specimen in question, and also to give insight into the relative age of such an individual.

Figure 22. Histology sample MGUAN-PA653, first embedded in resin (left) and afterwards ground into a thin section and mounted on a slide (right).

A 0.6 mm thick fragment of the MGUAN-PA653 ulna was chosen as the sample for histological analysis (Fig. 22) due to the fact that samples taken from long bones undergo the least metaplastic deformation throughout growth. Additionally, its already fragmentary nature meant that destructive sampling would not have as much of an impact on this bone as compared with the more complete bones, which are more valuable for morphological studies. Ulnae are also of particular interest in flying vertebrates because they are the main supporting bone of the zeugopodium that bears the brunt of the flight load and are especially subject to torsional forces. They endure a great amount of

shearing stress at the tissue level, and so compensate by having the highest laminarity of all bones (De Margerie, 2002).

In pterosaurs, identifying histological features also becomes more complex when compared with other tetrapods. Pterosaurs had the necessity of maintaining a thin cortical bone layer in order to reduce their overall weight for flight, and therefore have the thinnest bone walls of any tetrapod (de Ricqlès, 2000). However, flying animals also have to be especially flexible and resistant to the torsional factors that they endure by their behaviors in flight, especially as they grow larger and are more subject to flight factors, such as the duress of flapping wings (Padian, 2013). Thus, pterosaurs adapted to this need by developing a more lamellar configuration to their bones as the animals grew over time, wherein the faster-growing, well-vascularized fibrolamellar bone tissue in the periosteal layer of a juvenile would change to a slower-growing less-vascularized and more parallel-fibered or lamellar bone seen in subadult and adult animals (Steel, 2008; Chinsamy et al. 2009). Sexual maturity has, in the case of *Pterodaustro* specimens, been found to also be based on the transition of cortical fibrolamellar tissue to more parallel-fibered bone, which for that taxa happens at about 53% somatic growth (Chinsamy et al., 2009). This mature bone tissue, organized into a "plywood-like" structure of successive bone collagen fiber layers that orient at juxtaposing angles to each other, strengthen the overall bone (de Ricqlès, 2000). Functionally, this arrangement of lamellar bone helps in dealing with substantial aerodynamic loads and resisting the potentially hazardous factors of a volant lifestyle. However, this functional solution creates difficulty when it comes to histology, because thin-walled bones retain only a very sparse record of their growth dynamics. Considering that pterosaur bone tissue is quickly reabsorbed by osteoclasts from the inner medullary cavity as they outwardly grow, any primary bone evidence disappears rapidly, as well as any LAG that may have been previously recorded (Prondvai, 2012).

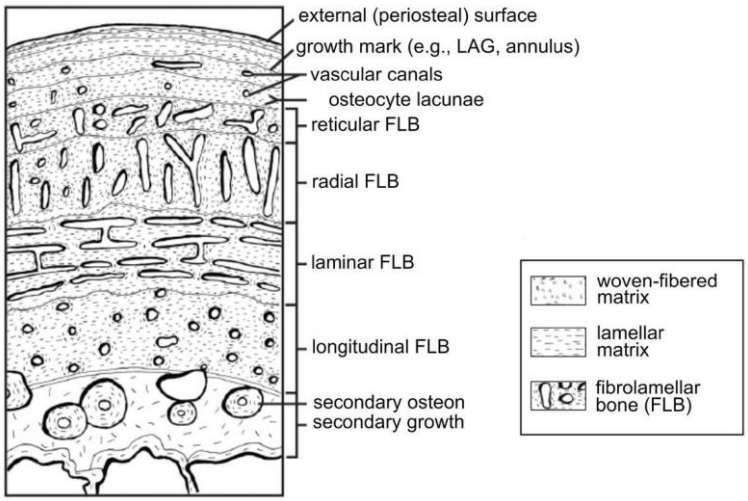

Figure 23. Histological diagram of bone (taken from Lamm, 2013).

The MGUAN-PA653 ulna is composed of a cortical layer with a periosteum that is mostly composed of mature bone with a plywood-like pattern (Fig. 24). Under crossed polarized light, which reveals the original orientation of collagen fibers, bone cells manifest as a spindle shape, which then orient themselves according to the orientation of the ply (Steel, 2018). This is visible here as the fibers

alternate in orientation, from longitudinal to circumferential (Fig. 24), and can also be seen as alternating colors under crossed polarized light with a lambda filter (Fig. 25). This type of poorly-vascularized parallel-fibered bone indicates an advanced arrangement of the tissue, which specifies that the sample is not juvenile.

The periosteum comprises a sparse array of vascular canals and primary osteons, until the poorly-visible inner endosteal limit is reached (Fig. 24). The endosteal region shows great irregularity, where bone has been previously remodeled and eroded away. There is a dense, organized network of osteocytes throughout the bone sample, visible as small simple lacunae and oriented longitudinally and circularly, which may also indicate secondary remodeling (Steel, 2008). It has also been suggested that these lacunae may potentially be a detection system for bone strain and damage (Cullinane, 2002). The tissue is moderately vascularized in a circumferential or longitudinal pattern, which is again a sign of maturity because juvenile bone is usually greatly vascularized in a reticular to laminar pattern (Steel, 2008). Approaching the innermost and outermost surfaces of the bone, this vascularization lessens and the bone becomes denser, which is a feature of mature animals that are no longer undergoing rapid growth (Bennett, 1993). Primary osteons are oriented longitudinally and are internally ringed with lamellar bone, which is visible under rotation with a lambda filter (Fig. 25), and are also sometimes connected by irregular and oblique anastomoses. Secondary osteons, commonly seen in adult animals, are not visible in the sample, which could be an indication of a sub-adult age (Bennett, 1993).

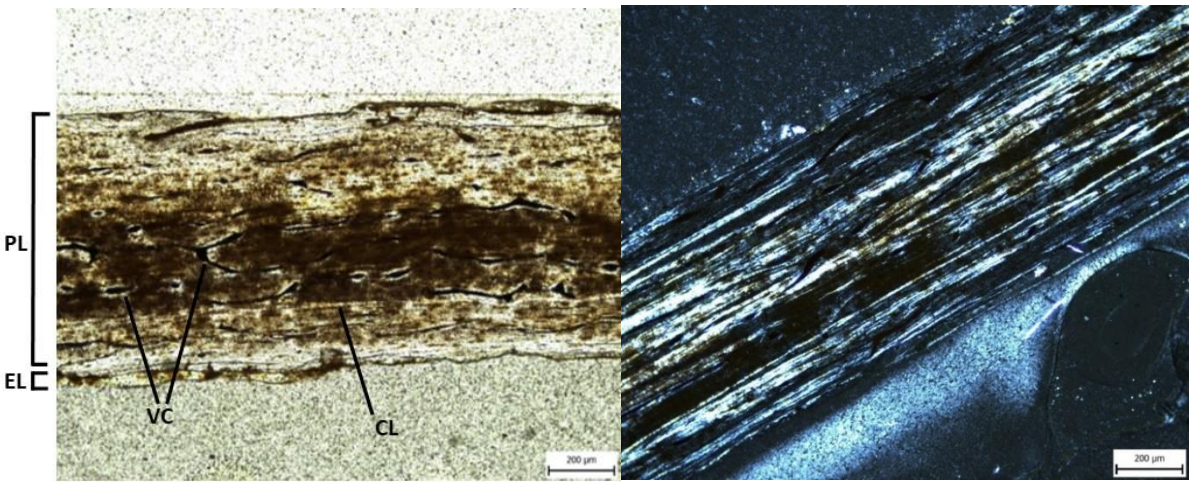

Figure 24. Thin section of MGUAN-PA653 ulna fragment under normal light (left) and cross-polarized light (right) Abbreviations: CL, circumferential lamella; EL, endosteal layer; PL, periosteal layer; VC, vascular canals;

In this sample, no trabeculae are visible, which is not surprising due to this being a mid-shaft sample, which would have been especially subject to secondary reworking (Woodward et al., 2013), erasing earlier records of growth. There is no sign of an external fundamental system, and a few vascular canals are seen to open onto the periosteal surface, which implies that the animal had not yet reached its final body size at the time of its death. In fact, the lack of an avascular outermost cortex implies that the animal was still growing. No LAG are here visible, and indeed are uncommon in pterodactyloids generally, although LAG do occur in some species including *Pteranodon* (Bennett,

2017; Sayão, 2003; Steel, 2008). In the absence of LAG, growth rates can be inferred by analyzing other aspects of bone type and the degree of vascularity (Lee et al., 2013). It is also worth mentioning that annual growth marks do not visibly appear in vertebrates that achieve full growth in less than one year (Woodward, 2013). Additionally, the presence of endosteal lamellae has been shown to be a sign of maturity in certain pterosaurs, because it is a correlate for the cessation of medullary expansion (Chinsamy et al. 2009; de Riqlès et al, 2000; Prondvai et al. 2012; Steel, 2008), but they are not visible here either.

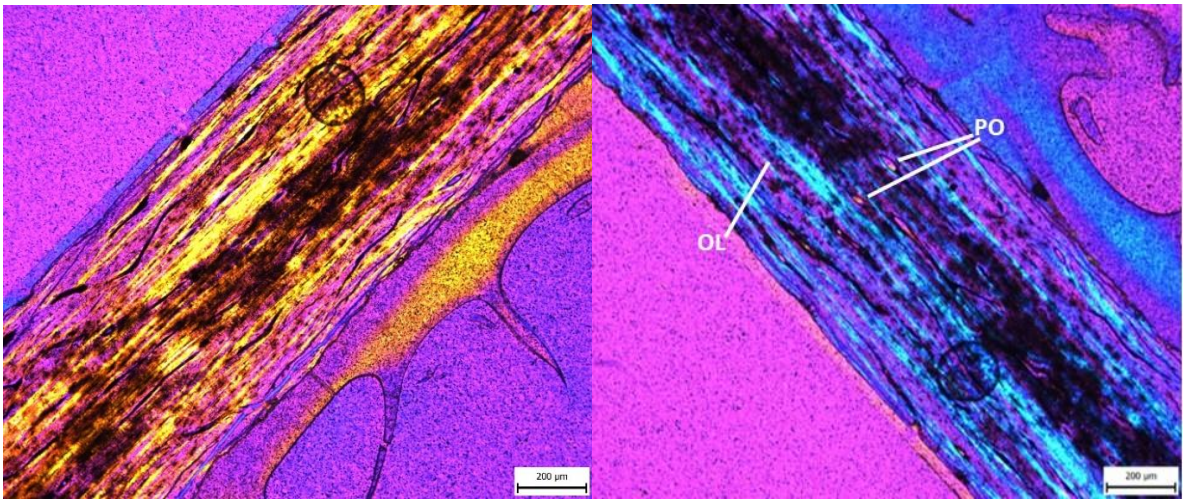

Figure 25. Thin section of MGUAN-PA653 ulna fragment under crossed polarized light, rotated under a λ filter. Abbreviations: OL, osteocyte lacuna; PO, primary osteon

The culmination of these histological observations implies that MGUAN-PA653 was likely a subadult to adult in age, although it had not yet reached its final determinate body size. This is not altogether unsurprising, considering that this ulna is one of the largest bones present in the Angolan fossil assemblage (despite size being an unreliable indicator of ontogeny). Although histology can be an informative foray into the maturity of an individual animal, its real strength lies in relative age, especially when several samples can be taken from entire populations. Therefore, more extensive sampling of other bones in the Angolan assemblage would yield much a more informative picture of the population at that time.

DISCUSSION

Morphologically, the bulk of the Angola material's taxonomic assignment to Pteranodontia is in keeping with the readily apparent overall similarities in the fossil remains to taxa such as *Pteranodon* sp., *Cretornis hlavaci* Averianov & Ekrt 2015, *Tethydraco regalis* Longrich et al. 2018*, Simurghia robusta* Longrich et al. 2018, and *Alcione elainus* Longrich et al. 2018, wherever characters are distinguishable on the bones (Fig. 26-28). In cases where multiple examples of the same bone element are represented in the Angolan fossil assemblage, all displayed the same evident morphological features despite size variation. A definitive individual specific designation is not

possible for the “Angola_pterosaurs” on the cladogram, since it changes position within Pteranodontia when dubious characters on *Cretornis hlavaci* Averianov & Ekrt 2015 are manipulated, and there is also a lack of discernable characters on single bones. However, most characteristic attributes are present in the “MGUAN_PA650&651” taxon (the only taxon with enough to make a specific diagnosis), and therefore this specimen is the only driver for categorizing this pterosaur recovered from Bentiaba to the specific level.

Although not enough of the humerus (MGUAN-PA650) is present to make many assertions about the shape as a whole, enough information is preserved to point out several aspects of the distal end. The Angolan specimen shares a straight humeral shaft with *Alcione elanus* and *Simurghia robusta* (Longrich et al. 2018). Additionally, if we use the above-mentioned size extrapolation of 213.5 mm overall humeral length, then we can presume just over half of the humerus is here preserved, which means that the mid-shaft shape of the humerus can also be assessed as it expands outward approaching the distal end. This measurement is also in keeping with the other species in the trichotomy, since the humerus of *Alcione elanus* averages 93-102 mm, and *Simurghia robusta* averages 165 mm (Longrich et al., 2018). Enough variability exists within the Angola pterosaur fossil assemblage to fall within that range comfortably, and the isometric scaling of the humeri discussed by Longrich et al. (2018) which differentiated *A. elainus* and *S. robusta* as separate species would also apply here in differentiating the MGUAN-PA650/MGUAN-PA651 taxon as a new species as well.

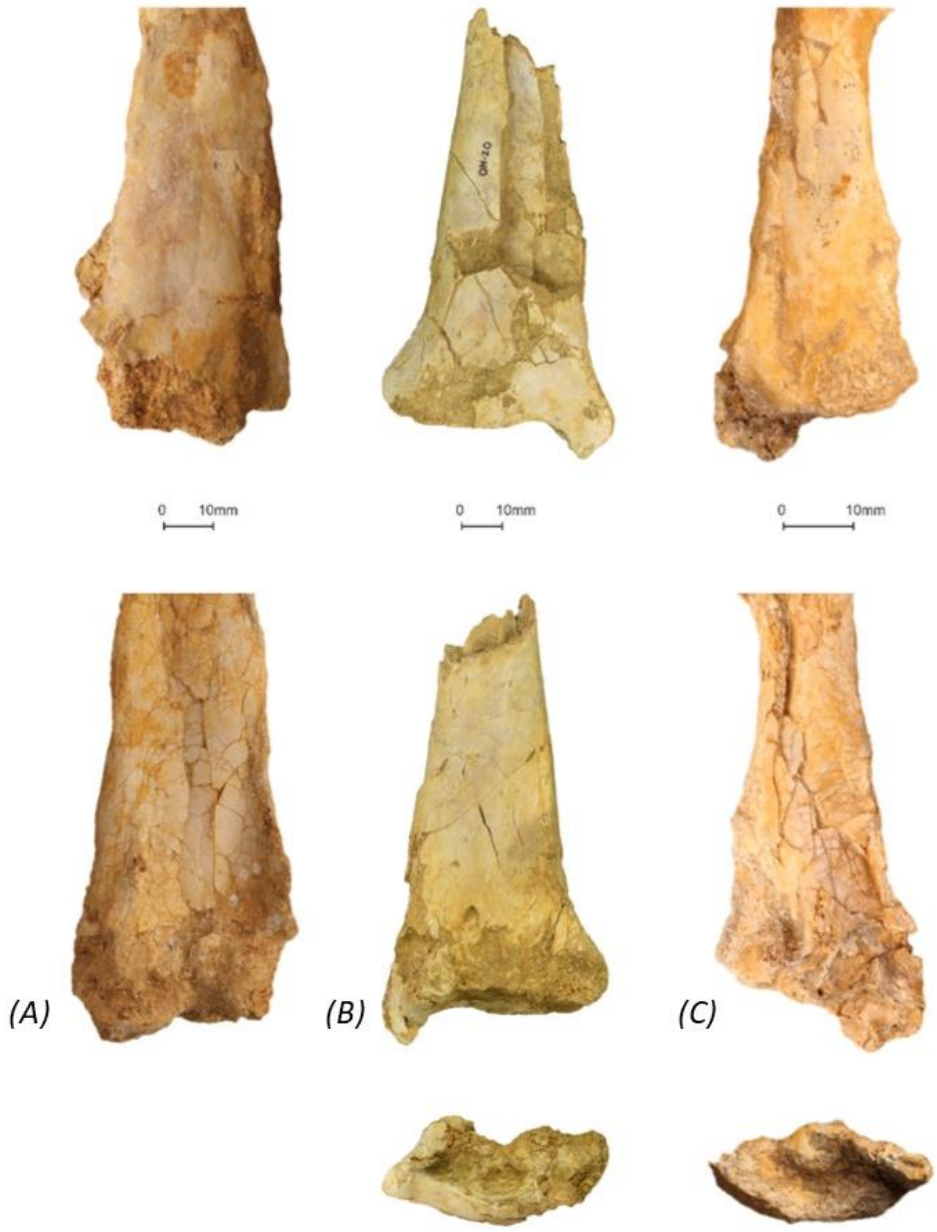

Figure 26. From left to right: distal humeri of (A) Simurghia robusta Longrich et al. 2018*, (B) Angola specimen MGUAN-PA650, and (C)* Alcione elanus Longrich et al. 2018*.*

The MGUAN-PA650 humerus displays a wider entepicondyle than ectepicondyle in anteroposterior width, with the entepicondyle of humerus projecting anteriorly (a pteranodontid feature), and distally, the distal projection being a characteristic shared by *Pteranodon* (Bennett, 2001) and Nyctosauridae (Longrich, 2018). The ectepicondyle projects posteriorly, a feature shared with both *Alcione elainus* and *Simurghia robusta* (Longrich et al., 2018), and *Pteranodon* (Bennett, 2001). This gives the humerus a very strong distal and trapezoidal expansion, also similar to both *Pteranodon, Tethydraco regalis* and *Alcione elainus*, in which the distal half of the shaft is expanded, a derived feature of pteranodontoids (Bennett, 2001a), but different from azhdarchoids that only have an expansion of the distal one-third of the humerus. In fact, the distal width of MGUAN-PA650 is already more than twice the width of the narrowest part of the preserved shaft, which is a

dimensional feature shared with *Tethydraco regalis* and previously found to be an autapomorphy (Longrich et al., 2018). MGUAN-PA650 also shares, in distal aspect, the trapezoidal humerus shape with a relatively straight dorsal surface that is a feature shared by pteranodontians and not azhdarchoids, which have convex dorsal margins (Longrich et al., 2018). An autapomorphy of *Simurghia robusta* (Longrich et al., 2018) was considered to be an unusually large supracondylar process, and although unfortunately the Angolan humerus is too eroded in that region to definitively assert that it shares such a feature, the edges of the process do form into a distinct ridge that would indicate such a great expansion. In *Alcione elainus* and also in the Angolan humerus, the supracondylar process is shifted proximal to the distal condyles of the humerus, which is a feature of nyctosaurids. In MGUAN-PA650, distal to the supracondylar process is the extreme hypertrophied projection from the entepicondyle, projecting anterodorsally, which is shared feature with pteranodontids, but the extent of the projection distally past the condyles is shared only between the Angolan humerus and *Alcione elainus*, in which it had been considered an autapomorphy. This process also shows significant muscle scarring on the cortical surface of the dorsal side of the bone, making it likely a place of muscle attachment for the carpus and digit extensors (Bennett, 2003), that may indicate a difference in function from other closely-related taxa.

Appendicular pneumatic foramina are absent in basal pterosaurs. However, they are present in the Angola specimens, gnathosaurines, and widespread in attributed “ornithocheiroids” including *Pteranodon* (Andres & Ji, 2008). As evidenced by the pneumatic foramina interspersed throughout their skeletons, these pterosaurs exhibited postcranial pneumatization by pulmonary air sacs, which gave them the lightweight and high-efficiency ventilation capabilities necessary for the strenuous active flapping required by flight (Claessens et al., 2009). The position and extent of these foramina along the pterosaur skeleton can also be a useful tool in distinguishing a clade, because their differing locations on the bones imply independent origins (Bennett, 2001). MGUAN-PA650 exhibits a large ovoid pneumatic foramen on the distal ventral end, proximal to the condyles of the humerus, similar to both *Alcione elainus* and *Simurghia robusta* (Longrich et al., 2018). Another foramen can be seen in distal view, inset into the dorsal margin of the distal fossa, which could be a potential autapomorphy.

With respect to ulnae, the better preserved MGUAN-PA651, when compared with MGUAN-PA661, is identical in morphology. The MGUAN-PA651 ulna exhibits a distal tuberculum on the ventral part of the distal end, which in MGUAN-PA661 is too eroded to be distinguished. In keeping with other pteranodontids, all shafts expand distally (Bennett, 2001; Kellner, 2010; Longrich, 2018). In both Angolan ulnae, the distal expansion is very gradual, with no clear distinction between the shaft and the distal end, which is very similar to *Tethydraco regalis.*

Figure 27. Ulnae of (A. and B.) cf. Pteranodon*, (C)* Cretornis hlavaci *Averianov & Ekrt 2015, (D) Angola specimen MGUAN-PA651, and (E)* Alcione elainus *Longrich et al 2018.*

The MGUAN-PA660 metacarpal IV proximal end fragment and MGUAN-PA654 distal end fragment, although from different individuals, when considered together give an overall good representation of the diagnostic characters of what a complete metacarpal IV for this taxon could be. MGUAN-PA660 appears to have had a subrectangular cross-section at the proximal end, and together with MGUAN-PA654, the shaft of the metacarpal IV appears to have a rounded rectangular shape. MGUAN-PA654 exhibits a flat surface between the distal condyles. This material shares traits with azhdarchids in that both are elongated with a non-tapering distal part of the diaphysis (Unwin & Lu 1997; Godfrey & Currie 2005; Witton & Naish 2008; Averianov 2010, 2014).

The wing digit IV first phalanx MGUAN-PA655 exhibits the presence of a pneumatic foramen on the ventral surface of the proximal end, as in other pterosaurs attributed to the “ornithocheiroids”. The wing digit IV phalanges 2 MGUAN-PA656 and MGUAN-PA652 show an oval shaft cross-section.

The MGUAN-PA163 femur was preliminarily assigned in an earlier publication to the “Ornithocheiroidea” sensu Unwin (2003) (Mateus et al., 2012), which corresponds to the Pteranodontoidea in this analysis, based on the femoral neck-shaft angle of >145 degrees (Unwin, 2003). The neck-shaft angle in the Angola femur lies close to the threshold, at the 146° cutoff mark, making the character difficult to code in this specimen. However, either coding for this character in the matrix did not change the phylogenetic results.

Femur shape was also a character of relative difficulty to code, because no specific angles are put forward to distinguish the character states of “strongly bowed” from “slight curvature” from each other. The Angola taxon was deemed as having a slight sigmoidal curvature in two planes, both anteroposteriorly and mediolaterally. However, either designation did not change the end result of where the Angola taxon was recovered. This medial curvature is also a shared trait with other Pteranodontidae and Nyctosauridae (Longrich et al. 2018). The shaft also expands in diameter gradually, but steadily, from the midpoint of the shaft onward, which is a feature of Nyctosauridae (Williston, 1903).

The MGUAN-PA163 femur also exhibited the following characters: a pneumatic foramen on the proximal end that is found in the “Ornithocheiroidea”, and a constricted femoral neck shape that is found in the Novialoidea.

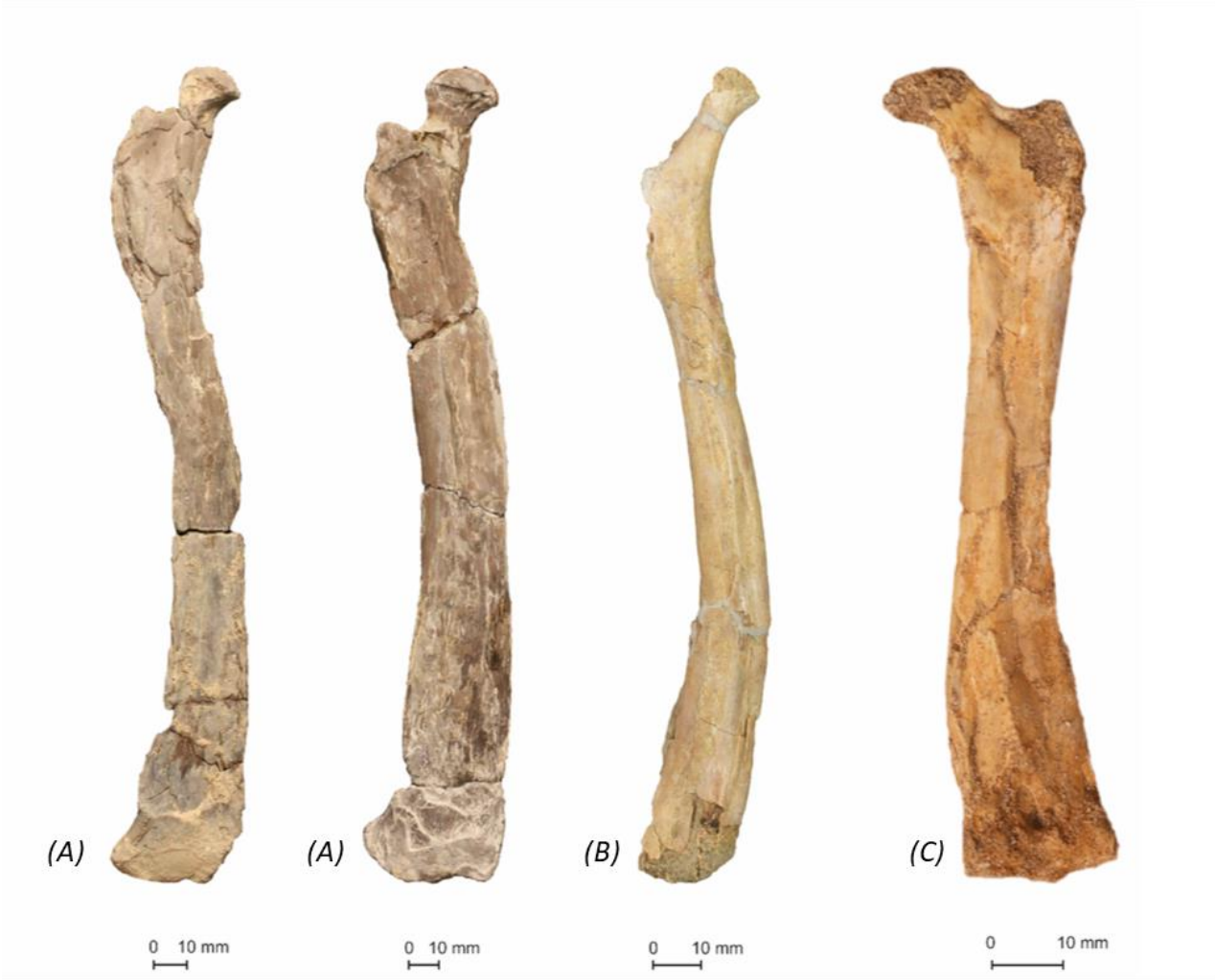

Figure 28. Femora of (A) Pteranodon sp. (*taken from Longrich et al 2018),*
(B) Angola specimen MGUAN-PA163, and Alcione elainus *Longrich et al 2018.*

Beyond the shared morphological features of Pteranodontia and Nyctosauridae throughout the Angolan fossil assemblage, geochronologically the presence of this group in Bentiaba is congruent with the temporal range of Nyctosauridae, which spans the Late Cretaceous (Longrich et al. 2018).

Although it was previously thought that the only pterosaur clade from the Maastrichtian was the Azhdarchidae, recent analyses have yielded other pterosaurs from this time period, namely nyctosaurids and pteranodontids (Longrich et al. 2018).

The paleoecological presence of Nyctosauridae in a marine environment is also congruent with this attribution, because subadults and adults of the pteranodontid *Pteranodon* and *Nyctosaurus* are often found preserved in marine environments (Bennett, 2017). This is in keeping with their piscivorous dietary preferences and also in their being viewed behaviorally as analogs to modern-day seabirds, where they would likely spend time flying around above open-water environments (Brower, 1983; Witton & Habib, 2010). The fact that bones in the Angolan assemblage are in such good condition would also indicate that they had not been transported far after death, and thus close to their actual habitats.

Ontogenetically, no trace of sutures could be found on the distal end of humerus MGUAN-PA650, fusion of the extensor tendon process on all first wing phalanges present in the assemblage appears to be fully completed, and there was no observable immature grain on limb bone shafts (Bennett, 1993). The MGUAN-PA652 digit IV phalanx 2 fragment exhibits possible surface pitting, but it is more likely due to poor preservation than any juvenile bone texturing.

CONCLUSION

Based on these fourteen remarkably well-preserved bones from the fossil assemblage within the locality of Bentiaba, Angola, further insights into the paleobiodiversity of the lower Maastrichtian of this region of Gondwana are drawn. The Late Cretaceous is of great significance when considering the geologic transitions that were in effect, and even more so when considering the resultant ecological shifts that were happening during this time period as well. Pterosaurs were no exception.

The attribution of the Angolan specimens described here to Pteranodontia, and one individual even further to Nyctosauridae, gen. et sp. nov., lends further support to the flourishing of these clades during the Maastrichtian. Although preliminary bone histology has proved fruitful in verifying the presence of subadult animals in the fossil assemblage, even further sampling and analysis is needed to derive more information about the taxa in terms of group dynamics and relative ages. Indeed, further sampling would extend the range of knowledge almost exponentially for many aspects of what exact specimens comprised the ecosystems of the Late Cretaceous. It is the hope of this work that, by illustrating the role that pterosaurs had within the grander paleontological scheme of Angola, further research endeavors will proliferate in the country, and contribute worldwide to the scientific understanding of Pterosauria itself.

Bibliography

Andres, B., Clark, J., & Xu, X. (2014). The earliest pterodactyloid and the origin of the group. *Current Biology, 24*(9), 1011-1016. doi:10.1016/j.cub.2014.03.030

Antunes, M. T. (1964). *O Neocretácico e o Cenozóico do litoral de Angola*. Lisboa, Portugal: Junta de Investigações do Ultramar.

Araújo, R., Polcyn, M.J., Schulp, A. S., Mateus, O., Jacobs,L.L., Gonçalves, A.O. & Morais, M.L. (2015a). A new elasmosaurid from the early Maastrichtian of Angola and the implications of girdle morphology on swimming style in plesiosaurs. *Netherlands Journal of Geosciences - Geologie en Mijnbouw*, *January 2015*, 1-12. doi:10.1017/njg.2014.44

Araújo, R., Polcyn, M.J., Lindgren, J. Jacobs,L.L., Schulp, A. S., Mateus, O., Gonçalves, A.O. & Morais, M.L. (2015b). New aristonectine elasmosaurid plesiosaur specimens from the Early Maastrichtian of Angola and comments on paedomorphism in plesiosaurs. *Netherlands Journal of Geosciences - Geologie en Mijnbouw, February 2015*, 1-16.

Averianov, A. O., Arkhangelsky, M. S. & Pervushov, E. M. (2008). A new Late Cretaceous azhdarchid (Pterosauria, Azhdarchidae) from the Volga Region. *Paleontological Journal, (42)*6, 634–642.

Averianov, A. (2010). The osteology of *Azhdarcho lancicollis* Nessov, 1984 (Pterosauria, Azhdarchidae) from the Late Cretaceous of Uzbekistan. *Proceedings of the Zoological Institute RAS, 314*(3), 264–317.

Averianov, A. (2014). Review of taxonomy, geographic distribution, and paleoenvironments of Azhdarchidae (Pterosauria). *Zookeys, 432*, 1-107. doi:10.3897/zookeys.432.7913

Averianov, A., & Ekrt, B. (2015). *Cretornis hlavaci* Frič, 1881 from the Upper Cretaceous of Czech Republic (Pterosauria, Azhdarchoidea). *Cretaceous Research, 55*, 164–175. https://doi.org/10.1016/j.cretres.2015.02.011

Bailleul, A.M., O'Connor, J., Schweitzer, M.H. (2019). Dinosaur paleohistology: review, trends and new avenues of investigation. *PeerJ, 7*:e7764, https://doi.org/10.7717/peerj.7764

Bardet, N., Pereda-Suberbiola, X., Iarochène, M., Amalik, M., & Bouya, B. (2005). Durophagous Mosasauridae (Squamata) from the Upper Cretaceous phosphates of Morocco, with description of a new species of *Globidens*. *Netherlands J Geosci. 84*(3):167–176.

Barrett, P. M., Butler, R. J., Edwards, N. P., & Milner, Andrew R. (2008). Pterosaur distribution in time and space: an atlas. *Zitteliana, B*(28), 61-107.

Bennett, S. C. (1992). Sexual dimorphism of *Pteranodon* and other pterosaurs, with comments on cranial crests. *Journal of Vertebrate Paleontology, 12*(4), 422-434.

Bennett, S.C. (1993). The ontogeny of *Pteranodon* and other pterosaurs. *Paleobiology, 19*, 92–106.

Bennett, S.C. (1994a). Taxonomy and systematics of the Late Cretaceous pterosaur *Pterandodon* (Pterosauria, Pterodactyloidea). *Occasional Papers of the Museum of Natural History, University of Kansas, Lawrence, 169*, 1–70.

Bennett, S.C. (1995). A statistical study of *Rhamphorhynchus* from the Solnhofen Limestone of Germany, year-classes of a single large species. *Journal of Paleontology, 69*, 569–580.

Bennett, S.C. (1996). Year-classes of pterosaurs from the Solnhofen Limestone of Germany: taxonomic and systematic implications. *Journal of Vertebrate Paleontology, 16*, 432–444.

Bennett, S. C. (2001a). The osteology and functional morphology of the Late Cretaceous pterosaur *Pteranodon*. Part I. General description and osteology. *Paleontographica A, 260*, 1-112.

Bennett, S. C. (2001b). The osteology and functional morphology of the Late Cretaceous pterosaur *Pteranodon*. Part II. Size and functional morphology. *Paleontographica A, 260*, 113-153.

Bennett, S. C. (2003). Morphological evolution of the pectoral girdle of pterosaurs: myology and function. *Geological Society, London, Special Publications, 217*, 191-215.

Bennett, S. C. (2017). New smallest specimen of the pterosaur *Pteranodon* and ontogenetic niches in pterosaurs. *Journal of Paleontology, 92*(2), 254-271.

Benson, R. B. J., Frigot, R. A., Goswami, A., Andres, B., & Butler, R. J. (2014). Competition and constraint drove Cope's rule in the evolution of giant flying reptiles. *Nature Communications, 5*(1), 3567. doi:10.1038/ncomms4567

Benton, M. J., Bouaziz, S., Buffetaut, E., Martill, D., Ouaja, M., Soussi, M., & Trueman, C. (2000). Dinosaurs and other fossil vertebrates from fluvial deposits in the Lower Cretaceous of southern Tunisia. *Palaeogeography, Palaeoclimatology, Palaeoecology, 157*(3), 227-246. doi:10.1016/S0031-0182(99)00167-4

Blackbeard, M. & Yates, A. (2007). The taphonomy of an Early Jurassic dinosaur bonebed in the northern Free State (South Africa) (Abstract). *Journal of Vertebrate Paleontology 27*(3 suppl.), 49A.

Blackburn, D.C. & Sereno, P.C. (2002). Two Early Cretaceous pterosaurs from Africa (Abstract). *Journal of Vertebrate Paleontology, 22*(3 suppl.), 37A.

Broom, R. (1913a). Note on *Mesosuchus browni*, Watson and on a new South African Triassic pseudosuchian (*Euparkeria capensis*). *Rec. Albany Mus. 2*, 394-396.

Brower, J. C. (1983). The aerodynamics of *Pteranodon* and *Nyctosaurus*, two large pterosaurs from the Upper Cretaceous of Kansas. *Journal of Vertebrate Paleontology, 3*(2), 84-124.

Butler, R. J., Benson, R. B. J., & Barrett, P. M. (2013). Pterosaur diversity: Untangling the influence of sampling biases, lagerstätten, and genuine biodiversity signals. *Palaeogeography, Palaeoclimatology, Palaeoecology, 372*, 78-87. doi:10.1016/j.palaeo.2012.08.012

Cavin, L., Tong, H., Boudad, L., Meister, C., Piuz, A., Tabouelle, J., Aarab, M., Amoit, R., Buffetaut, E., Dyke, G. J., Hua, S. & Le Loeuff, J. (2010). Vertebrate assemblages from the early Late Cretaceous of southeastern Morocco: An overview. *Journal of African Earth Sciences, 57*(5), 391-412. doi:10.1016/j.jafrearsci.2009.12.007

Chinsamy, A., Codorniú, L., & Chiappe, L. (2009). Palaeobiological Implications of the bone histology of *Pterodaustro guinazui*. *The Anatomical Record, 292*(9), 1462–1477. doi:10.1002/ar.20990

Choffat, P. (1890). Nouvelles publications sur les dépots mésozoïques du Brésil. *Rev. Sc. Nat. Soc., I*, 115-121.

Choffat, P. (1905). *Contributions a la connaisance géologique des colonies Portugasies d'Afrique*. Imprimerie de L'Académie Royale des Sciences.

Claessens, L., O'Connor, P. M., & Unwin, D. M. (2009). Respiratory evolution facilitated the origin of pterosaur flight and aerial gigantism. *PloS One, 4*(2), e4497. doi:10.1371/journal.pone.0004497

Cohen, J. E., Hunt, T. C., Frederickson, J. A., Berry, J. L., & Cifelli, R. L. (2018). Azhdarchid pterosaur from the Upper Cretaceous (Turonian) of Utah, USA. *Cretaceous Research, 86*, 60-65. doi:10.1016/j.cretres.2017.12.013

Cooper, M.R. (2003a). Upper Cretaceous (Turonian-Coniacian) ammonites from São Nicolau, Angola. *Annals of the South African Museum, 110*(2), 89-146.

Cooper, M.R., (2003b). Stratigraphy and paleontology of the Upper Cretaceous (Santonian) Baba Formation at São Nicolau, Angola. *Annals of the South African Museum, 110*(3), 147-170.

Costa, F. R., & Kellner, A. W. A. (2009). On two pterosaur humeri from the Tendaguru beds (Upper Jurassic, Tanzania). *Anais Da Academia Brasileira De Ciências, 81*(4), 813-818. doi:10.1590/S0001-37652009000400017

Costa, F. R., Sayão, J. M., & Kellner, A. W. A. (2014). New pterosaur material from the Upper Jurassic of Tendaguru (Tanzania), Africa. *Historical Biology, 27*(6), 646-655. doi:10.1080/08912963.2014.901314

Cullinane, D.M. (2002). The role of osteocytes in bone regulation: Mineral homeostasis versus mechanoreception. *The Journal of Musculoskeletal and Neuronal Interactions, 2*(3), 242-244.

Currey, J. D. & Alexander, R. McN. (1985). The thickness of the walls of tubular bones. *Journal of the Zoological Society of London, 206*, 453–468.

Dal Sasso, C. & Pasini, G. (2003). First record of pterosaurs (Diapsida, Archosauromorpha, Pterosauria) in the Middle Jurassic of Madagascar. *Atti della Società Italiana di scienze naturali e del Museo Civico di Storia Naturale di Milano, 144*(II): 281-296.

de Margerie, E. (2002). Laminar bone as an adaptation to torsional loads in flapping flight. *Journal of Anatomy, 201*, 521-526.

de Ricqlès, A. J., Padian, K., Horner, J. R., & Francillon-Vieillot, H. (2000). Palaeohistology of the bones of pterosaurs (Reptilia: Archosauria): anatomy, ontogeny, and biomechanical implications. *Zoological Journal of the Linnean Society, 129*(3), 349-385.

Dean, C. D., Mannion, P. D., Butler, R. J., & Benson, R. (2016). Preservational bias controls the fossil record of pterosaurs. *Palaeontology, 59*(2), 225-247. doi:10.1111/pala.12225

do Nascimento, J. P. (1898). *Exploração Geographica e Minerologica no Districto de Mossamedes em 1894-1895*. Lisboa Typ. da Companhia Nacional Editora.

Eaton G.F. (1910). Osteology of *Pteranodon*. *Memoirs of the Connecticut Academy of Arts and Sciences, 2*:1-38.

Fanti, F., Contessi, M., & Franchi, F. (2012). The "Continental Intercalaire" of southern Tunisia: Stratigraphy, paleontology, and paleoecology. *Journal of African Earth Sciences, 73-74*, 1-23.

Flynn, J.J., Fox, S.R., Parrish, J., Ranivoharimanana, L. & Wyss, A.R. (2006). Assessing diversity and paleoecology of a Middle Jurassic microvertebrate assemblage from Madagascar. *New Mexico Museum of Natural History and Science Bulletin, 37*, 476-489.

Galton, P. M. (1980). Avian-like tibiotarsi of pterodactyloids (Reptilia: Pterosauria) from the Upper Jurassic of East Africa. *Paläontologische Zeitschrift, 54*(3/4), 331-342.

Gauthier, J. A. (1986). Saurischian monophyly and the origin of birds. In K. Padian (Ed.), *The Origin of Birds and the Evolution of Flight* (pp. 1-55). California Academy of Sciences, Memoir 8.

Godfrey, S. J. & Currie, P. J. (2005). Pterosaurs of the Dinosaur Park Formation. In P. J. Currie & E. B. Koppelhus (Eds.), *Dinosaur Provincial Park: A Spectacular Ancient Ecosystem Revealed* (pp. 292-311). Indiana University Press.

Goloboff, P. & Catalano, S. (2016). T.N.T., version 1.5, with a full implementation of phylogenetic morphometrics [computer software]. Cladistics. doi:10.1111/cla.12160.

Goloboff, P.A., Farris, J.S., and Nixon, K.C. (2008). T.N.T., a free program for phylogenetic analysis. *Cladistics, 24*, 774–786.

Google Earth 9.3.105.0. 2020. Angola Pterosaur Localities. 3D map, viewed 29 February 2020. https://earth.google.com/web/@4.26720835,12.362375,24.51550583a,1384.69827754d,3y,0h,0t,0r.

Huntley B. J. (2019). Angola in outline: physiography, climate and patterns of biodiversity. In Huntley B., Russo V., Lages F., & Ferrand N. (Eds.), *Biodiversity of Angola* (pp.15-42). Springer Open.

Ibrahim, N., Unwin, D. M., Martill, D. M., Baidder, L., & Zouhri, S. (2010). A new pterosaur (Pterodactyloidea: Azhdarchidae) from the Upper Cretaceous of Morocco. *PloS One, 5*(5), e10875. doi:10.1371/journal.pone.0010875

Ifrim, C., Padilla Gutiérrez, J. M., Elgin, R. A., González González, A. H., Giersch, S., Frey, E., & Stinnesbeck, W. (2012). A new specimen of nyctosaurid pterosaur, cf. *Muzquizopteryx* sp. from the Late Cretaceous of northeast Mexico. *Revista Mexicana De Ciencias Geológicas, 29*(1), 131-139.

Jacobs, L.L., Mateus, O., Polcyn, M.J., Schulp, A.S., Antunes, M.T., Morais, M.L. & Tavares, T. da S. (2006). The occurrence and geological setting of Cretaceous dinosaurs, mosasaurs, plesiosaurs, and turtles from Angola. *Journal of the Paleontological Society of Korea, 22*: 91-110.

Jacobs, L.L., Mateus, O., Polcyn, M.J., Schulp, A.S., Scotese, C.R., Goswami, A., Ferguson, K.M., Robbins, J.A., Vineyard, D.P., and Neto, A.B. (2009). Cretaceous paleogeography, and amniote biogeography of the low and mid-latitude South Atlantic Ocean. *Bulletin of the Geological Society of France, 180*: 333-341.

Jacobs, L. L., Polcyn, M. J., Mateus, O., Schulp, A. S., Gonçalves, A. O., & Morais, M. L. (2016). Post-Gondwana Africa and the vertebrate history of the Angolan Atlantic coast. *Memoirs of Museum Victoria, 74*, 343-362. doi:10.24199/j.mmv.2016.74.24

Jacobs, M. L., Martill, D. M., Ibrahim, N., & Longrich, N. (2019). A new species of *Coloborhynchus* (Pterosauria, Ornithocheiridae) from the mid-Cretaceous of north Africa. *Cretaceous Research, 95*: 77-88. doi:10.1016/j.cretres.2018.10.018

Kellner, A.W.A. & Mader, B.J. (1996). First report of pterosauria (Pterodactyloidea, Azhdarchidae) from Cretaceous rocks of Morocco (Abstract). *Journal of Vertebrate Paleontology, Illinois, 16*(3): 45A.

Kellner, A.W.A. & Mader, B.J. (1997). Archosaur teeth from the Cretaceous of Morocco. *Journal of Paleontology, 71*(3), 525-527. Retrieved from http://www.jstor.org/stable/1306632

Kellner, A. W. A., Mello, A. M. S., & Ford, T. (2007). A survey of pterosaurs from Africa with the description of a new specimen from Morocco. In I.S. Carvalho, et al. (Eds.), *Paleontologia: Cenários da Vida*, *1*, 257-267.

Kellner, A. W. A. (2010). Comments on the Pteranodontidae (Pterosauria, Pterodactyloidea) with the description of two new species. *Anais da Academia Brasileira de Ciências, 82*(4), 1063-1084.

Knoll, F. (2000). Pterosaurs from the Lower Cretaceous (?Berriasian) of Anoual, Morocco. *Annales De Paléontologie, 86*(3), 157-164. doi:10.1016/S0753-3969(00)80006-3

Lamm, E. (2013). Preparation and sectioning of specimens. In K. Padian & E. Lamm (Eds.), *Bone Histology of Fossil Tetrapods* (pp.55-160). University of California Press.

Lapão, L. G. P. (1972). *Carta Geologica*. Direcção Provincial dos Serviços de Geologia e Minas.

Lee, A.H., Huttenlocker, A.K., Padian, K. & Woodward, H.N. (2013). Analysis of growth rates. In K. Padian & E. Lamm (Eds.), *Bone Histology of Fossil Tetrapods* (pp.195-215). University of California Press.

Longrich, N. R., Martill, D. M., & Andres, B. (2018). Late Maastrichtian pterosaurs from North Africa and mass extinction of Pterosauria at the Cretaceous-Paleogene boundary. *PLoS Biology, 16*(3), e2001663. doi:10.1371/journal.pbio.2001663

Lourenço, J. M. C. (2019). Foreward. In B. Huntley, V., Russo, F. Lages & N. Ferrand (Eds.), *Biodiversity of Angola* (pp.vii-viii). Springer Open.

Mader, B. & Kellner, A. W. A. (1999). A new anhanguerid pterosaur from the Cretaceous of Morocco. *Boletim do Museu Nacional, 45,* 1-11.

Marsh, O. C. (1876). Principal characters of American pterodactyls. *American Journal of Science, 3*(12), 479–480.

Martill, D. M. & Ibrahim, N. (2015). An unusual modification of the jaws in *cf. Alanqa*, a mid Cretaceous azhdarchid pterosaur from the Kem Kem beds of Morocco. *Cretaceous Research*, *53*, 59-67.

Martill, D. M., Ibrahim, N., & Bouaziz, S. (2018). A giant pterosaur in the early Cretaceous (Albian) of Tunisia. *Journal of African Earth Sciences, 147*, 331-337. doi:10.1016/j.jafrearsci.2018.05.008

Martill, D. M., Smith, R., Unwin, D. M., Kao, A., McPhee, J. & Ibrahim, N. (2020). A new tapejarid (Pterosauria, Azhdarchoidea) from the mid-Cretaceous Kem Kem beds of Takmout, southern Morocco. *Cretaceous Research, 112.*

Martill, D. M., Unwin, D. M., Ibrahim, N., & Longrich, N. (2018). A new edentulous pterosaur from the cretaceous Kem Kem beds of south eastern Morocco. *Cretaceous Research, 84*, 1-12. doi:10.1016/j.cretres.2017.09.006

Masse, P. & Laurent, O. (2015). Geological exploration of Angola from Sumbe to Namibe: A review at the frontier between geology, natural resources and the history of geology. *Comptes Rendus Geoscience, 348*(1), 80-88.

Mateus, O., Jacobs, L., Polcyn, M., Schulp, A. S., Vineyard, D., Neto, A. B., & Antunes, M. T. (2009). The oldest African eucryptodiran turtle from the Cretaceous of Angola. *Acta Palaeontologica Polonica, 54*(4), 581-588. doi:10.4202/app.2008.0063

Mateus, O., Polcyn, M.J., Jacobs, L.L., Araújo, R., Schulp, A.S., Marinheiro, J., Pereira, B., & Vineyard, D. (2012). Cretaceous amniotes from Angola: dinosaurs, pterosaurs, mosasaurs, plesiosaurs, and turtles. In P. H. Hurtado, F. T. Fernández-Baldor & J. I. Canudo Sanagustín (Eds.), *Actas de V Jornadas Internacionales sobre Paleontología de Dinosaurios y su Entorno* (71-105). Burgos: Colectivo Arqueológico y Paleontológico de Salas, C.A.S.

Mateus, O., Callapez, P.M., Polcyn, M.J., Schulp, A.S., Gonçalves, A. O. & Jacobs, L.L. (2019). The fossil record of biodiversity in Angola through time: a paleontological perspective. In B. Huntley, V. Russo, F. Lages & N. Ferrand (Eds.), *Biodiversity of Angola* (pp.53-76). Springer Open.

Monteillet, J., Lappartient, J. R. & Taquet, P. (1982). Un ptérosaurien géant dans le Crétacé supérieur de Paki (Sénégal). *C. R. Acad. Sc. Paris, 295*(3), 167-172.

Novas, F. E. (1993). New information on the systematics and postcranial skeleton of *Herrerasaurus ischigualastensis* (Theropoda; Herrerasauridae) from the Ischigualasto Formation (Upper Triassic) of Argentina. *Journal of Vertebrate Paleontology, 13*, 400-423.

Ntamak-Nida, M.J., Ketchemen-Tandia, B., Ewane, R.V., Lissok, J.P. & Courville, P. (2006). Nouvelles données sur les Mollusques et autres macro-organismes campaniens de Sikoum (Centre-Est du sous bassin de Douala-Cameroun): intérêts bio-chronologiques et paléo-écologiques. *Africa Geoscience Review, 13*(4), 385-394.

O'Connor, P. M., Sertich, J. J. W., & Manthi, F. K. (2011). A pterodactyloid pterosaur from the Upper Cretaceous Lapurr sandstone, West Turkana, Kenya. *Anais Da Academia Brasileira De Ciências, 83*(1), 309-315. doi:10.1590/S0001-37652011000100019

Padian, K. (1995). Bone histology determines identification of a new fossil taxon of pterosaur (Reptilia: Archosauria). *Comptes rendus de l'Académie des sciences: La vie des sciences, 320*(1), 77-84.

Padian, K. 2004. The nomenclature of Pterosauria (Reptilia, Archosauria). In Laurin, M. (ed) First *International Phylogenetic Nomenclature Meeting* (pp. 27). Paris: Muséum National d'Histoire Naturelle.

Padian, K. (2013). Why study the bone microstructure of fossil tetrapods? In K. Padian & E. Lamm (Eds.), *Bone Histology of Fossil Tetrapods* (pp.1-11). University of California Press.

Padian, K. & Smith, M. (1992). New light on Late Cretaceous pterosaur material from Montana. *Journal of Vertebrate Paleontology, 12*(1), 87-92.

Padian, K., Horner, J., & De Ricqlès, A. (2004). Growth in small dinosaurs and pterosaurs: the evolution of archosaurian growth strategies. *Journal of Vertebrate Paleontology, 24*(3), 555-571.

Pereda Suberbiola, X., Bardet, N., Jouve, S., Iarochene, M., Bouya, B. & Amaghzaz, M. (2003). A new azhdarchid pterosaur from the Late Cretaceous phosphates of Morocco. *Geological Society, London, Special Publications, 217*, 79-90.

Polcyn, M. J., Jacobs, L. L., Schulp, A. S., & Mateus, O. (2010). The north African mosasaur *Globidens phosphaticus* from the Maastrichtian of Angola. *Historical Biology, 22*, 175-185.

Prondvai, E., Stein, K. H. W., Osi, A., & Sander, M.P. (2012). Life history of *Rhamphorhynchus* inferred from bone histology and the diversity of pterosaurian growth strategies. *PLoS ONE, 7*(2) doi:10.1371/journal.pone.0031392

Prondvai E. & Stein K. H. W. (2014). Medullary bone-like tissue in the mandibular symphyses of a pterosaur suggests non-reproductive significance. *Scientific Reports, 4*(6253), 1-9.

Prondvai, E. (2017). Medullary bone in fossils: Function, evolution and significance in growth curve reconstructions of extinct vertebrates. *Journal of Evolutionary Biology, 30*(3), 440–460.

Reck, H. (1931). Die deutschostafrikanischen flugsaurier . *Centralblatt für Mineralogie, Geologie und Paläontologie, 1931*, 321-336.

Rocha, R. B. D. & Kullberg, J. C. (2008). Paul Léon Choffat: Uma vida dedicada à ciência. In J.J.C. Pais, R.E.B. Rocha & J. C. R. Kullberg (Eds.), *Paul Choffat na Geologia Portuguesa* (pp. 23-44). Universidade Nova de Lisboa / Instituto Nacional de Engenharia, Tecnologia e Inovação.

Rodrigues, T., Kellner, A. W. A., Mader, B. J., & Russell, D. A. (2011). New pterosaur specimens from the Kem Kem beds (Upper Cretaceous, Cenomanian) of Morocco. *Rivista Italiana Di Paleontologia e Stratigrafia, 117*(1) doi:10.13130/2039-4942/5967

Rodrigues, T., Kellner, A. W. A. (2013). Taxonomic review of the Ornithocheirus complex (Pterosauria) from the Cretaceous of England. *ZooKeys, 308*, 1–112. doi: 10.3897/zookeys.308.5559

Romer, A. S. (1978). *Osteology of the Reptiles*. Chicago: The University of Chicago Press.

Sampson, S. D., Witmer, L. M., Forster, C. A., Krause, D. W., O'Connor, P. M., Dodson, P., & Ravoavy, F. (1998). Predatory dinosaur remains from Madagascar: Implications for the Cretaceous biogeography of Gondwana. *Science, 280*(5366), 1048-1051. doi:10.1126/science.280.5366.1048

Sayão, J. M. (2003). Histovariability in bones of two pterodactyloid pterosaurs from the Santana Formation, Araripe Basin, Brazil: preliminary results. *Geological Society, London, Special Publications, 217*(1), 335-342.

Schulp, A. S., Polcyn, M. J., Mateus, O. Jacobs, L. L., Morais, M. L., & da Silva Tavares, T. (2006). New mosasaur material from the Maastrichtian of Angola, with notes on the phylogeny, distribution and palaeoecology of the genus *Prognathodon*. *Publicaties van het Natuurhistorisch Genootschap in Limburg Reeks XLV aflevering, 1*, 57-67.

Schulp, A. S., Polcyn, M. J., Mateus, O., Jacobs, L. L., and Morais, M. L. (2008). A new species of *Prognathodon* (Squamata, Mosasauridae) from the Maastrichtian of Angola, and the affinities of the mosasaur genus *Liodon*. *Proceedings of the Second Mosasaur Meeting, Fort Hays Studies Special Issue, 3*, 1-12.

Sereno, P. C., Forester, R. R. & Monetta, A. M. (1993). Primitive dinosaur skeleton from Argentina and the early evolution of dinosaurs. *Nature, 361*, 64-66.

Sereno, P. C., & Brusatte, S. L. (2008). Basal abelisaurid and carcharodontosaurid theropods from the Lower Cretaceous Elrhaz Formation of Niger. *Acta Palaeontologica Polonica, 53*(1), 15-46. doi:10.4202/app.2008.0102

Steel, L. (2008). The palaeohistology of pterosaur bone: an overview. In D.W.E. Hone &E. Buffetaut (Eds.), *Zitteliana: An International Journal of Paleontology and Geobiology, B28* (pp.109 125). Bayerische Staastssammlung fur Palaontologie und Geologie.

Strganac, C., Jacobs, L. L., Polcyn, M. J., Mateus, O., Myers, T. S., Salminen, J., May, S. R., Araújo, R., Ferguson, K. M., Olímpio Gonçalves, A., Morais, M. L., Schulp, A. S. & da Silva Tavares, T. (2014). Geological setting and paleoecology of the Upper Cretaceous Bench 19 marine vertebrate bonebed at Bentiaba, Angola. *Netherlands Journal of Geosciences, 94*(1), 121 136.

Strganac, C., Jacobs, L. L., Polcyn, M. J., Ferguson, K. M., Mateus, O., Olímpio Gonçalves, A., Morais, M. L. & da Silva Tavares, T. (2015). Stable oxygen isotope chemostratigraphy and paleotemperature regime of mosasaurs at Bentiaba, Angola. *Netherlands Journal of Geosciences, February 2015*. doi:10.1017/njg.2015.1

Swinton, W. E. (1948). A Cretaceous pterosaur from the Belgian Congo. *Bull. Soc. Belge Geol. Paléont. Hydr. Liège, 77*, 234–238.

Upchurch, P., Andres, B., Butler, R. J., & Barrett, P. M. (2015). An analysis of pterosaurian biogeography: Implications for the evolutionary history and fossil record quality of the first flying vertebrates. *Historical Biology, 27*(6), 697-717. doi:10.1080/08912963.2014.939077

Unwin, D. M., & Heinrich, W. (1999). On a pterosaur jaw from the Upper Jurassic of Tendaguru (Tanzania). *Fossil Record, 2*(1), 121-134. doi:10.5194/fr-2-121-1999

Unwin, D. M. & Lu, J. (1997). On *Zhejiangopterus* and the relationships of pterodactyloid pterosaurs. *Historical Biology, 12*, 199-210.

U.S. Geological Survey. (2002). Geological Map of Africa. Retrieved from http://www.uni-koeln.de/sfb389/e/e1/

Wellnhofer, P. & Buffetaut, E. (1999). Pterosaur remains from the Cretaceous of Morocco. *Palaontologische Zeitschrift, 73*(1/2), 133-142.

Williston, S. W., & Museum, F. C. (1903). *On the osteology of Nyctosaurus (Nyctodactylus), with notes on American pterosaurs*. Chicago: Field Columbian Museum Geological Series.

Witton, M. P. (2013). *Pterosaurs: Natural history, evolution, anatomy*. Princeton: Princeton University Press.

Witton, M. P., & Habib, M. B. (2010). On the size and flight diversity of giant pterosaurs, the use of birds as pterosaur analogues and comments on pterosaur flightlessness. *PloS One, 5*(11), e13982. doi:10.1371/journal.pone.0013982

Witton, M. P., & Naish, D. (2008). A reappraisal of azhdarchid pterosaur functional morphology and paleoecology. *PloS One, 3*(5), e2271. doi:10.1371/journal.pone.0002271

Woodward, H. N., Padian, K. & Lee, A. H. (2013). Skeletochronology. In K. Padian & E. Lamm (Eds.), *Bone Histology of Fossil Tetrapods* (pp.195-215). University of California Press.

APPENDIX:

Data Matrix

nstates cont;

nstates 32 ;

xread 'Data saved from TNT'

271 134

&[cont]

Euparkeria_capensis 0.184 0.057 0.646 0.036 0.000 0.000 0.679 0.453 ? ? 0.419 0.612 0.144 1.000 0.665 0.056 0.088 0.074 ? 0.398 0.044 0.019 0.446 0.000 0.079 0.294 0.795 ? 0.000 ? 0.204 0.628 ? 0.042 0.082 0.712 ? ? ? ? ? 0.130 0.000 0.631 0.014 0.995 0.655 0.241 0.056 0.148 0.216

Ornithosuchus_longidens 0.093 0.137 0.564 0.043 0.397 ? 1.000 0.425 ? ? 0.540 0.454 ? ? 0.677 0.032 0.666 0.000 ? ? 0.096 0.026 0.153 0.125 0.087 0.188 0.530 ? 0.135 ? 0.165 0.999 ? 0.001 0.106 0.235 ? ? ? ? ? 0.112 0.022 0.668 0.000 0.995 0.831 0.434 0.294 0.379 0.685

Herrerasaurus_ischigualastensis 0.133 ? 0.795 0.010 0.071 0.186 0.583 0.572 ? ? 0.374 0.851 ? 0.863 0.726 0.064 0.704 0.118 ? 0.417 0.062 ? 0.128 0.000 0.107 0.105 ? ? 0.061 ? 0.208 0.788 ? 0.021 0.051 0.487 0.000 ? ? ? ? 0.085 0.078 1.000 0.061 1.000 0.932 0.334 0.071 0.142 ?

Scleromochlus_taylori ? 0.182 0.633 0.161 0.080 ? 0.495 0.937 ? ? 0.995 1.000 0.122 0.697 0.523 0.050 0.072 0.214 ? 0.390 0.046 0.000 0.733 0.250 0.121 0.216 0.999 ? 0.350 ? 0.228 0.525 ? 0.000 0.000 1.000 0.001 ? ? ? ? 0.000 0.238 0.754 0.199 0.995 0.828 0.529 0.321 0.255 0.340

Eudimorphodon_ranzii 0.166 0.267 0.473 0.280 0.399 0.415 0.079 0.000 ? ? 0.757 ? ? ? 0.814 0.109 0.042 0.250 ? 0.754 0.010 0.075 0.760 0.250 ? ? 0.315 ? 0.327 ? 0.632 0.469 0.292 0.170 0.487 0.572 ? ? ? ? 0.271 ? ? 0.245 ? ? ? ? ? ? ?

Eudimorphodon_rosenfeldi 0.076 0.231 0.344 0.280 0.504 0.573 0.208 0.384 ? ? 1.000 0.430 ? 0.392 0.664 0.054 0.254 0.178 ? 0.802 0.012 0.077 0.801 ? 0.835 0.978 0.250 ? 0.386 ? 0.550 0.448 0.249 0.114 0.425 0.465 0.406 0.410 0.682 0.760 ? ? 0.132 0.118 0.490 0.918 0.623 1.000 0.220 0.465 1.000

Eudimorphodon_cromptonellus ? ? ? ? ? ? ? ? ? ? ? ? ? ? ? 0.036 ? ? ? ? ? ? ? ? ? 0.409 0.596 ? ? ? 0.368 0.603 ? 0.116 0.420 0.485 0.268 0.593 0.827 ? ? ? ? 0.338 0.168 0.679 1.000 ? ? ? ?

Peteinosaurus_zambellii ? ? ? ? ? ? ? ? ? ? ? ? ? ? ? 0.137 ? 0.580 ? 0.341 ? 0.716 ? ? 0.163 ? ? 0.865 0.488 ? ? ? ?

Caviramus_schesaplanensis ? ? ? ? ? ? ? ? ? ? ? ? ? ? ? 0.056 0.116 0.075 ?

Raeticodactylus_filisurensis 0.129 0.201 0.511 0.286 0.271 0.277 0.445 0.478 ? ? 0.482 0.593 ? ? 0.644 0.066 0.229 0.124 ? 0.589 0.028 0.109 0.871 ? ? ? ? ? 0.562 ? 0.515 ? 0.127 ? ? ? 0.381 0.431 0.726 ? ? ? ? 0.040 0.535 0.431 0.621 ? ? ? ?

Austriadactylus_cristatus 0.206 0.198 0.373 0.167 0.465 0.269 0.291 0.305 ? ? 0.481 0.301 0.216 0.576 0.679 0.089 0.113 0.236 ? 0.662 0.015 0.050 ? ? 0.456 0.492 0.335 ? 0.385 ? 0.567 0.527 ? 0.107 ? ? 0.333 0.487 0.742 0.764 ? ? ? ? ? ? ? ? ? ? ?

Preondactylus_buffarinii 0.162 0.628 0.495 0.111 0.671 0.519 0.500 0.340 ? ? 0.473 ? ? ? 0.794 0.058 0.036 0.348 ? 0.601 0.024 0.047 0.505 0.250 1.000 0.511 ? ? 0.779 ? 0.565 0.498 0.172 0.110 0.435 0.649 0.301 0.597 0.846 0.683 1.000 ? 0.194 0.305 0.432 0.610 0.583 0.944 0.468 0.895 ?

Dimorphodon_macronyx 0.176 0.407 0.531 0.202 0.999 0.143 0.495 0.079 ? ? 0.204 ? ? ? 0.732 0.113 0.116 0.201 0.000 0.716 0.018 0.093 0.718 0.250 0.239 0.788 0.321 ? 0.379 ? 0.513 0.411 0.102 0.108 0.547 0.756 0.311 0.546 0.933 0.884 0.227 0.484 0.221 0.234 0.507 0.430 0.405 0.712 0.607 0.999 0.954

Parapsicephalus_purdoni 0.203 ? ? ? ? 0.260 ? 0.530 ? ? 0.380 ? 0.162 0.791 ?

Campylognathoides_liasicus 0.152 0.166 0.442 0.245 0.647 0.249 0.137 0.454 ? ? 0.722 0.421 0.004 0.602 0.747 0.044 0.106 0.213 ? 0.740 0.038 0.073 1.000 0.375 0.325 0.543 0.230 ? 0.265 ? 0.474 0.377 0.271 0.116 0.659 0.471 0.514 0.527 0.634 0.650 0.065 0.371 0.617 0.100 0.333 0.561 0.711 0.451 0.104 0.197 0.533

Campylognathoides_zitteli 0.089 0.000 0.608 0.336 0.465 0.388 0.216 0.488 ? ? 0.650 ? ? ? 0.724 0.054 0.176 0.112 ? 0.694 0.032 0.025 0.739 0.375 0.223 1.000 0.425 ? 0.162 ? 0.334 0.498 0.196 0.101 0.344 0.559 0.827 0.506 0.516 0.526 ? 0.373 0.652 ? 0.395 0.942 0.693 0.453 0.236 0.218 0.735

Sericipterus_wucaiwanensis 0.224 0.211 ? 0.322 ? ? ? ? ? ? ? 0.488 ? ? ? 0.016 ? ? ? ? 0.057 0.084 0.800 ? ? ? 0.135 ? 0.210 ? ? 0.713 ? ? ? ? 0.350 0.391 ? 0.815 ? ? ? ? ? ? ? ? ? ? ?

Angustinaripterus_longicephalus 0.218 ? 0.488 0.334 0.462 0.999 0.929 1.000 ? ? 0.508 ? ? ? 0.616 0.024 0.143 0.299 ?

Harpactognathus_gentryii 0.185 ? ? ? ? ? ? ? ? ? ? ? ? ? ? 0.016 ?

Cacibupteryx_caribensis 0.138 ? ? ? ? 0.245 ? 0.728 ? ? 0.311 ? 0.088 0.747 ?
0.028 ?
? ? ? ? ? ? ? ? ? ? ?

Rhamphorhynchus_muensteri 0.183 0.294 0.298 0.374 0.241 0.410 0.000 0.689 ? ? 0.628 0.325
0.033 0.212 0.698 0.024 0.562 0.252 ? 0.744 0.032 0.067 0.780 0.250 0.256 0.699 0.198 ? 0.243
0.352 0.778 0.493 0.136 0.150 0.609 0.549 0.713 0.410 0.554 0.763 0.134 0.601 0.581 0.172 0.509
0.406 0.824 0.916 0.529 0.507 0.935

Qinglongopterus_guoi ? 0.096 0.726 0.359 0.543 ? 0.604 ? ? ? ? ? ? 0.661 0.779
0.016 0.429 0.343 ? 0.690 0.013 0.064 0.588 0.250 0.302 0.311 0.097 ? 0.230 ? 0.745 0.714
0.044 0.133 0.310 0.624 0.497 0.471 0.631 0.506 0.261 ? ? 0.042 0.345 0.587 0.635 0.347 0.533
0.244 0.591

Nesodactylus_hesperius ? ? ? ? ? ? ? ? ? ? ? ? ? ? ? ? ? ? ?
? 0.018 0.076 0.879 0.250 0.106 0.629 0.099 ? 0.274 0.271 0.845 0.358 ? 0.155 0.452 0.784
0.833 ? ? ? 0.149 ? ? ? ? ? ? ? ? ? ?

Dorygnathus_banthensis 0.179 0.251 0.551 0.405 0.662 0.533 0.400 0.308 ? ? 0.445 0.287
0.240 0.508 0.771 0.028 0.411 0.204 ? 0.649 0.033 0.099 0.858 0.250 0.259 0.633 0.295 ? 0.321
? 0.768 0.634 0.090 0.131 0.573 0.474 0.338 0.655 0.890 0.877 0.157 0.541 0.536 0.155 0.432 0.501
0.603 0.377 0.588 0.247 0.549

Scaphognathus_crassirostris 0.103 0.331 0.327 0.281 0.343 0.168 0.345 0.301 ? ? 0.480 0.535
? 0.347 0.656 0.012 0.237 0.130 ? 0.570 0.013 0.098 0.976 0.250 0.135 0.461 0.266 ? 0.350 ?
0.830 0.593 0.084 0.129 0.557 0.640 0.329 0.547 0.741 0.866 0.186 0.404 0.603 0.241 0.257 0.245
0.502 0.258 0.121 0.050 0.591

Sordes_pilosus 0.170 0.343 0.242 0.206 0.408 0.236 0.508 0.469 ? ? 0.532 0.641 0.042 0.633
0.597 0.014 0.380 0.295 ? 0.480 0.000 0.085 0.915 0.375 0.225 0.395 0.183 ? 0.540 ? 0.783
0.623 0.109 0.095 0.592 0.630 0.291 0.539 0.729 0.662 0.668 0.363 0.695 0.120 0.476 0.275 0.486
0.139 0.139 0.061 0.116

Darwinopterus_modularis 0.276 0.621 0.420 0.373 ? ? ? ? 0.569 0.387 0.527 0.282 ? ?
0.574 0.042 0.259 0.530 ? 0.575 0.067 0.089 0.559 0.375 0.492 0.737 0.148 ? 0.416 ? 0.648
0.686 0.438 0.164 0.542 0.798 0.324 0.600 0.914 0.979 0.079 0.601 0.659 0.209 0.425 ? 0.461
0.194 0.370 0.144 0.318

Wukongopterus_lii 0.231 ? 0.468 0.289 ? ? ? ? 0.684 ? ? ? ? ? 0.587 0.044
0.223 0.230 ? ? 0.069 ? ? 0.375 ? 0.567 0.290 ? ? ? 0.754 ? 0.010 0.161 ? 0.633
0.323 0.690 0.970 1.000 ? ? 0.715 0.194 0.577 0.235 0.477 0.324 0.999 0.147 0.287

Pterorhynchus_wellnhoferi 0.119 0.848 0.581 0.347 ? ? ? ? 0.728 0.521 0.551 ? ? 0.321
0.611 0.026 0.205 0.259 ? 0.499 0.035 0.190 0.474 0.375 0.366 0.754 ? ? 0.887 ? 0.869
0.443 0.199 0.146 0.692 ? 0.302 0.698 0.836 0.702 ? 0.554 0.636 0.134 0.273 0.225 ? ? ?
? ?

Changchengopterus_pani ? 0.010 0.029 0.365 0.125 0.107 0.243 0.239 ? 0.188 ? 0.614 0.788 0.521 0.165 0.540 ? 0.427 0.526 0.692 ? ? ? ? 0.136 0.292 0.371 0.538 ? ? ? ?

Batrachognathus_volans ? 0.159 0.681 0.000 ? ? ? ? 0.100 0.000 0.690 0.550 0.318 ? 0.772 0.036 0.018 0.192 ? ? 0.010 0.056 0.621 ? ? ? 0.145 ? 0.640 ? 0.759 0.568 ? 0.069 ? 0.779 ? ? ? ? ? ? ? 0.000 0.646 0.160 0.614 0.197 0.000 0.076 0.259

Jeholopterus_ningchengensis 0.101 0.031 0.841 0.077 ? ? ? ? 0.240 0.006 0.474 ? 0.225 ? 0.842 0.016 0.064 0.229 ? 0.689 0.007 0.055 0.475 0.375 0.000 0.010 0.394 ? 0.640 ? 0.501 0.563 0.062 0.069 0.267 0.760 0.410 0.362 0.337 0.138 0.159 ? 0.830 0.055 0.258 0.354 0.770 0.187 0.002 0.062 0.107

Anurognathus_ammoni 0.000 0.208 0.524 0.024 ? ? ? ? 0.102 0.035 0.556 0.665 0.251 ? 0.579 0.018 0.177 0.226 ? 0.347 0.025 0.118 0.357 0.375 0.022 0.012 0.238 ? 0.688 ? 0.623 0.588 0.041 0.054 0.490 0.596 0.469 0.275 0.171 ? ? 0.382 0.855 0.125 0.519 0.376 0.806 0.355 0.165 0.217 0.504

Dendrorhynchoides_curvidentatus ? 0.103 0.874 0.099 ? ? ? ? ? ? ? ? 0.237 ? ? ? 0.000 0.361 ? ? ? ? 0.481 ? 0.078 0.008 0.219 ? 0.751 ? 0.518 0.674 0.000 0.062 0.336 0.790 0.451 0.298 0.332 ? ? ? ? 0.070 0.420 0.426 0.770 0.133 0.247 0.159 0.245

Kryptodrakon_progenitor ? 0.313 ? 0.751 ? ? ? ? ? ? ? ? ? ? ? ? ? ? ?

Gnathosaurus_subulatus 0.999 ? ? 0.554 ? ? ? ? 0.299 0.488 0.735 0.114 0.372 0.275 0.686 0.129 ?

Gnathosaurus_macrurus ? ? ? ? ? ? ? ? ? ? ? ? ? ? ? 0.109 0.540 1.000 ? 0.587 0.483 ?

Plataleorhynchus_streptophorodo ? ? ? ? ? ? ? ? ? ? ? ? ? ? ? 0.113 ?

Huanhepterus_quingyangensis 0.731 ? ? ? ? ? ? ? ? ? ? ? ? ? ? 0.089 ? ? ? ? 0.486 0.371 0.000 0.375 ? ? ? ? 0.260 ? 0.790 0.615 ? 0.260 0.503 0.190 0.410 0.355 0.406 0.552 0.000 ? ? 0.225 0.999 ? 0.319 ? 0.137 ? ?

Moganopterus_zhuiana 0.916 ? 0.564 1.000 ? ? ? ? 0.168 1.000 0.406 ? ? 0.060 0.338 0.052 0.407 0.766 ? 0.362 0.418 ?

Elanodactylus_prolatus ? 0.176 0.268 0.388 ? ? ? 0.289 ? 0.584 ? 0.371 0.560 ? 0.251 0.432 0.197 0.387 0.596 0.740 0.613 0.055 0.532 0.563 ? ? ? ? 0.118 0.263 0.032 ?

Kepodactylus_insperatus ? 0.114 ? ? ? ? ? ? ? ? ? ? ? ? ? ? 0.000 ? ? ? ? ? ? ? 0.171 ? ? ? ? ? ? ?

Ctenochasma_elegans 0.598 0.589 0.369 0.681 ? ? ? ? 0.000 0.266 0.918 0.296 0.430 0.153 0.738 0.398 0.841 0.516 ? 0.797 0.214 0.188 ? 0.375 0.011 0.036 0.246 ? 0.560 ? 0.470 0.496 0.598 0.320 0.971 0.067 0.387 0.388 0.419 0.582 0.116 0.626 0.927 0.170 0.502 0.201 0.592 0.103 0.233 0.031 0.078

Pterodaustro_guinazui 0.845 0.857 0.652 0.768 ? ? ? ? 0.028 0.331 0.593 0.057 ? ? 0.890 1.000 0.855 0.561 ? 1.000 0.220 0.214 0.298 0.625 0.061 0.226 0.148 ? 0.537 ? 0.625 0.486 ? 0.322 ? 0.356 0.446 0.440 0.453 0.523 0.120 0.770 ? 0.169 0.597 0.441 0.905 0.224 0.382 0.091 0.152

Beipiaopterus_chenianus ? 0.199 0.378 0.132 0.375 0.000 0.031 0.190 0.427 1.000 ? 0.558 0.563 0.242 0.316 0.561 0.253 0.251 1.000 1.000 0.977 ? ? ? 0.058 0.960 0.264 0.524 0.078 0.640 0.085 0.365

Gegepterus_changae 0.768 0.878 0.469 0.748 ? ? ? ? 0.111 0.403 0.557 0.196 ? ? 0.490 0.140 ? 0.684 ? 0.479 0.178 0.207 0.145 ? ? ? ? 0.291 ? ? ? ? ? ? ? ? ? 0.477 ? ? ? 0.544 ? ? ? ? ? ? ? ? ?

Feilongus_youngi 0.808 ? 0.528 0.662 ? ? ? ? 0.179 0.618 ? 0.071 ? 0.048 0.330 0.064 0.622 0.637 ? 0.329 0.359 ?

Cycnorhamphus_suevicus 0.255 0.381 0.408 0.440 ? ? ? ? 0.377 0.306 0.710 0.650 0.863 ? 0.000 0.000 0.400 0.286 ? 0.000 0.081 0.151 0.335 0.375 0.004 0.082 0.157 ? 0.379 ? 0.524 0.552 0.922 0.523 0.570 0.311 0.596 0.294 0.300 0.429 0.098 0.395 0.712 0.390 0.535 0.215 0.265 ? ? ? ?

Ardeadactylus_longicollum 0.374 0.581 0.426 0.546 ? ? ? ? 0.330 0.287 0.633 0.301 1.000 ? 0.567 0.046 0.561 0.526 ? 0.491 0.290 0.296 0.344 0.375 0.004 0.048 0.207 ? 0.529 ? 0.512 0.483 0.726 0.534 0.654 0.144 0.576 0.255 0.175 0.333 0.100 0.528 0.614 0.383 0.554 0.082 0.204 ? ? ? ?

Pterodactylus_antiquus 0.417 0.577 0.362 0.501 ? ? ? ? 0.217 0.263 0.744 0.244 ? ? 0.543 0.067 0.528 0.483 ? 0.527 0.273 0.286 0.352 0.375 0.012 0.042 0.307 ? 0.463 ? 0.550 0.608 0.583 0.300 0.683 0.177 0.360 0.412 0.537 0.558 0.089 0.531 0.859 0.272 0.457 0.255 0.578 0.087 0.441 0.043 0.193

Normannognathus_wellnhoferi 0.300 ?

Germanodactylus_cristatus 0.247 0.533 0.271 0.427 ? ? ? ? 0.411 0.174 0.512 0.200 ? ? 0.621 0.040 0.564 0.328 ? 0.673 0.154 0.132 0.276 0.375 0.014 0.070 0.261 ? 0.658 ? 0.500 0.555 0.647 0.336 0.705 0.308 0.381 0.410 0.523 0.628 0.189 0.483 0.932 0.245 0.495 0.267 0.504 0.110 0.156 0.010 0.000

Germanodactylus_rhamphastinus 0.267 0.761 0.471 0.335 ? ? ? ? 0.511 0.246 0.452 0.090 ? ? 0.625 0.046 0.660 0.341 ? 0.517 0.112 0.204 0.200 0.375 ? ? 0.255 ? 0.538 ? 0.635 0.633 ? 0.327 0.680 0.038 0.395 0.300 0.471 0.616 0.093 0.512 1.000 0.300 0.526 0.369 0.468 ? ? ? ?

Haopterus_gracilis 0.199 0.527 0.395 0.464 ? ? ? ? 0.411 0.763 ? ? ? ? 0.646 0.040 0.660 0.231 ? 0.733 0.025 0.113 0.163 ? ? ? 0.022 ? 0.548 ? 0.627 0.649 0.390 0.366 ? ? 0.587 0.276 0.352 0.277 ? ? ? ? ? ? ? ? 0.287 0.000 0.107

Aetodactylus_halli ? ? ? ? ? ? ? ? ? ? ? ? ? ? ? 0.097 0.559 0.649 ? 0.835 ?

Anhanguera_santanae 0.271 0.646 0.582 0.558 ? ? ? ? 0.353 0.216 0.293 0.167 ? 0.347 0.822 0.068 0.704 0.304 0.335 0.624 0.072 0.144 0.328 0.375 ? ? 0.000 ? ? ? ? 0.144 ? ? 0.551 0.309 ? ? ? ? ? 0.492 0.531 ? ? ? ? 0.005 ? ? ?

Anhanguera_piscator 0.349 0.566 0.440 0.522 ? ? ? ? 0.298 0.221 0.996 0.148 ? 0.336 0.785 0.077 0.677 0.306 0.337 0.725 0.025 0.104 0.184 0.375 0.050 0.175 0.015 ? 0.500 ? 0.697 0.123 ? 0.305 0.670 0.376 ? ? ? ? ? 0.715 ? 0.215 0.315 ? 0.213 0.000 0.785 ? ?

Anhanguera_blittersdorffi 0.402 ? 0.433 0.554 ? ? ? ? 0.315 0.278 0.398 0.153 0.172 0.414 0.804 0.087 ? 0.338 0.316 0.733 ?

Anhanguera_araripensis 0.373 ? ? 0.583 ? ? ? ? 0.235 0.226 0.274 0.071 0.190 0.450 0.796 0.085 ? ? ? ? ? 0.144 ? ? ? ? ? ? ? ? ? ? ? ? ? 0.097 ? ? ? ? ? ? ? ? ? ? ? ? ? ? ?

Liaoningopterus_gui 0.470 ? ? ? ? ? ? ? ? ? ? ? ? ? ? 0.056 0.487 0.206 ? ? 0.080 ?

Siroccopteryx_moroccensis ?

Tropeognathus_mesembrinus 0.319 ? 0.449 0.495 ? ? ? ? 0.441 0.302 0.269 0.081 0.133 0.484 0.671 0.036 0.388 0.328 0.283 0.709 ?

Coloborhynchus_clavirostris ?

Coloborhynchus_wadleighi ? ? ? ? ? ? ? ? ? ? ? ? ? ? ? ? ? ?
? ?
? ? ? ? ? ? ?

Ornithocheirus_simus ?
? ?
? ? ? ? ?

Brasileodactylus_araripensis ? ? ? ? ? ? ? ? ? ? ? ? ? ? ? ? ? ?
? ?
? ? ? ? ? ? ?

Ludodactylus_sibbicki 0.265 ? 0.524 0.558 ? ? ? ? 0.321 0.204 0.394 0.090 ? 0.171
0.842 0.068 0.520 0.272 ? 0.764 ? ? ? ? ? ? ? ? ? ? ? ? ? ? ? ? ?
? ? ? ? ? ? ? ? ? ? ? ? ? ?

Boreopterus_cuiae 0.390 ? 0.451 0.613 ? ? ? ? 0.179 0.350 0.473 ? ? ? 0.809 0.101
0.940 0.409 ? 0.864 0.079 ? ? ? ? 0.136 ? ? ? ? 0.591 ? 0.442 0.370 ? 0.294
0.483 0.365 0.416 0.553 ? ? ? 0.305 0.134 ? 0.110 ? ? ? ?

Guidraco_venator 0.255 ? 1.000 0.597 ? ? ? ? 0.222 0.260 0.369 0.076 ? ? 0.771
0.076 0.761 0.245 ? 0.807 0.017 ? ? ? ? ? ? ? ? ? ? ? ? ? ? ? ? ?
? ? ? ? ? ? ? ? ? ? ? ? ?

Zhenyuanopterus_longiristris 0.603 0.694 0.555 0.610 ? ? ? ? 0.267 0.354 0.597 0.066 ?
? 1.000 0.161 0.801 0.435 ? 0.978 0.110 0.192 ? 0.500 0.028 0.025 0.295 ? 0.593 ? 0.480
0.200 0.487 0.337 0.688 0.038 0.478 0.244 0.288 0.455 ? ? ? 0.276 0.094 0.367 0.000 ? ?
? ?

Cearadactylus_atrox 0.293 ? 0.442 0.467 ? ? ? ? 0.357 0.152 ? ? 0.373 ? 0.484
0.050 0.276 0.253 ? 0.456 ? ? ? ? ? ? ? ? ? ? ? ? ? ? ? ? ? ?
? ? ? ? ? ? ? ? ? ? ? ? ?

Hongshanopterus_lacustris ? ? ? 0.540 ? ? ? ? 0.276 ? ? 0.244 0.330 0.452 0.593
0.060 ? ? ? ? 0.021 ? ? ? ? ? ? ? ? ? ? ? ? ? ? ? ? ? ? ?
? ? ? ? ? ? ? ? ? ? ?

Piksi_barbarulna ?
? ? ? ? ? ? ? ? ? ? 0.494 ? ? ? ? ? ? ? ? ? ? ? ? ? ?
? ? ? ? ?

Lonchodectes_compressirostris 0.485 ? ? ? ? ? ? ? ? ? ? ? ? ? ? ? ? ?
? ?
? ? ? ? ? ? ? ?

Lonchodraco_giganteus 0.147 ? ? ? ? ? ? ? ? ? ? ? ? ? ? ? ? ? ?
? ? ? ? ? ? ? ? ? ? ? ? 0.395 ? ? ? ? ? ? ? ? ? ? ? ?
? ? ? ? ? ? ?

Cimoliopterus_cuvieri 0.316 ? ? ? ? ? ? ? ? ? ? ? ? ? ? ? ? ? ?
? ?
? ? ? ? ? ?

Cimoliopterus_dunni 0.855 ? ? ? ? ? ? ? ? ? ? ? ? ? ? ? ? ? ?
? ?
? ? ? ? ? ?

Nurhachius_ignaciobritoi 0.324 0.575 0.506 0.411 ? ? ? ? 0.845 0.626 0.693 0.186 0.854 ?
0.396 0.035 0.422 0.448 ? 0.356 0.087 0.124 0.412 ? ? ? 0.034 ? 0.437 ? 0.837 0.111
0.399 0.347 0.454 0.213 0.566 0.296 0.342 ? ? 0.461 ? 0.354 0.348 ? 0.056 0.118 0.198 ?
?

Liaoxipterus_brachyognathus ? ? ? ? ? ? ? ? ? ? ? ? ? ? ? 0.032
0.367 0.467 ? 0.314 ?
? ? ? ? ? ? ? ? ? ? ?

Istiodactylus_sinensis 0.329 0.853 0.544 0.217 ? ? ? ? 0.924 0.423 0.595 0.153 ? ?
0.240 0.048 0.106 0.332 ? 0.174 0.071 0.121 0.288 ? ? ? 0.077 ? 0.726 ? 0.869 0.147 ?
0.390 0.526 0.270 0.573 0.363 0.416 ? ? ? ? 0.430 0.245 ? ? ? ? ? ?

Istiodactylus_latidens 0.429 0.847 0.276 0.177 ? ? ? ? 0.545 0.321 0.502 0.119 0.478 ?
0.000 0.040 0.177 0.366 ? 0.170 ? 0.140 0.220 ? ? ? 0.027 ? 0.478 ? 0.855 0.096 0.209
? 0.408 ? ? ? ? ? ? ? ? 0.209 ? ? ? ? ? ? ?

Pteranodon_longiceps 0.289 ? 0.486 0.776 ? ? ? ? 0.179 0.138 0.236 0.114 0.415 0.000 ?
? 0.919 0.305 ? ? 0.071 ? ? 1.000 ? ? 0.081 ? ? ? 0.573 0.389 0.280 0.706 0.355
0.263 0.684 0.290 0.298 0.246 0.083 0.618 0.537 0.263 0.473 0.188 0.472 0.107 0.457 0.016 0.116

Pteranodon_sternbergi 0.415 0.985 0.566 0.798 ? ? ? ? 0.095 0.127 0.204 0.033 ? 0.006
? ? 0.999 0.316 ? ? 0.076 0.162 0.113 ? 0.063 0.005 0.086 ? 0.668 ? 0.633 0.467 0.389
0.780 0.477 0.169 0.666 0.275 0.287 0.270 0.123 0.515 0.574 0.278 0.464 0.187 0.310 ? ? ? ?

Tethydraco_regalis ?
? ? ? ? ? ? ? ? 1.000 ? ? ? ? ? ? ? ? ? ? ? ? ? ? ? ?
? ? ? ? ?

Alamodactylus_byrdi ?
? ? ? ? ? ? ? ? ? 0.851 ? ? ? ? ? ? ? ? ? ? ? ? ? ? ?
? ? ? ? ? ?

Nyctosaurus_grandis ?
0.089 ? ? ? ? ? ? ? ? 0.269 0.000 0.389 ? 0.272 0.811 0.375 ? ? ? ? ? ?
? 0.186 ? ? ? ? ? ? ?

Alcione_elainus ?
? ? ? ? ? 0.128 ? ? 0.222 0.500 0.434 ? 0.479 0.452 ? ? ? ? ? ? ? ?
0.278 ? ? ? ? ? ? ?

Simurghia_robusta ?
? ? ? ? ? ? ? ? 0.168 ? ? ? ? ? ? ? ? ? ? ? ? ? ? ? ?
? ? ? ? ?

Cretornis_hlavaci ?
? ?
? ? ? ?

Nyctosaurus_gracilis 0.386 0.685 0.513 0.741 ? ? ? ? 0.256 0.214 0.484 0.253 0.143 0.528
? ? 0.800 0.446 ? ? 0.078 0.140 0.209 0.875 0.008 0.005 0.078 ? 0.351 0.067 0.936 0.412
0.999 1.000 0.487 0.188 1.000 0.273 0.162 0.318 0.021 0.999 0.565 0.212 0.427 0.160 0.371 ? ?
? ?

Nyctosaurus_nanus ?
? ? 0.150 ? ? ? ? ? 0.206 0.000 ? ? ? ? ? ? ? ? ? ? ? ? ? ?
? ? ? ? ? ? ?

Nyctosaurus_lamegoi ?
? ? ? ? ? ? ? ? ? 0.323 ? ? ? ? ? ? ? ? ? ? ? ? ? ? ?
? ? ? ? ? ?

Muzquizopteryx_coahuilensis 0.223 ? ? ? ? ? ? ? ? 0.206 0.915 ? ? ? ? ?
? ? ? ? ? ? ? 0.750 ? ? ? ? ? 0.238 0.591 0.506 0.728 ? ? ? ? ? ?
? 0.036 0.618 ? 0.253 0.464 ? 0.207 ? ? ? ?

Tupandactylus_navigans 0.127 ? ? 0.267 ? ? ? ? 0.626 0.136 0.240 0.363 0.111 0.082 ?
? ?
? ? ? ? ? ? ? ? ? ?

Tupandactylus_imperator 0.172 ? ? 0.188 ? ? ? ? 0.994 0.205 0.244 0.000 ? ? ?
? 0.720 0.226 0.737 ?
? ? ? ? ? ? ? ? ? ? ? ?

Bakonydraco_galaczi ? ? ? ? ? ? ? ? ? ? ? ? ? ? ? ? 0.704 0.410
0.688 ?
? ? ? ? ? ? ? ?

Tapejara_wellnhoferi 0.073 0.230 0.304 0.234 ? ? ? ? 0.630 0.119 0.331 0.497 0.000 0.008
? ? 0.608 0.078 0.540 ? 0.114 0.089 0.107 ? 0.024 0.046 0.241 0.602 0.151 ? 0.602 0.527
0.564 0.414 0.817 0.066 0.550 0.310 0.349 0.371 ? 0.532 0.668 0.391 0.350 0.389 0.407 ? ? ?
?

Europejara_olcadesorum ? ? ? ? ? ? ? ? ? ? ? ? ? ? ? ? 0.312 0.193
0.332 ?
? ? ? ? ? ? ? ?

Vectidraco_daisymorrisae ? ? ? ? ? ? ? ? ? ? ? ? ? ? ? ? ? ? ?
? ? ? 0.629 0.125 ? ? ? ? ? ? ? ? ? ? ? ? ? ? ? ? ? 0.515 ?
? ? ? ? ? ? ? ?

Caiuajara_dobruskii ? ? ? ? ? ? ? ? ? 0.077 0.269 ? ? 0.000 ? ? 0.496
0.148 0.393 ? 0.047 ? 0.187 0.500 0.013 0.000 ? 0.492 0.576 ? 0.543 0.260 ? 0.538 ?
0.450 0.540 0.377 0.649 0.240 0.178 ? ? 0.282 0.321 ? ? ? ? ? ?

Huaxiapterus_benxiensis 0.157 ? 0.320 0.362 ? ? ? ? 0.617 0.242 ? 0.358 ? ? ? ?
0.762 0.301 0.801 ? 0.126 ? ? ? ? ? ? ? ? ? 1.000 0.610 0.583 0.703 0.768 0.009
0.802 0.220 0.263 ? ? ? ? 0.877 0.446 ? 0.263 ? ? ? ?

Huaxiapterus_corallatus 0.185 0.356 0.457 0.329 ? ? ? ? 0.567 0.165 ? ? ? ? ? ?
0.831 0.252 0.999 ? 0.042 0.089 ? ? ? ? 0.216 0.744 0.432 ? 0.659 0.547 0.638 0.632
0.542 0.234 0.613 0.128 0.127 0.154 0.047 ? ? 0.514 0.561 0.152 0.202 0.076 0.551 0.040 0.147

Eopteranodon_lii 0.219 0.227 0.630 0.324 ? ? ? ? 0.578 0.144 ? ? ? ? ? ? 0.882
? ? ? 0.103 0.117 0.189 ? ? ? ? ? 0.227 ? 0.671 0.661 0.643 0.491 0.560 0.256
0.567 0.252 0.229 0.291 ? 0.831 0.682 0.412 ? ? ? ? ? ? ?

Huaxiapterus_jii 0.201 0.387 0.557 0.102 ? ? ? ? 0.718 0.151 ? ? ? ? ? ? 0.441
0.273 0.994 ? 0.160 0.178 0.262 ? ? ? ? 0.390 0.468 ? 0.660 0.594 0.597 0.538 0.642
0.276 0.573 0.264 0.273 0.229 0.006 ? ? 0.475 0.475 0.234 0.295 ? ? ? ?

Sinopterus_dongi 0.166 0.657 0.214 0.158 ? ? ? ? 0.999 0.240 0.311 ? ? ? ? ?
0.732 0.232 0.721 ? 0.096 0.158 0.242 0.375 ? ? 0.163 0.737 0.503 ? 0.639 0.566 0.563
0.505 0.776 0.092 0.557 0.242 0.232 0.193 0.145 ? 0.680 0.445 0.479 0.061 0.220 0.078 0.187
0.038 0.131

Bennettazhia_oregonensis ? ? ? ? ? ? ? ? ? ? ? ? ? ? ? ? ? ? ?
? ? ? 0.163 ? ? ? ? ? 0.449 ? ? ? ? ? ? ? ? ? ? ? ? ? ? ?
? ? ? ? ? ? ?

Dsungaripterus_weii 0.238 0.701 0.335 0.430 ? ? ? ? 0.351 0.137 0.534 0.344 0.033 0.385
0.420 0.032 0.575 0.220 ? 0.672 0.021 0.157 0.220 0.625 0.020 0.186 0.342 ? 0.357 ? 0.757
0.557 ? 0.600 0.747 0.305 0.675 0.249 0.497 0.504 ? 0.294 ? 0.604 0.609 ? 0.112 ? ? ?
?

Domeykodactylus_ceciliae ? ? ? ? ? ? ? ? ? ? ? ? ? ? ? 0.052 ? ?
? ?
? ? ? ? ? ? ?

Noripterus_parvus 0.185 ? 0.453 0.515 ? ? ? ? 0.382 0.129 0.470 0.291 ? 0.248 0.570
0.040 0.761 0.377 ? 0.261 0.031 0.071 0.553 ? ? ? ? ? 0.179 ? 0.607 0.568 0.646 0.623
0.589 0.303 0.573 0.330 0.369 0.430 ? 0.395 ? 0.472 0.563 0.173 ? ? ? ? ?

Noripterus_complicidens ? ? ? ? ? ? ? ? ? ? ? ? ? ? ? 0.016 ? ?
? ? 0.145 0.143 0.716 0.625 0.030 0.196 ? ? 0.400 ? 0.573 0.666 ? 0.606 0.313 0.302
0.643 0.196 ? ? 0.199 0.618 0.264 0.384 0.832 0.075 0.202 0.045 0.361 0.184 0.619

Tupuxuara_longicristatus 0.138 ? ? ? ? ? ? ? ? ? ? ? ? ? ? ? ? ? ?
? ?
? ? ? ? ? ? ?

Tupuxuara_leonardii 0.425 0.999 0.216 0.257 ? ? ? ? 0.515 0.213 0.123 0.028 0.174 0.342 ? ? 0.894 0.368 ? ? 0.053 0.147 0.189 ? ? ? 0.222 ? 0.364 ? 0.487 0.408 0.610 0.506 0.773 0.248 0.613 0.101 0.121 ? ? ? ? 0.478 0.416 0.226 0.254 ? 0.423 0.032 0.108

Alanqa_saharica 0.813 ?

Aerotitan_sudamericanus 0.560 ?

Thalassodromeus_sethi 0.149 ? 0.522 0.431 ? ? ? ? 0.664 0.149 0.007 0.081 ? ? ? ? ? 0.225 ?

Chaoyangopterus_zhangi 0.225 ? ? ? ? ? ? ? ? ? ? ? ? ? ? ? 0.647 0.567 ? ? 0.182 0.233 0.216 ? ? ? 0.195 0.000 0.487 ? 0.573 0.529 ? 0.640 0.510 0.121 0.609 0.145 0.101 0.194 ? 0.404 0.347 0.604 0.599 0.286 0.297 ? 0.179 ? ?

Jidapterus_edentus 0.135 0.578 0.531 0.573 ? ? ? ? 0.547 0.107 ? ? ? ? ? ? 0.811 0.398 ? ? 0.106 0.187 0.297 ? ? ? 0.198 ? 0.437 ? 0.620 0.400 0.751 0.621 0.473 0.296 0.598 0.191 0.143 0.172 ? 0.605 ? 0.472 0.544 0.319 0.297 0.098 0.423 0.061 0.135

Eoazhdarcho_liaoxiensis ? ? ? ? ? ? ? ? ? ? ? ? ? ? ? ? 0.616 0.604 ? ? 0.167 0.175 0.244 ? ? ? 0.197 0.897 0.512 ? 0.563 0.000 0.499 0.478 0.463 0.226 0.554 0.260 0.229 0.231 ? ? ? 0.309 0.718 ? ? ? ? ? ?

Shenzhoupterus_chaoyangensis 0.090 ? 0.000 0.552 ? ? ? ? 0.856 0.141 0.000 ? ? ? ? ? 0.704 0.228 ? ? 0.163 ? ? ? ? ? 0.129 ? ? ? 0.745 ? ? 0.694 ? 0.222 0.626 0.165 0.172 0.198 ? ? ? 0.682 0.436 ? 0.385 ? ? ? ?

Radiodactylus_langstoni ?

Microtuban_altivolans ? 0.269 0.226 0.206 ? 0.569 0.416 ? 0.585 0.843 0.092 0.560 0.322 0.179 0.000 ? ? ? ? ? ? ? ? ? ? ?

Aralazhdarcho_bestobensis ?

Volgadraco_bogolubovi ? ? ? ? ? ? ? ? ? ? ? ? ? ? ? ? ? ? ? 0.093 0.193 0.027 ?

Eurazhdarcho_langendorfensis ? ? ? ? ? ? ? ? ? ? ? ? ? ? ? ? ? ?
? ? 0.355 ? ? ? ? ? ? ? ? ? ? ? ? ? ? 0.009 ? ? ? ? ? ? ?
? ? ? ? ? ? ? ?

Montanazhdarcho_minor ? ? ? ? ? ? ? ? ? ? ? ? ? ? ? ? ? ? ?
? 0.256 ? ? ? ? ? ? 0.999 ? ? 0.793 0.439 ? 0.461 0.526 0.652 ? ? ? ? ?
? ? ? ? ? ? ? ? ? ?

Phosphatodraco_mauritanicus ? ? ? ? ? ? ? ? ? ? ? ? ? ? ? ? ? ?
? ? 0.351 ?
? ? ? ? ? ? ? ?

Zhejiangopterus_linhaiensis 0.346 ? 0.499 0.487 ? ? ? ? 0.457 0.206 0.401 0.157 ? ?
? ? 0.806 0.430 ? ? 0.544 0.506 0.412 0.625 ? 0.001 0.236 ? 0.564 ? 0.694 0.513 0.763
0.678 0.999 0.093 0.543 0.260 ? ? ? ? ? 0.600 0.618 0.000 0.265 0.132 0.476 0.066 0.121

Azhdarcho_lancicollis 0.422 ? ? ? ? ? ? ? ? ? ? ? ? ? ? ? ? ? ?
? 0.284 ? 0.236 ?
? ? ? ? ? ? ?

OCP_DEK_GE_716 ?
0.461 ?
? ? ? ? ? ?

Hatzegopteryx_thambena ? ? ? ? ? ? ? ? ? ? ? ? ? ? ? ? ? ? ?
? ?
? ? ? ? ? ?

Arambourgiania_philadelphiae ? ? ? ? ? ? ? ? ? ? ? ? ? ? ? ? ? ?
? ? 1.000 ?
? ? ? ? ? ? ? ?

Quetzalcoatlus_spp 0.525 ? ? ? ? ? ? ? ? 0.301 ? ? 0.189 ? ? ? 0.740
0.572 ? ? 0.789 1.000 0.109 ? ? ? 0.199 0.934 ? ? 0.621 0.296 0.673 0.755 0.521 0.285
0.633 0.000 0.000 ? 0.138 ? ? ? 0.292 0.009 ? ? ? ? ?

MGUAN_PA650&651 ?
? ?
? ? ? ? ?

&[num]

Euparkeria_capensis
0?100?00000001000000?000000000??????00000000100??0000?0000000?0000000000000000??
00000010000?000000000000?00100??0010?01000000000100011000000000000000000000000000
000000000000000000000?0????00000???000??0000000000000010

Ornithosuchus_longidens
0?1?0?00000001?000000?2001001?0??????000000000?0??1010?0000000?000000000???0?????0

?0?0010000?000000???????00100??0010?000000000001000110000?000000000[01]00?0000000000
0101000000000001000?00??????000??0??000??0000000000001?0?

Herrerasaurus_ischigualastensis
0?1?0?0000000100001000?000000000???????00002000000??1000?0000000?000000000000000????
0?0?0010000?00000000?????00200??0010?000000000001000110000000000?0000100000000???
??????000010001010000?0????00110000000??0000001000000030

Scleromochlus_taylori
1??00?000010?1??01000?00?0?0100???????010000000?0??1??0?0?020???10???001?0000?????0
0??0?10000?00?00000?????00120??0010???0000?????1???1???00???10000??000000000000???
?????0?01???1000?????????01??????000??00000001?00?004?

Eudimorphodon_ranzii
1?100?000010?10101000?001110200???????01003000000??1000?0002100?100000010???0?00??
01??002000100000000010000?00110??000101100201100110421101O?10???000?00?1???0?000020
10110100011000101000??0??1000010??????00??000?01?0?00???

Eudimorphodon_rosenfeldi
1?1?0?00001??10101000?001110200???????01003000000??1?00?0002100?10000?01000100?????
???00100010000000010000?00110??000101000201100110421101O?10?000000?0???0000?000101
01001??01100?101000000?000000100000000??00?00?01???0?020

Eudimorphodon_cromptonellus
???????00??00?0??100?????????????????????010?200?00?????0??0????0???0???0???0??????????????
?01000??000?00???????????0???00101000?01100[01]1042?10????0???0?????0???00?00?0101?0
001?0?11?001010????0????0?010??0?????????????100000?20

Peteinosaurus_zambellii
??0??????????????????????00
??000?0???0000?????0??????000101000201?0002022??000?????????????????????0?????????????
?????????????????????0010000000??00000?0????????0

Caviramus_schesaplanensis
????0?????????????1???0
100011111100000?????00020??00???100010??0?[01]1032??010?????????????????????????????
??

Raeticodactylus_filisurensis
1?1?0?00001??10101100?00?0102010101000010020000000???000?0002000?100000010???0?????
01???012001111100000?????00021??000121100101000110321101O?10?0000???00????????0????
?????00?11???1010000????0?000??0?0?????????????1000?0??0

Austriadactylus_cristatus
1?1?0??00010?101?1000?00?0001?10102000010010010000??1000?00?1000??00000??0??10?????0
?????20000?000?0000?????00120??0001[01]1100201000010111100O????00000000???000000?01
????001???11????01000??????00001???0?00????000?01????????

Preondactylus_buffarinii
1?1?0?00001??10101000??0???0100???????01001001000????0?????1000?10000??1????????????
???010000?00000000?????00110???00101?00201000010111110000????0?00???0???000?0?01????
??????11????01000?????00000100?000000000000001?00?0020

Dimorphodon_macronyx
1?1?0?00001??00111000?203000210???????01111001000??110??0001000?10000001???10?????0
1???012000?000000000000?20132001001?41002110000011??11000011???000??0010020?00012??
??00?00011100102000??000200001000010113001001010000020

Parapsicephalus_purdoni
???0???01010000111000?203000210???????01112001000??1000?0001000?10000001000100000??
01000?????????????????????????????????0???????0?1????[01]1???????0?????????????????????????????
??

Campylognathoides_liasicus
1?100?000010010111000?002110210???????02102000000??1000?0002000?000100000010000??
01??0122000?0000001?0000?10130??1000?00002111000011??10010010?000000000000200000021
1110001001111??101000001?020000100011011310?00?0101100021

Campylognathoides_zitteli
1?1?0?000010?10111000?00???0210???????02102000000??1000?00??000?000100?0????0?0????
???0122000?0000001?000??10130??1000?00002111000011??10010????00000??0000020?00002?1
10001?01111??1010??001??2000010?011011310100101011?0021

Sericipterus_wucaiwanensis
311?10101010111111101??????0?11001?001011?20000?0?????0?0?02001?1?00??11?0??00?0???
???11??????1001001?0000?00?31??1020?2211220111121??00??0?1000000????0??????00?02???
????000111?010300100???????????02201?????????????????

Angustinaripterus_longicephalus
311?10101010111111101?0021102?1001?00101102000000??1?0??0002101?10000011??????????
01???112010?1001011????0?00131??1020?2211120111121??000?0????????????????????????????
??

Harpactognathus_gentryii
30101010121011111?110???????0??1001?001001?200?0??????????????????????????????00??01
???1????????????????????????????020????1220???[01]2???00??0????????????????????????????
??

Cacibupteryx_caribensis
??10???01010111110101?002000?10???????00102000000??0000?0001001??000000?000100000??
0100?1????????????????????????????020????0?2????[01]2????00?0????????????????????????????
??????????????????????0????????????????????????????????

Rhamphorhynchus_muensteri
2?100?000010111110101?002110210???????00102000000??0000?0012201?100000?100010000??

01001102000?1000001?0000?01131??1020?2210220110221??000100110000000000010020000002
110100[12]000111001060000100020010101012011[12]011001010110012[12]

Qinglongopterus_guoi
3?1?0??0?0?01?1??1101?002?1?2??????????0???20000?????????0???200???00?00???001?????0??
??11200??1?0?0?1??????0?130??1020?20112201111?1??0001??10???000?00?1?020000002????0
0????111??103000?00??3?0101?100?011101?????1?1100121

Nesodactylus_hesperius
??????????????????????????0??????????????????????????????????1?0??????????????????????????
??1?0000???????020?00?02?11000200?1
11??1060000100??001010?01???00?100010??1??????

Dorygnathus_banthensis
1?100?0000101111111101?002110210???????00102000000??1000?0002001?1000000100010000??
0100111200101000001?0200?00131??1020?20102201101l1??10010010?000000000010020000002
110100300111100103000010003001010100201l[13]0110010101100122

Scaphognathus_crassirostris
1?1?0?0000103101111100?002110210???????01102000000??1000?0002001?100000010??10?????
01?00112000?1000001??????00131??1020?20102201000l1??100000??000000000000020000002l1
1??002000110??1030000100020010101002?11101[01]0000101100122

Sordes_pilosus
1?100?0000101101110l1000?002110210???????01102001000??1000?0012101?100010?100010000??
01?00110000?1000001?0001010130??1020?3000220100011??10000011?000000000100200000021
?110004001111??1000000000?[45]00101010020111011000010l100122

Darwinopterus_modularis
1?100?00001011?11??100004110?1111220000????001010??1000?00121010100110?11??10?0100
01???110000?1000001??????10100??1020?3000220101031??200001???10100?00?1?020000002?
1??00200?110???12000????04?010??0?0201131100000l?1100122

Wukongopterus_lii
1?1?0?00001011?1???1?0?????0??????????0??????????????????2???01??????1??????????01??
?110000?1000001??????10100??1020?3000220101031??20000??0?10?0010001002000000l2????0
02??0110??1???????0??4?010100???????01?00001?11?0122

Pterorhynchus_wellnhoferi
1?100?00001011?11??100004110??110110000????001000????00?00?22010100010?100010??????
????110000?1000001??????10100??1020?3000220101011??100001?0???00????0100200?0??????
???????110??102000?????0001010??0201??01000101???0??2?

Changchengopterus_pani
??
??0?100001?0???010?00?02????00?00?1
11???00000?????400101??00201??01?0???1?11?1121

Batrachognathus_volans
1?1?0?0001?030?0???100000111?10???????0????0????0??1?00?00?001?0?00110??????0?????10
?1011010??0020001?0000?1?220??1010?3000220100011??10000?????001??00?????000020100
004000110??1000000??????010101??????1?0100?01?1??00??

Jeholopterus_ningchengensis
1?1?0?0001?030?0???100000111?10???????0????0????0??1000?00?001?0?001?0??????0?????10
?1?110100??02000????00?1?22????010?3000220100011??10000????10??1100??0100000002????
00??001110?10400000???5001010100??11100100?01?11?0020

Anurognathus_ammoni
1?1?0?00011030?0???1000001?1?10???????0????0???00??1000?00?001?0?00110??????00????10
?10110100?0020001?0000?1?220??1010?3000220100011??100001???????1?000101000000002???
?????00111??104000??0??50010101??101??00100?0101100020

Dendrorhynchoides_curvidentatus
1?1?0?0001?030?0?????0?????1??0???????0??????????????????????01???????????001??????10?1
0?10100?002000??0?00?1???0???010?300022?100011?????00????10??1??0???100000002????00
4?001110?100000??0??500101?1?01????00?00??1???0?021

Kryptodrakon_progenitor
??
??0????????2???????00??1?
???0??????000?10?000?00?????????????????????

Gnathosaurus_subulatus
1?10110002101??11??110004110?1110310000????001000??1000?1113201010010?121100??0??
0101?110210?100?001??????1???0??1020?2011120?01231??100?0??????????????????????????
??

Gnathosaurus_macrurus
?????10?0??01??
10210?10??001?1000?10?2????020????1120???23?????00??01?22101??????????????????????????
??

Plataleorhynchus_streptophorodo
1?10100002?01??1???1????????????????????????????????????1??????????????????10??0???
??1????????????????????????????02?????1120???13???10000??????????????????????????????
??

Huanhepterus_quingyangensis
1?1?100000101?????????????????1103?000??
?110010?100000???????????0???020?20101201011 31??10000????22?0110001??0???0??2??????1
?0?1?1??1050?????????0?1????????1301001?01?1??0???

Moganopterus_zhuiana
1?100?00001??2?11??10100 4110?11101000?0????001100??0?01311?3201??0?0?0???2?100??????

?????12000?1000001??????00020??1020?2010120111111??10000????221?????????????????????
??

Elanodactylus_prolatus
??
??221011000?????000002?101001?011
11?0105000000?040011000?030113010011O?011?0133

Kepodactylus_insperatus
??
??01012101?????????????????????00111
1?0105000??0??????100??0?????0??????1????????

Ctenochasma_elegans
1?100?00000112?11??100004110?1[01]103?0000????001200??1100?111320101000l0?12??00?10
??0?0??110000?1000001?1000?00120??1010?2011110101211??10000?0??1010010001??0000000
2??00002000111??105000000??4??1100?0?3011301001?0101100133

Pterodaustro_guinazui
1?000?00001112?11??100004110?10???????0????001200??1100?1113101?100000?12??00?10??0
????100000?1000001?100??20020??1010?2010200201001??00000?0101010?10??1100000000211
00002000?110?1050??000004???1000003??130100110101l1?133

Beipiaopterus_chenianus
??
??1010?100?1?100?00022????00?00?1
1???1050???0???4???10000?????????????1?????133

Gegepterus_changae
??0????0001112?11??10000?110?11??300000????001200??1100?1?131010100000?12???0?10??0
????10?????00??001???0??00020??1010?2010?1?101201???0??0001?10100?????????????22????
002?????????????????????[01]???0?003????0??????1???0????

Feilongus_youngi
1?100?000010?2?11??101?04110?1110100000????001000??010101113?010100010?12?100?10??
0???0112000?1000001??????00020??1020?2010120111111??10000????22101?????????????????
??

Cycnorhamphus_suevicus
1?000?10021012?11??1000021l0?1[01]12220000????001100??1101111132010100010?1211?0?10
??01010100200?1001001????0?01111??10???20101??100011??1??000000000l?0??1??00000?02
?110002000111??108000000??4?011000003011301000001011001331

Ardeadactylus_longicollum
1?101000001012?11??110004110?10???????0????001?00??1100?1103201010001011121?00?10??0
1010110010?1??0001?1001010120??1020?5010120101131??10000001022101100001??00000002??
0100110?0110?105000000??4?01100?0?3011301001101011001??

Pterodactylus_antiquus
1?100?00001011?11??100004110?10???????0????001100??1100?1113201010010?12???0?10??0
????110000?1000001?0?00?00130??1020?3000120100011??10000000?10001100010100000002010
0100400011100105000000004001100100301130100110101100133

Normannognathus_wellnhoferi
1?000?000?10?2?1?????????????1122?000?????????????????????????????????????10??????
?1?0200?1?0000??100??????????020?2010110100?11??11000????????????????????????????
??

Germanodactylus_cristatus
2?100?00001011?11??100004110?1110320000????001100??1100?20132010100010?11???0?1???
?????111000?1000001?0?0??10130??1020?3000120100011??010100?????001100010??0000002??
??0020001110?1050??000??4??110010?30113010000101011001 33

Germanodactylus_rhamphastinus
2?100?00001011?11??100004110?1110320000????001100??1100?20132010100010?11???0?1???
?????111000??000001?0?0??10130??1020?3000120100011??110000???10001??0?10???0000?20?
00002?0?111??1?????0?00?4??1?0010?301130?000?01011001??

Haopterus_gracilis
1?100?00001011?1???1?000??10??0???????0????010000???000?0?1230??1????0?1????0?0?????
???112000?1?0?0?1??????10100???020?3000220100011??10000??????001?00??????1000020101
??2000011???07100?????4?01?00100?????????????????1??

Aetodactylus_halli
?????000?2?10??????????????????0??100????1
110210?1020001?1000?1?101??1010?51?0120101131????001????????????????????????????????
??

Anhanguera_santanae
1?1010001010 01?10??110102110?111040?110????0110110211110001230111010 10?1111001010
0011111100?0?1000001?1010?00102?11021251?0121111131??10101101101101010010 10?11100
2????11?00100???20711000011401?1????0211??1110100?011?????

Anhanguera_piscator
1?1?1000101001?10??110102110?1110400110????0110110211110001230111010 10?11110010???
?1??1110010?1000001????0?00102011021251101211111 31??10101101101101010010101?11002
00101120010010120711 00?0114?1?101110211???110110101101?4?

Anhanguera_blittersdorffi
1?1010001010 01?10??110102110?1110400110????1????10211110001230111010 10?1111001010 0
01111110010?100?0?1?10????01?201?021251101211111 31??10101????????????????????????
??

Anhanguera_araripensis
1?1010?0101001?10??110102110?1110400110?????????10211110001230111010 10?11110010100

011111??0???10??001????0?0010???102125??0121111131??101?1?????????????????????????????
???0010010120?110?00114?1?1?????????????????????????

Liaoningopterus_gui
1?1010001010?1?10??1101[02]2110??110400110?????????????1??0012301?101010?1???????10
0????11100?0??00?001??????00102???021251101211011 31??10101?01???101?????????????????
??

Siroccopteryx_moroccensis
0?101100?0?00?????????????????1004?01???101????
?1?????????????????????????????02?25?0012??01131??2?0????????????????????????????????
??

Tropeognathus_mesembrinus
1?1010001010 01?10??110102110??100400110????1????1021111000123011101010?11110010100
01111110010?1000001?1000?0013201?021251?0121101131??10001?????????????????????????
??

Coloborhynchus_clavirostris
0?11120??0?????????????????????1004?011???101????
?1?????????????????????????????02?25??0121???13????2?0????????????????????????????????
??

Coloborhynchus_wadleighi
0?11120??0100?????????????????1004?011???101????
?1?????????????????????????????02?25??0121??1131??2?0????????????????????????????????
??

Ornithocheirus_simus
0?10100??0?????????????????????1004?011???101????
?1?????????????????????????????02?25??01?????03???1????????????????????????????????????
??

Brasileodactylus_araripensis
?????0?????00???1
10010?1000001?101??????1???021250?0121?01131????001?????????????????????????????????
??

Ludodactylus_sibbicki
1?101000101??1?10??110102110?10???????0????011011111111200122011101000?111100?0101
010?1110010?1000011?100??101000?102125110121101131??10001?????????????????????????
??

Boreopterus_cuiae
1?1?0?10101??1?1???11010?110?10???????0?????????10211?100012201?100010?11???????????
???112000?1001011??????0010[01]??1000?2010220100111??10000????01101??????10?????0???
???????10?????????????????11???1?0????????????1?11?114?

Guidraco_venator
1?1?1000101??1?10??110102110?10???????0?????????12111112001220111000??11???0?????0
?0?111?010?1000011??????10100??10212511012110111??10001?01???101?????????????????????
??

Zhenyuanopterus_longiristris
1?1?0?00101??1?11??110104110?1112310??0????011001021101000122010100010?11???0??????
?0??11?000?1000011??????0010[01]??1000?2010220100011??10000??1?01101?1111?10?111102
??????2?0?001??207110?????4??110?1???????0??????1?11?114?

Cearadactylus_atrox
1?1010001010012?10??11010?110??1?0100110????01100?????????012301010101??1??????01000
1111110010?1000001?1010?10101??10212501012110113 1??10001????????????????????????????
??

Hongshanopterus_lacustris
2?100?1010?01??????110?0?110??????????0????01000????????0?1?[23]0??1?001??11110??0100
01?111?????????????????????????????020?0000220?01031??100?0101?01101?????????????????
??

Piksi_barbarulna
??
??1
002?????00????????????????????????????????

Lonchodectes_compressirostris
??10???0131011???????0????????0????????????????????????????0?????????????0100?????
11?30???????????00??????1???000????0?10???03????0000????????????????????????????????
??

Lonchodraco_giganteus
1?1?0?00?01011?????1?0?????0??1105?011?????????????????????????????????????1000???
?110000?10000???1?1??????200?00125000210101031??10000?????????????????1????2???????
?0???1??2071????????????????????????????????????

Cimoliopterus_cuvieri
1?101000?011?1?????????????????1104?011??100????
?1????????????????????????????020?5100120?01131??120?1????????????????????????????????
??

Cimoliopterus_dunni
1?101000?011?1?????????????????1104?011??100????
?1????????????????????????????020?5??0120?01131??120?1????????????????????????????????
??

Nurhachius_ignaciobritoi
1?1?0?00001011?10??10010?110?10???????0????010000??1110?0013301?100110?11???0??1110

?0?0112000?1000001?1000?101[02]0??1020?4000110101011??10001101?01101??1???????11?02
1?1010200?0010??0711010?1?4?1?10011?3??????001101?1?01?4?

Liaoxipterus_brachyognathus
???????????11??
1?200?10??0?1????0?1012????020?4000000?01011????00??????????????????????????????????
???

Istiodactylus_sinensis
1?1?0?000211?1?10??100012110?10???????0????1????0??1?10?00134011100121?11???0??1110
?0?0112?00?1000001??????10120??1020?4300000101011??100011???01?01??1????????1?02???
?00??00001???071???00???01??00??0311?????????1?1?0????

Istiodactylus_latidens
1?1?0?00021111?10??100012110??0???????0????1????0??1110?0013401?100121?11????10?????
0?0112200?1000001????0?10120??1020?4300000101011??10001????0?10??111?????1111021010
10?00?00101207110100114???100?1?311?????????111101???

Pteranodon_longiceps
2?000?00101002??0??110104110?10???????0????010?01200101200124011101010?111100100??
01011111000?1100011?0001100101??11??????????????????????01011011010111110111010200
101011000001030711000011402110011010112011011011110114?

Pteranodon_sternbergi
2?0?0??0101002??0??110104110?10???????0????0100?1200101200123011101010?11??00??????
?0??111000?110?011??????00101???1??????????????????????????????0?????11??1?????20?101
01?0?0?01?3?7????0?1?20??100??0????????????1???01???

Tethydraco_regalis
??
???0?001
10307110?????????????????????????????????????

Alamodactylus_byrdi
??
??10000
10?306110??????????00?????????????????????????

Nyctosaurus_grandis
??
???????????11????????10???????????????????????????????????101???????????????2???????10001
???31601000?????????????????????????1111?1???

Alcione_elainus
??
??110?02?01110?00000
00031601000???????100?10?????????????111101???

Simurghia_robusta
??
??00?
????60?0??????????????????????????????????????

Cretornis_hlavaci
??
??10000
10031?110??0????2??00??0??????????????????????

Nyctosaurus_gracilis
2?100?10101001??0??110002110?10???????0????1????120110110012301110010?111100?00??0
1?11111000?1101011?0001001101??11??????????????????????0100103101011111101110002001
11011000110031601000011?21100?102011201101101111011??

Nyctosaurus_nanus
??1
???????????11??????0?10???1??????????????????????????????????1??????????02????10?10001
?00?16010??????????????????????????????????

Nyctosaurus_lamegoi
??
??01?
???160??????????????????????????????????

Muzquizopteryx_coahuilensis
????????1?1????????110002110?10???????0????1???00??110110012201?100010?11???0???????
???1???????????11??????0103???11????????????????????????01???03?01??111?10?11000??0?1??
1?0?001???16010?????102?1????????120?101??1?11?114?

Tupandactylus_navigans
2?210?110010?0??1??100124110?1111011100????00110???010?000123010100110?11??0??0????
?1????????????????????????????????1????????????????????0????????????????????????????????
??

Tupandactylus_imperator
2?2?0?1?0010?0?????1?0123110?1111011100????1????1120?013001230101001l0?11???1?0????
????122001010????1?010??001?210?1????????????????????????0????????????????????????????
??

Bakonydraco_galaczi
???????????00??11
2100111001111?01010001020111??
??

Tapejara_wellnhoferi
2?210?11001000??1??100124110?1111010110????00110112010130012301010011O?111101110??

0101012100111001111?0101000102100?????????????????????0?011001010100????010012211
1000110101100108011111004 1??100010311??00111?111111014?

Europejara_olcadesorum
????????0??0???????1????411???????????0?????????????1???00?2?0?010???0?1??????1???010?
0121001110?1111?01????010210?1?????????????????????0?????????????????????????????????
??

Vectidraco_daisymorrisae
??
??10??????????????????
??????????????????????311???011111?????????

Caiuajara_dobruskii
2?210?11001000?????100124110??111011110?????????112???13?01?[34]0?0100110?11?101?00?
?0???012200111001011?010??001021001?????????????????????0??110010???0?1?10010012 2?1
?00?21?101???108011??1004???100?102??12??111?1111110???

Huaxiapterus_benxiensis
2?2?0?1?0010?0?????100????10?1112610110????0?10?1120?013?013301010011 0?11??????????
????12100101001111?010??2012201?1?????????????????????0?01???101??0????????????????
?????01????080??????0??2110?110???????????1??????4?

Huaxiapterus_corallatus
2?2?0?110010?0?????1?0?2???0?1112610110????????????0??10???????01??????1????1????????
??12100101001?11??????20?220111?????????????????????0?01???101??0???????00?22??1000?
???01????0801?111??4?2110?110???13???11?111?1??14?

Eopteranodon_lii
2?210?11001000?????100?????0??110410110?????????????????1??0?01?011??11????????????
?1?21001010??1?1?00?????1????11?????????????????????0????00101???????????0?22????00??
0?01???10801??1???4?????0??020113011111 11?1110???

Huaxiapterus_jii
2?210?1??010?0?????100??4110??110410?10????00?10???????0??13?01?1?011??1???????0??0?
???1210010100???1?00???201220111?????????????????????0???????01??0???1??????22??1000
210?01???108011?????411110?110???13???????1?1110???

Sinopterus_dongi
2?2?0?110010?0??1??10002?1?0?1110410110????0011011201?130?133?101?011??11???1??????
????12100101001?11??????201220111?????????????????????0????00101??0??110?1?0?22?110
00210?011??10801111100412110011 0?0?13?1111111???1?14?

Bennettazhia_oregonensis
??
??10??????????????????10100
100108011?????????????????????????????????????

Dsungaripterus_weii
30000?10001001?11??100012110?1112330101????1????112000122012201011011O?11110110100
01011101000?1001001?1001000101??1020?1000220101041??02010101100101011111100100112
1110001???0?0??108011111?0?10?1001123?1????1111?001210???

Domeykodactylus_ceciliae
???????????0??????????????0??1?2???10??
11?0???10??001????10?0??1???020?1??0220???04?????01????????????????????????????????
??

Noripterus_parvus
30100?10001001?11??100012010?1111330101????1????112000122012201?110110?111101?0100
010?1111000?1001001?1001100101??1020?1000220101031??0101010110010101111?????00?12?
???00?000011001080111110041?1100?02??1?????????001210???

Noripterus_complicidens
???????????00??1
??000?100?00??100110???1???020?10?0220??1?31????????01100101??1?11100????12????00?00
10111010801111100??01100?0210113?111111001210?4?

Tupuxuara_longicristatus
???00?100010???????100?????0?11005?012?????????????????????1????0??0???????????11110??
??????????????????????????????1?????????????????????0???????0?????????????????????0????
?????????????????21?0??1?????????????????????

Tupuxuara_leonardii
2?100?10001001??1??100124110?1100530120????1????11000012201230101001l0?11110111111
01111111000?1001011?0001000101??11?????????????????????0101100101??11??????001121?
10001100??11?108011111004???100110?????????????1112101??

Alanqa_saharica
2?100?10?31??1???0121?????
01??00?1??101??101??????????1?????????????????????0????????????????????????????????
??

Aerotitan_sudamericanus
2?100?10?31??1???012??????
0????????????????????????????1?????????????????????0????????????????????????????????
??

Thalassodromeus_sethi
2?100?10101001??1??100124110?1100530120????0100011000012201230101001l0?11?1?110111
011?111?000?100?011?1211000101??11?????????????????????0????????????????????????????
??

Chaoyangopterus_zhangi
2?100?100010?2?????1?0?????1??0???????0?????????????????????1????????????????????????

?111000?1101001??????????1???1??????????????????????0?00?12111?????????00?2211100 02?
?0011??10????1?1??4?11100??02011300000?01?121014?

Jidapterus_edentus
2?100?10001002??1??1?0?????1??0???????0?????????????????????1???101??????1??????00??????
?111000?1101001??????0?101??11?????????????????????????0?00?12111????1??????0??21?10001?
??01??0???????110?4?1110011?3??13???11?111121??33

Eoazhdarcho_liaoxiensis
???????????00???0????????????????????????
11000?1??1001?00010??10???11?????????????????????????00?12?11??1????????0?22????00??0?
01??0?080??111??4?2110??10?????????????1???1????

Shenzhoupterus_chaoyangensis
2?1?0????01??2??1??10012?111?10???????0????1????1101?01301?2301?100020?11???1???????
???111000?110???1??????001?1???1?????????????????????0????12?11?10???????00?22????????
???01???1080??????0??21?0?1?0????????????1?1??014?

Radiodactylus_langstoni
??
??10001?
01108011?????????????????????????????????

Microtuban_altivolans
??
??1???????100?22????????0001
10??08011??1??4?2110???0?????????????112?0???

Aralazhdarcho_bestobensis
????????0???????0???1?1??????1?????????????1
??????????????????????????????1?????????????????????????0???1??????????1001????????????
??????????????????????3?????????????112?????

Volgadraco_bogolubovi
???????????0???1
11000?1101?????00??????1???1?????????????????????????01101101?11????????????????????
??????????????????????????????????????1??????

Eurazhdarcho_langendorfensis
??
??00122?11????????????????????????
??????????????????1?0??3?????????????????????

Montanazhdarcho_minor
???????????0???1
1?000?1?0100??000??????0???1?????????????????????????00?12?11?????????100122?010???110
01101108001?110??1??100??0?????????????????????

Phosphatodraco_mauritanicus
??
??0002211?1????????????????????????
??

Zhejiangopterus_linhaiensis
2?100?10001??0?????100124110?10???????0????1????0????00?01123010101010?12???1???????
0??111000?1101001??????01101???1?????????????????????01???22?110?1111100?00?22??10?
?1???01???1180??11???4?2?10?1?310113?1111?11?1210?4?

Azhdarcho_lancicollis
2?100?100010?1?????1???????0?10?????????????????????????????0??????????????00??????
1111000?1?01????00?????1?1???1?????????????????????0100122111?11??????100122101000?
1?00110111801?11100?????00?13???????????111211???

OCP_DEK_GE_716
??
??0012211????????????????????????????
??

Hatzegopteryx_thambena
????????0??1??01?1??????121??0?????0?1?1
??001
????18011????????????????????????????????????

Arambourgiania_philadelphiae
??
??0012211????????????????????????????
????????????????????1?????????????????????

Quetzalcoatlus_spp
2?100?10001000??1??10012??10?11?16[23]0110????1???????100????12301?101010?1??????00?
?011?1111000?1001001?0001001101??11?????????????????????0100122111011?????1001221
11000?11000101118011111100412?100?13??113??1111111121014?

MGUAN_PA650&651
??
??000
003?????01?????????????????????????????????

;

Ccode

+[/1 0 +[/1 1 +[/1 2 +[/1 3 +[/1 4

+[/1 5 +[/1 6 +[/1 7 +[/1 8 +[/1 9

+[/1 10 +[/1 11 +[/1 12 +[/1 13 +[/1 14

+[/1 15 +[/1 16 +[/1 17 +[/1 18 +[/1 19

+[/1 20 +[/1 21 +[/1 22 +[/1 23 +[/1 24

+[/1 25 +[/1 26 +[/1 27 +[/1 28 +[/1 29

+[/1 30 +[/1 31 +[/1 32 +[/1 33 +[/1 34

+[/1 35 +[/1 36 +[/1 37 +[/1 38 +[/1 39

+[/1 40 +[/1 41 +[/1 42 +[/1 43 +[/1 44

+[/1 45 +[/1 46 +[/1 47 +[/1 48 +[/1 49

+[/1 50 +[/1 51 -[/1 52 +[/1 53 -[/1 54

-[/1 55 -[/1 56 -[/1 57 -[/1 58 -[/1 59

-[/1 60 -[/1 61 -[/1 62 +[/1 63 +[/1 64

-[/1 65 -[/1 66 -[/1 67 -[/1 68 -[/1 69

-[/1 70 -[/1 71 -[/1 72 -[/1 73 -[/1 74

-[/1 75 -[/1 76 -[/1 77 -[/1 78 +[/1 79

-[/1 80 -[/1 81 -[/1 82 +[/1 83 -[/1 84

+[/1 85 -[/1 86 -[/1 87 -[/1 88 -[/1 89

-[/1 90 -[/1 91 -[/1 92 -[/1 93 -[/1 94

-[/1 95 -[/1 96 +[/1 97 -[/1 98 -[/1 99

-[/1 100 +[/1 101 -[/1 102 -[/1 103 -[/1 104

-[/1 105 -[/1 106 -[/1 107 -[/1 108 -[/1 109

+[/1 110 +[/1 111 -[/1 112 -[/1 113 -[/1 114

-[/1 115 -[/1 116 -[/1 117 -[/1 118 +[/1 119

-[/1 120 -[/1 121 -[/1 122 -[/1 123 -[/1 124

-[/1 125 -[/1 126 -[/1 127 -[/1 128 -[/1 129

-[/1 130 -[/1 131 -[/1 132 -[/1 133 -[/1 134

-[/1 135 -[/1 136 -[/1 137 -[/1 138 +[/1 139

+[/1 140 -[/1 141 -[/1 142 -[/1 143 -[/1 144

-[/1 145 -[/1 146 -[/1 147 -[/1 148 -[/1 149

-[/1 150 -[/1 151 -[/1 152 -[/1 153 -[/1 154

-[/1 155 -[/1 156 -[/1 157 +[/1 158 -[/1 159

+[/1 160 -[/1 161 -[/1 162 -[/1 163 -[/1 164

-[/1 165 -[/1 166 +[/1 167 -[/1 168 -[/1 169

-[/1 170 -[/1 171 -[/1 172 -[/1 173 +[/1 174

+[/1 175 -[/1 176 +[/1 177 -[/1 178 -[/1 179

+[/1 180 -[/1 181 -[/1 182 +[/1 183 +[/1 184

+[/1 185 -[/1 186 -[/1 187 -[/1 188 -[/1 189

-[/1 190 -[/1 191 -[/1 192 -[/1 193 +[/1 194

-[/1 195 -[/1 196 -[/1 197 -[/1 198 -[/1 199

-[/1 200 -[/1 201 -[/1 202 -[/1 203 -[/1 204

-[/1 205 +[/1 206 -[/1 207 -[/1 208 -[/1 209

-[/1 210 -[/1 211 -[/1 212 +[/1 213 -[/1 214

-[/1 215 -[/1 216 -[/1 217 -[/1 218 -[/1 219

-[/1 220 -[/1 221 -[/1 222 -[/1 223 -[/1 224

-[/1 225 -[/1 226 -[/1 227 -[/1 228 -[/1 229

-[/1 230 -[/1 231 -[/1 232 -[/1 233 -[/1 234

-[/1 235 -[/1 236 -[/1 237 -[/1 238 -[/1 239

-[/1 240 -[/1 241 +[/1 242 -[/1 243 -[/1 244

-[/1 245 -[/1 246 -[/1 247 -[/1 248 -[/1 249

+[/1 250 -[/1 251 -[/1 252 -[/1 253 -[/1 254

-[/1 255 -[/1 256 -[/1 257 -[/1 258 -[/1 259

-[/1 260 -[/1 261 -[/1 262 -[/1 263 -[/1 264

+[/1 265 -[/1 266 -[/1 267 -[/1 268 +[/1 269

+[/1 270 ;

cnames

{0
Skull_aspect_ratio,_length_relative_to_height_at_most_posterior_point_preserved_between_anterior_margin_of_external_naris_or_nasoantorbital_fenestra_and_jaw_articulation_exclusive_of_cranial_crests:_continuous;

{1 Skull,_length_to_squamosal_relative_to_dorsal_vertebra_length:_continuous;

{2 Mandble,_length_relative_to_skull_length_to_squamosal:_continuous;

{3
Rostrum,_length_to_external_naris_(or_nasoantorbital_fenestra)_relative_to_skull_length_to_squamosal:_continuous;

{4 External_naris,_length_relative_to_skull_length_to_squamosal:_continuous;

{5 External_naris,_length_relative_to_height:_continuous;

{6 Antorbital_fenestra,_length_relative_to_skull_length_to_squamosal:_continuous;

{7 Antorbital_fenestra,_length_relative_to_height:_continuous;

{8 Nasoantorbital_fenestra,_length_relative_to_skull_length_to_squamosal:_continuous;

{9 Nasoantorbital_fenestra,_length_relative_to_height:_continuous;

{10 Orbit,_length_relative_to_height:_continuous;

{11 Supratemporal_fenestra,_length_relative_to_skull_length_to_squamosal:_continuous;

{12 Subtemporal_fenestra,_length_relative_to_width:_continuous;

{13 Basipterygoid_processes,_angle_divided_by_100:_continuous;

{14
Rostral_tooth_row,_length_to_posterior_margin_relative_to_skull_length_to_squamosal:_continuous;

{15 Teeth,_maximum_number_divided_by_1000:_continuous;

{16 Mandibular_symphysis,_length_relative_to_mandible_length:_continuous;

{17 Mandible_length,_relative_to_ramus_mid-depth:_continuous;

{18 Mandibular_crest,_length_relative_to_mandible_length:_continuous;

{19 Mandibular_tooth_row,_length_relative_mandible_length:_continuous;

{20 Mid-cervical_vertebra,_maximum_length_relative_to_mid-width:_continuous;

{21 Mid-cervical_vertebra,_maximum_length_relative_to_dorsal_vertebra_length:_continuous;

{22 Dorsal_vertebra,_length_relative_to_maximum_diameter:_continuous;

{23 Synsacral_verebra,_number:_continuous;

{24 Caudal_vertebra,_length_relative_to_dorsal_vertebra_length:_continuous;

{25 Caudal_vertebra,_length_relative_to_diameter:_continuous;

{26 Scapula,_length_relative_to_coracoid_length:_continuous;

{27 Deep_coracoid_flange,_length_relative_to_coracoid_length:_continuous;

{28 Humerus,_length_relative_to_dorsal_vertebra_length:_continuous;

{29
Humerus,_deltopectoral_crest,_proximodistal_constriction_width_relative_to_anterior_terminus_proximodistal_width:_continuous;

{30 Ulna_or_radius,_length_relative_to_humerus_length:_continuous;

{31 Radius,_diameter_relative_to_ulna_diameter:_continuous;

{32 Pteroid,_length_relative_to_ulna_length:_continuous;

{33 Metacarpal_IV,_length_relative_to_humerus_length:_continuous;

{34 Metacarpal_IV_mid-width_relative_to_combined_ulna_and_radius_mid-width:_continuous;

{35 Metacarpal_IV_proximal_end,_dorsoventral_width_relative_to_mid-width:_continuous;

{36 Manual_digit_IV_first_phalanx,_length_relative_to_humerus_length:_continuous;

{37 Manual_digit_IV_second_phalanx,_length_relative_to_first_phalanx_length:_continuous;

{38 Manual_digit_IV_third_wing_phalanx,_length_relative_to_first_phalanx_length:_continuous;

{39 Manual_digit_IV_fourth_wing_phalanx,_length_relative_to_first_phalanx_length:_continuous;

{40 Prepubis,_length_relative_to_width:_continuous;

{41 Pubis,_dorsoventral_depth_relative_to_acetabulum_anteroposterior_length:_continuous;

{42 Ilium_anterior_process,_length_relative_to_posterior_process_length:_continuous;

{43 Femur,_length_relative_to_humerus_length:_continuous;

{44 Tibia,_length_relative_to_femur_length:_continuous;

{45 Fibula,_free_length_relative_to_tibia_length:_continuous;

{46 Metatarsal_III,_length_relative_to_tibia_length:_continuous;

{47 Pedal_digit_III_second_phalanx_length,_relative_to_mid-width:_continuous;

{48 Pedal_digit_IV_first_phalanx,_length_relative_to_mid-width:_continuous;

{49 Pedal_digit_IV_second_phalanx,_length_relative_to_mid-width:_continuous;

{50 Pedal_digit_IV_third_phalanx,_length_relative_to_mid-width:_continuous;

{51 Rostrum_anterior_margin,_shape: flat_surface blunt sharp_tip rostral_process;

{52 Rostral_process_cross-section,_shape: triangular elliptical;

{53 Rostrum_anterior_end,_orientation:_ordered upturned straight downturned;

{54 Palate_anterior_end,_shape: absent present;

{55 Rostrum,_anterior_end,_lateral_expansion: absent present;

{56 Jaws,_anterior_expansion,_horizontal_outline_shape: elliptical triangular quadrangular;

{57 Rostrum,_anterior_occlusal_margins,_shape: rounded_edges sharp_or_ridged;

{58 Rostrum,_middle_expansion: absent present;

{59 Rostrum,_posterior_occlusal_margins,_shape: rounded sharp_or_ridged;

{60 Rostrum,_shape: laterally_attenuated anteroposteriorly_shortened dorsoventrally_depressed laterally_flattened;

{61 Rostrum,_dorsal_taper: subparallel attenuated;

{62 Jaws,_anterior_end,_lateral_taper: attenuated subparallel;

{63 Skull,_entire_margin,_lateral_shape: concave straight_attenuated convex _;

{64 Skull_dorsal_margin,_curvature_exclusive_of_cranial_crests:_ordered convex straight concave;

{65 External_naris_dorsal_and_ventral_margins,_orientation: acute_angle subparallel;

{66
External_naris_(or_nasoantorbital_fenestra)_anterior_margin,_position_relative_to_premaxillary_toothrow: dorsal posterior;

{67 Antorbital_(or_nasoantorbital)_fossa_on_jugal: present absent;

{68 Antorbital_fenestra_dorsal_and_ventral_margins,_orientation: subparallel acute_angle;

{69 Antorbital_fenestra_ventral_margin,_position_relative_to_external_naris_ventral_margin: same_level ventral;

{70 External_naris_and_antorbital_fenestra,_configuration: separate confluent;

{71 Antorbital_(or_nasoantorbital_fenestra)_posterior_margin,_shape: subangular beveled;

{72 Nasoantorbital_fenestra_dorsal_and_ventral_margins,_orientation: acute_angle subparallel;

{73 Orbit_outline,_shape: subcircular piriform inverted_triangle;

{74 Orbit,_dorsal_position:
middle_of_the_skull_with_the_ventral_margin_of_the_orbit_below_the_middle_of_the_antorbital_(or_nasoantorbital)_fenestra_and_the_dorsal_margin_of_the_orbit_above_the_dorsal_margin_of_the_antorbital_(or_nasoantorbital)_fenestra
high_in_the_skull_with_the_ventral_margin_of_the_orbit_the_same_level_or_above_the_middle_of_the_antorbital_(or_nasoantorbital)_fenestra
low_in_the_skull_with_the_entire_orbit_lower_than_the_dorsal_margin_of_the_antorbital_(or_nasoantorbital)_fenestra;

{75 Infratemporal_fenestra,_shape: trapezoidal inverted_triangle upright_triangle oval elliptical;

{76 Infratemporal_fenestra,_position_relative_to_orbit: posterior_to_orbit reaches_under_orbit;

{77 Infratemporal_fenestra,_orientation: subvertical inclined;

{78 Premaxillary_bar_(internasal_process),_width: wide narrow;

{79 Premaxilla,_maxillary_process,_position:_ordered contacts_nasal reaches_posterior_half_of_external_naris anterior_to_middle_of_external_naris;

{80 Premaxilla,_posterior_process,_posterior_margin_position: terminate_between_nasals contacts_frontals;

{81 Premaxillary_crest: absent present;

{82 Premaxillary_crest_anterior_margin,_position_relative_to_skull_anterior_margin: level posterior;

{83 Premaxillary_crest_anterior_margin,_orientation:_ordered inclined_posteriorly subvertical curving_anterodorsally;

{84 Premaxillary_crest,_shape: tall_triangle_decreasing_in_height_posteriorly low_blade low_with_anterior_humped_margin comb-like_with_straight_dorsal_margin semicircular tall_triangle_increasing_in_height_posteriorly rectangular;

{85 Premaxillary_crest_posterior_margin,_position:_ordered anterior_to_external_naris_(or_nasoantorbital_fenestra)_anterior_margin between_external_naris_(or_nasoantorbital_fenestra)_anterior_margin_and_orbit above_orbit above_occipital_region;

{86 Premaxillary_crest_dorsal_spine: absent present;

{87 Premaxillary_crest,_thickness: single_plate two_plates_separated_by_trabeculae;

{88 Premaxillary_crest,_texture: striated smooth branching_system_of_grooves;

{89 Maxilla_posterior_end,_shape: narrow ventrally_expanded;

{90 Maxilla_ascending_process,_shape: broad tapered slender;

{91 Antorbital_fossa_on_maxilla: present absent;

{92 Maxilla_and_nasal_contact,_position: maxilla_contacts_main_body_of_nasal maxilla_contacts_only_descending_process_of_nasal;

{93 Maxilla,_premaxillary_and_jugal_processes,_shape: jugal_process_wider both_narrow premaxillary_process_wider both_wide;

{94 Nasal_descending_process: present absent;

{95 Nasal_descending_process,_position: lateral medial;

{96 Nasal_descending_process,_length: short elongate;

{97 Nasal_descending_process,_orientation:_ordered inclined_anteriorly ventral inclined_posteriorly;

{98 Nasal_process,_lateral_pneumatic_foramen: absent present;

{99 Frontal_crest: absent present;

{100 Frontal_crest,_shape: low_and_blunt low_and_elongated high_and_expanded;

{101 Frontal_crest_anterior_margin,_position: anterior_to_orbit above_orbit posterior_to_orbit;

{102 Frontal_anterior_margin,_position_relative_to_preorbital_bar_anterior_margin: anterior posterior;

{103 Lacrimal_foramen: absemt present;

{104 Lacrimal_descending_process_posterior_margin,_shape: flat orbital_process;

{105 Parietal_crest: absent present;

{106 Parietal_crest,_shape: blunt expanded_into_rounded_margin tapered_into_triangular_process elongate_process;

{107 Squamosal,_shape: unexpanded rounded expanded;

{108 Squamosal,_position: above_base_of_lacrimal_process_of_jugal below_or_level_with_base_of_lacrimal_process_of_jugal;

{109 Jugal_posterior_process: present absent;

{110 Quadrate,_inclination_relative_to_ventral_margin_of_skull:_ordered anteriorly subvertical 120˚_posteriorly 150˚_posteriorly;

{111 Mandibular_articulation,_position_relative_to_center_of_orbit:_ordered posterior_to_orbit posterior_to_center_below_orbit underneath_center_below_orbit anterior_to_center_below_orbit anterior_to_orbit;

{112 Quadrate,_shape: wide thin_and_cylindrical;

{113 Jugal_ventral_margin,_shape: straight concave;

{114 Jugal_anterior_margin,_position_relative_to_nasoantorbital_fenestra_anterior_margin: posterior same_level_or_anterior;

{115 Jugal_maxillary_process: absent present;

{116 Jugal_postorbital_process_and_lacrimal,_configuration: do_not_contact contact_to_form_lower_orbital_bar;

{117 Jugal_ascending_and_postorbital_processes,_shape: separated_by_distinct_angle infilled_by_concave_flange;

{118 Jugal_ascending_process_base,_width: broad narrow;

{119 Jugal_ascending_process,_inclination:_ordered anterodorsal vertical posterodorsal;

{120 Jugal_postorbital_process_anterior_margin,_shape: flat orbital_process;

{121 Jugal_posterior_process,_orientation: posterior ventral;

{122 Jugal_maxillary_process: absent present;

{123 Occiput,_orientation:_ordered posterior posteroventral ventral;

{124 Basioccipital,_length_relative_to_width: shorter_than_wide longer_than_wide;

{125 Basisphenoid_body,_length: shorter_than_wide at_least_longer_than_wide;

{126 Elongate_basipterygoid_processes: absent present;

{127 Supraoccipital_crest: absent present;

{128 Supraoccipital,_pneumatic_foraminae: absent present;

{129 Palate,_posterior_end,_shape: concave convex;

{130 Palatal_ridge: absent present;

{131 Palatal_ridge,_position: tapering_anteriorly confined_posteriorly _;

{132 Palatal_ridge_shape: narrow_strip strong_keel;

{133 Palatines,_shape: broad_and_flat thin_bars;

{134 Internal_nares_and_maxilla,_configuration: contact do_not_contact;

{135 Pterygoids,_ventral_position_relative_to_jaw_margin: level_or_dorsal ventral;

{136 Interpterygoid_opening,_length_relative_to_subtemporal_fenestra_length: at_least_subtemporal_fenestra shorter_than_subtemporal_fenestra;

{137 Mandible_articulation_condyles,_orientation: parasagittal oblique;

{138 Foramina_positioned_in_a_row_along_the_lateral_margin_of_the_jaws: present absent;

{139 Mandible_anterior_end,_orientation:_ordered upturned straight downturned;

{140 Mandible_anterior_margin,_shape: blunt sharp_tip prow;

{141 Mandible_anterior_end,_shape: compressed_laterally shortened_anteroposteriorly depressed_dorsoventrally _;

{142 Mandible,_anterior_expansion: absent present;

{143 Mandible_anterior_end_dorsal_jaw_margins,_shape: level eminence;

{144 Mandible_anterior_end_distinct_eminence,_height: low high;

{145 Mandibular_symphysis,_fusion: unfused fused;

{146 Mandibular_symphysis,_orientation: subparallel_to_rami oblique_to_rami;

{147 Mandible,_anterior_end_lateral_surfaces,_texture: flat large_foramina pitted;

{148 Mandible,_anterior_occlusal_margins,_shape: rounded_edges sharp_or_ridged;

{149 Mandible,_distinct_middle_expansion: absent present;

{150 Mandible,_posterior_occlusal_margins,_shape: rounded sharp_or_ridged;

{151 Mandibular_rami_distinct_dorsal_eminence: present absent;

{152 Mandibular_rami_dorsal_eminence,_shape: rounded pointed;

{153 Mandibular_sulcus: absent present;

{154 Mandible_symphysis_occlusal_surface_anterior_end,_shape: flat_or_concave fossa keel;

{155 Mandible,_dorsal_surface,_parasagittal_ridges: absent present;

{156 Mandible,_symphyseal_cavity: absent present;

{157
Mandibular_symphyseal_cavity,_dorsal_shelf,_posterior_margin_relative_to_ventral_symphysis_posterior_margin:
dorsal_shelf_posterior_margin_extends_posterior_to_ventral_symphysis_posterior_margin
ventral_shelf_posterior_margin_extends_at_least_posterior_to_dorsal_symphysis_posterior_margin;

{158 Mandibular_rami_dorsal_margin,_shape:_ordered convex straight concave;

{159 Mandibular_rami,_orientation: straight_to_upturned downcurved;

{160 Retroarticular_process,_orientation_relative_to_mandible:_ordered posteroventral subhorizontal posterodorsal;

{161 Retroarticular_process,_shape: triangular subcircular elongate blunt;

{162 Mandible_ventral_margin,_shape: flat keel crest;

{163 Mandibular_crest,_shape: blade_like_and_low massive_and_deep;

{164 Mandibular_crest_anterior_margin,_position: posterior_to_mandible_anterior_margin mandible_anterior_margin;

{165 Dentary,_length: do_not_separate_angular_and_surangular separate_angular_and_surangular;

{166 Teeth: present absent;

{167 Teeth,_spacing_along_jaws:_ordered mesial_teeth_spaced_wider_apart even_along_the_jaws distal_teeth_spaced_wider_apart;

{168 Teeth,_variation_in_shape_along_tooth_row: isodont heterodont;

{169 Mesial_heterodont_teeth,_shape: recurved_triangle slender_needle recurved_spike;

{170 Teeth,_shape: recurved_triangle bulbous_triangle slender_needle recurved_cone labiolingually_compressed_triangle recurved_spike;

{171 Teeth,_texture: smooth striated sharp_mesial_and_distal_keels medial_carinae;

{172 Teeth,_maximum_crown_height_relative_to_basal_width: less_than_four_times_width at_least_four_times_width;

{173 Teeth,_lateral_orientation: vertical inclined_laterally;

{174 Mesial_teeth,_average_spacing_between_successive_teeth: nearly_touching at_most_diameter_of_teeth more_than_diameter_of_teeth;

{175 Cheek_teeth,_average_spacing_between_successive_teeth:_ordered nearly_touching at_most_diameter_of_teeth more_than_diameter_of_teeth;

{176 Teeth,_size_variation: transition_along_tooth_row disparity_in_size_between_mesial_and_distal_teeth;

{177 Upper_dentition,_size_relative_to_lower_dentition:_ordered upper_dentition_significantly_larger subequal upper_dentition_significantly_smaller;

{178 Teeth,_maximum_curvature: displacement_of_curvature_less_than_tooth_diameter displacement_of_curvature_at_least_tooth_diameter;

{179 Teeth,_curvature_orientation: posterior lingual;

{180 Teeth,_inclination:_ordered upright mesial_teeth_procumbent procumbent;

{181 Cheek_alveoli,_shape: set_in_grooves low undulating_occlusal_margins raised_rims inflated;

{182 Cheek_teeth,_denticles: present absent;

{183 Teeth_largest_denticles,_shape:_ordered serrations cuspules crenulations low_cusps tall_cusps;

{184 Teeth,_maximum_denticle_number:_ordered more_than_50 between_six_and_49 five;

{185 Rostral_tooth_row,_anterior_end,_position: posterior_to_tip_of_rostrum tip_of_rostrum anterior_surface_of_rostrum;

{186 Maxillary_teeth,_position_of_largest_teeth: mesial middle distal;

{187 Fifth_and_sixth_teeth,_distinctly_smaller_than_fourth_and_seventh_and_subequal_in_size: absent present;

{188 Mandibular_tooth_row,_anterior_end,_position: tip_of_mandible posterior_to_tip_of_mandible;

{189 Occlusal_margin,_orientation_with_respect_to_jaw_margin: parallel dorsally_reflected;

{190 Atlantoaxis,_fusion: unfused fused;

{191 Mid-cervical_vertebra_neural_arch_lateral_surface,_pneumatic_foramen: absent present;

{192 Mid-cervical_vertebra_centrum_lateral_surface,_pneumatic_foramen: absent present;

{193 Cervical_vertebra_lateral_to_neural_canal,_pneumatic_foramina: absent present;

{194 Mid-cervical_vertebra_neural_spines,_height:_ordered tall low extremely_reduced;

{195 Mid-cervical_vertebrae_neural_spines,_lateral_outline_shape: blade triangular ridge fan;

{196 Mid-cervical_vertebra,_postexapophyses: absent present;

{197 Mid-cervical_vertebra_neural_arch_and_centrum,_configuration: distinct confluent;

{198 Mid-cervical_vertebra_ribs,_shape: elongate reduced;

{199 Cervical_8_neural_spine,_height: tall low;

{200 Cervical_9,_shape: similar_to_dorsal_vertebrae similar_to_cervicals;

{201 Notarium: absent present;

{202 Anterior_dorsal_vertebra_neural_spines,_shape: unfused supraneural_plate;

{203 Sacral_ribs,_configuration: contact_at_ilium contact_medial_to_ilium;

{204 Synsacral_supraneural_plate: absent present;

{205 Caudal_vertebra,_number: more_than_15 at_most_15;

{206 Caudal_vertebra_zygapophyses,_length: short elongate extremely_elongate;

{207 Caudal_vertebra_centrum,_shape: single duplex;

{208 Scapulocoracoid,_orientation_relative_to_vertebral_column: subparallel rotated_laterally;

{209 Scapula_proximal_end,_shape: elongate_andcompressed suboval_and_expanded;

{210 Scapula,_shape: elongate_process stout_with_constricted_shaft;

{211 Scapula_articulates_with_vertebral_column: absent present;

{212 Coracoid_ventral_margin,_shape: rounded broad_tubercle deep_flange;

{213 Coracoid,_shape:_ordered semicircular broad_shaft narrow_shaft;

{214 Sternocoracoid_articulations,_position_with_respect_to_one_another: lateral anterior_and_posterior;

{215 Sternum,_constriction_posterior_to_sternocoracoid_articulations: present absent;

{216 Cristopine,_shape: shallow deep;

{217 Cristospine,_length: stout elongate;

{218 Sternocoracoid_articulations,_shape: flattened oval;

{219 Sternocoracoid_articulations,_posterior_expansion: absent present;

{220 Sternum_plate,_shape: narrow quadrangular semicircular triangular laterally_expanded;

{221 Humerus_proximal_end_ventral_surface,_pneumatic_foramen: absent present;

{222 Humerus_proximal_end,_cross_section: crescent horseshoe;

{223 Humerus_proximal_end_dorsal_surface,_pneumatic_foramen: absent present;

{224 Humerus_shaft,_shape: straight bowed;

{225 Humerus,_mid-shaft,_shape: tapered subcylindrical;

{226 Humerus_entepicondyle,_anteroposterior_width_relative_to_ectepicondyle_anteroposterior_width: entepicondyle_wider_than_ectepicondyle ectepicondyle_at_most_entepicondyle_width;

{227 Humerus,_between_distal_condyles,_pneumatic_foramen: absent present;

{228 Humerus_distal_aspect,_pneumatic_foramen: absent present;

{229 Humerus_distal_aspect,_shape: hourglass crescentic_or_D-shape triangular trapezoidal;

{230 Deltopectoral_crest,_position_on_humerus: proximal more_distally_on_shaft;

{231 Humerus_deltopectoral_crest,_shape: subtriangular_with_proximal_apex proximally_leaning_trapezoid proximally_curving_hook oblong_process_with_constricted_neck low_and_rectangular elongate_and_proximally_expanded hatchet-shape distally_leaning_trapezoid tall_rectangular_process;

{232 Humerus_deltopectoral_crest,_curvature: parallel_to_shaft warped_distally;

{233 Ulnar_crest_of_humerus,_size: reduced developed;

{234 Humerus_ulnar_crest,_orientation: posterior ventral;

{235 Ulna_shaft_proximal_anterior_surface,_shape: flat longitudinal_ridge;

{236 Ulna_distal_tubercle,_position: middle_of_the_distal_end ventral_part_of_the_distal_end;

{237 Radius_distal_end_cross-section,_shape: suboval subtriangular_with_large_anterior_process;

{238 Distal_syncarpal_ventral_articular_facet_for_Metacarpal_IV,_size_relative_to_dorsal_facet: ventral_facet_larger subequal_in_size;

{239 Distal_syncarpal,_cross-section_shape: rectangular triangular;

{240 Pteroid,_shape: angled_at_midsection stout_hook straight_and_tapered_with_expanded_proximal_end straight_with_expanded_ends curved_slender_rod curved_and_subparallel-sided;

{241 Preaxial_carpal,_shape: longer_than_wide at_most_long_as_wide;

{242 Metacarpals,_number_articulating_with_carpus:_ordered four_or_more two one;

{243 Metacarpals_I_to_III_distal_ends,_positions: disparate approximate;

{244 Metacarpal_IV_proximal_cross-section,_shape: anteroposteriorly_compressed subrectangular;

{245 Metacarpal_IV_shaft_cross-section,_shape: rounded_rectangle anteroposteriorly_compressed_oval;

{246 Metacarpal_distal_end_between_condyles,_shape: flat median_ridge;

{247 Manual_unguals,_size_relative_to_pedal_unguals: less_than_twice_the_size_of_pedal_unguals at_least_twice_the_size_of_pedal_unguals;

{248 Manual_digit_IV_first_phalanx_proximal_end_ventral_surface,_pneumatic_foramen: absent present;

{249 Manual_digit_IV_second_or_third_phalanges_shaft_cross-sections,_shape: round_to_subtriangular concave_posteriorly oval ventral_ridge;

{250 Pubis_anterior_margin,_shape_in_lateral_view:_ordered convex straight slightly_concave deeply_concave;

{251 Pubis_and_ischium_contact,_shape: confluent_along_length partially_separated_by_oval_opening;

{252 Ischium_ventral_margin,_shape: straight convex;

{253 Prepubis_shaft,_constriction: absent present;

{254 Prepubis,_shape: elongate_paddle medially_curved_with_short_lateral_process triradiate expanded_fan;

{255 Ilium_preactetabular_anterior_margin,_shape: rounded pointed;

{256 Ilium_preacetabular_process,_orientation: straight dorsiflected;

{257 Ilium_postacetabular_process,_orientation: subhorizontal posterodorsal;

{258 Ilium_postacetabular_process_shaft,_constriction: absent present;

{259 Ilium_postacetabular_process,_terminal_expansion: absent present;

{260 Acetabulum,_shape: anteroposteriorly_ovate subcircular;

{261 Ilium_postacetabular_process_apex,_shape: flat torus;

{262 Femur,_shape: strongly_bowed slight_curvature;

{263 Femur_proximal_end,_pneumatic_foramen: absent present;

{264 Femoral_neck,_shape: indistinct constricted;

{265 Greater_trochanter,_shape:_ordered reduced distinct_process anteriorly-curved_hook;

{266 Femur_distal_end,_epicondyles_size: reduced_and_confluent_with_distal_condyles expanded_into_distinct_distal_flanges;

{267 Femoral_head,_angle_relative_to_shaft: at_most_145° greater_than_145°;

{268 Metatarsal_IV,_length_relative_to_metatarsals_I_to_III: subequal significantly_shorter;

{269 Pedal_digit_V,_number_of_phalanges:_ordered four three two one zero;

{270 Pedal_digit_V_ultimate_phalanx,_shape:_ordered straight curved bent_at_midsection nubbin;

;

;

Ancstates

-0 -1 -2 -3 -4 -5 -6 -7 -8 -9

-10 -11 -12 -13 -14 -15 -16 -17 -18 -19

-20 -21 -22 -23 -24 -25 -26 -27 -28 -29

-30 -31 -32 -33 -34 -35 -36 -37 -38 -39

-40 -41 -42 -43 -44 -45 -46 -47 -48 -49

-50 -51 -52 -53 -54 -55 -56 -57 -58 -59

-60 -61 -62 -63 -64 -65 -66 -67 -68 -69

-70 -71 -72 -73 -74 -75 -76 -77 -78 -79

-80 -81 -82 -83 -84 -85 -86 -87 -88 -89

-90 -91 -92 -93 -94 -95 -96 -97 -98 -99

-100 -101 -102 -103 -104 -105 -106 -107 -108 -109

-110 -111 -112 -113 -114 -115 -116 -117 -118 -119

-120 -121 -122 -123 -124 -125 -126 -127 -128 -129

-130 -131 -132 -133 -134 -135 -136 -137 -138 -139

-140 -141 -142 -143 -144 -145 -146 -147 -148 -149

-150 -151 -152 -153 -154 -155 -156 -157 -158 -159

-160 -161 -162 -163 -164 -165 -166 -167 -168 -169

-170 -171 -172 -173 -174 -175 -176 -177 -178 -179

-180 -181 -182 -183 -184 -185 -186 -187 -188 -189

-190 -191 -192 -193 -194 -195 -196 -197 -198 -199

-200 -201 -202 -203 -204 -205 -206 -207 -208 -209

-210 -211 -212 -213 -214 -215 -216 -217 -218 -219

-220 -221 -222 -223 -224 -225 -226 -227 -228 -229

-230 -231 -232 -233 -234 -235 -236 -237 -238 -239

-240 -241 -242 -243 -244 -245 -246 -247 -248 -249

-250 -251 -252 -253 -254 -255 -256 -257 -258 -259

-260 -261 -262 -263 -264 -265 -266 -267 -268 -269

-270 ;

xgroup

;

agroup

;

taxcode

+0 +1 +2 +3 +4 +5 +6 +7

+8 +9 +10 +11 +12 +13 +14 +15

+16 +17 +18 +19 +20 +21 +22 +23

+24 +25 +26 +27 +28 +29 +30 +31

+32 +33 +34 +35 +36 +37 +38 +39

+40 +41 +42 +43 +44 +45 +46 +47

+48 +49 +50 +51 +52 +53 +54 +55

+56 +57 +58 +59 +60 +61 +62 +63

+64 +65 +66 +67 +68 +69 +70 +71

+72 +73 +74 +75 +76 +77 +78 +79

+80 +81 +82 +83 +84 +85 +86 +87

+88 +89 +90 +91 +92 +93 +94 +95

+96 +97 +98 +99 +100 +101 +102 +103

+104 +105 +106 +107 +108 +109 +110 +111

+112 +113 +114 +115 +116 +117 +118 +119

+120 +121 +122 +123 +124 +125 +126 +127

+128 +129 +130 +131 +132

;

blocks 0 51 ;

proc/;